NASA CR-159,728

NASA CR-159728

BAT REPORT NO. D2536-941001

AEROELASTIC AND DYNAMIC FINITE ELEMENT ANALYSES OF A BLADED SHROUDED DISK

by

G.C.C. SMITH
V. ELCHURI

BELL AEROSPACE TEXTRON

P.O. BOX 1

Buffalo, New York 14240

NATIONAL AERONAUTICS AND SPACE ADMINISTRATION

CONTRACT NAS3-20382

NASA LEWIS RESEARCH CENTER
CLEVELAND, OHIO

MARCH 1980

NASA CR-159728

BAT REPORT NO. D2536-941001

AEROELASTIC AND DYNAMIC FINITE ELEMENT ANALYSES OF A BLADED SHROUDED DISK

by

G.C.C. SMITH
V. ELCHURI

BELL AEROSPACE TEXTRON

P.O. BOX 1

Buffalo, New York 14240

NATIONAL AERONAUTICS AND SPACE ADMINISTRATION

CONTRACT NAS3-20382

NASA LEWIS RESEARCH CENTER
CLEVELAND, OHIO

MARCH 1980

ABSTRACT

A computer program based on state-of-the-art compressor and structural analysis technologies applied to bladed shrouded discs is described. It is operational in NASTRAN Level 16.

Problems encompassed include aeroelastic analyses, modes, flutter and approaches to forced vibration.

Mathematical extensions from the tuned disc to mistuned disc analyses are presented.

SUMMARY

The objective of the work described herein was the delivery and demonstration of a computer program for the analysis of aeroelastic and dynamic properties of tuned and mistuned bladed discs.

The scope was defined as:

- aerothermoelastic "design", "analysis" and transient characteristics of tuned bladed discs.
- modes, flutter, subcritical roots and forced vibration of tuned bladed discs.
- modes, flutter, subcritical roots and forced vibration of mistuned bladed discs.

The program was to use state-of-the-art structural and aerodynamic technologies, be coded and delivered in NASTRAN Level 16 and demonstrated on the UNIVAC 1100 System at NASA/Lewis.

The currently delivered program accomplishes -

- aerothermoelastic "design" and "analysis" of tuned bladed discs.
- modes, flutter and subcritical roots of tuned bladed discs.

Mathematical formulations of modes of mistuned bladed discs were developed but not programmed. Approaches to flutter and forced vibration of mistuned discs, and transient aerothermoelasticity were also formulated.

The bases of the current capabilities use three aerodynamic theories:

- o a three-dimensional axial flow compressor code.
- o a subsonic two-dimensional unsteady cascade theory.
- o a supersonic two-dimensional unsteady cascade theory.

Additionally, three existing Rigid Formats in the NASTRAN general purpose structural analysis program have been used:

- o Statics with Differential Stiffness
- o Normal Modes Using Cyclic Symmetry
- o Modal Flutter Analysis

The program consists of three principal parts:

- o Blade-mesh generator.
- o A Rigid Format 16 for Static Aerothermoelastic Analysis.
- o A Rigid Format 9 for Cyclic Modal Flutter Analysis.

Program documentation consists of updates to NASTRAN Theoretical, User, Programmer and Demonstration Example Manuals. In addition, aeroelastic, modal and flutter analyses of a NASA/Lewis Rotor 12 were performed.

Limitations of current cascade theories related to mistuned systems are discussed.

ACKNOWLEDGEMENT

The authors take this opportunity to express their deep appreciation of the contributions of Dr. Kari Appa as Technical Director during the earlier stages of this program, Ms. Beverly Dale and Mr. A. Michael Gallo for the entire programming efforts and Dr. Joseph Padlog for his technical suggestions.

TABLE OF CONTENTS

LIST OF TABLES

LIST OF ILLUSTRATIONS

INTRODUCTION

The jet engine designer, striving for improved performance of turbomachinery components is finding, as did the aircraft designer, that aeroelastic effects on performance, stability and life are of ever-increasing significance. In seeking higher thrust to weight and volume ratios, lower specific fuel consumption and longer life, he is using higher tip speeds, temperatures and pressure ratios, fewer and larger stages, thinner components and exotic materials. His problems are further compounded by the complex aerodynamics of the axial flow machine, the deviations (mistuning) from perfection of the ideal cyclic structure, and the interactions of multiple stages.

There is little wonder that, compared with the systematic approaches routinely exercised for flight vehicle aeroelastic analyses, the engine field exhibits a high degree of empiricism and a relatively piecemeal approach. The panel discussion terminating the workshop of Reference 1, illustrates this well with comments from panel members such as:

- "What this field of aeroelasticity is all about"...
- "No longer able to decouple modes from aerodynamics".
- "A well-described structural model...as part of a series of aeroelastic calculations...".
- "Aerodynamics... and structures linked together (as) one does (in) lifting surface theory".
- "We're going to be in a business where you really have to marry elasticity in all its complications

with aerodynamics and a good deal of its complications".

Progress in the analysis of turbomachinery aeroelastics (static and dynamic) is principally constrained by the fluid dynamics aspect. Reference 1 was heavily weighted with papers on steady and unsteady, unstalled and stalled, transonic and other flow regimes. Since then, reviews such as those of References 2-6 have concentrated largely on this aspect. In November 1978, NASA/Lewis conducted the workshop introducing the establishment and program of the new Internal Computational Fluid Mechanics Group. This has far reaching plans for the analytical development and experimental evaluation of fluid mechanics and its application in turbomachinery design and analysis methodology.

However, the tremendous strides made in finite element techniques of structural mechanics (and eventually of fluid mechanics?) are directly applicable to the required methodology. General purpose finite element structural programs are legion and will be typified for obvious reasons by the NASA sponsored NASTRAN Program (Reference 7).

From both fluid and structural aspects, the cyclic geometric nature of bladed discs is one feature affording some analysis simplification. Indeed the NASTRAN program itself (Reference 7), has special capability in this respect. Later developments of a related nature were References 8 and 9. Advantages of this feature should be retained in a general purpose capability. Even here, however, structural and geometric tolerances result in significant deviations in sector-to-sector

dynamic properties, the so-called MISTUNING effect.

This has received attention (References 10-18) mostly in the context of modal analysis and forced mechanical vibration. No significant literature appears to exist on the flutter of mistuned systems per se, though the problem is very real.

This report discusses the details and application of a computer program based within the NASTRAN Level 16 capability for analyzing aeroelastic problems of bladed shrouded discs in compressible flows. It was evolved under NASA/Lewis Contract NAS3-20382 for "Finite Element Modal Analysis Of A Bladed Shrouded Disc".

NASA recognized a need to properly couple structural and aerodynamic aspects of the system for the study of static and dynamic (flutter) stability, and modal and subcritical forced vibration characteristics in a practical computer program. While generally constraining the program to state-of-the-art aerodynamics (2 dimensional linear cascade theories), structural and aeroelastic techniques, NASA also required that the mistuning problem, in general, be addressed. The work encompassed definition, development, documentation, delivery and demonstration of a computer program suitable for systematic studies of aeroelastic phenomena of bladed discs.

The generic problem spectrum consists of three (3) groups:

(1) "Steady" aeroelastic performance .

(2) Dynamics of ideal cyclic (tuned) systems.

(3) Dynamics of real cyclic (mistuned) systems.

In (1) the elasticity of the system causes changes in geometry and, hence, in performance, with differential effects on the system stiffness, which can affect problem groups (2) and (3). Thus static aeroelastic solutions should precede and contribute to tuned system dynamics studies. The mistuned systems (3) are perturbations of the tuned system (2). Proper understanding of tuned system behavior should guide approaches to and understanding of problem group (3).

This interdependence makes it desirable to construct a computer program approach that can progress logically through the whole spectrum.

At the same time, as specific facets of the problem will develop, such as cascade theories, a modular program architecture is desirable to enable easy updating, improvement and expansion of the program.

The basic steps necessary are then;

(1) Adequate mathematical formulations of flow dynamics, elasticity and vibration and thermal conduction processes in an appropriate integro-differential continuum form.

(2) Discretization of (1) in space and time.

(3) Algorithm definition and computer program creation for practical (time, cost) solutions.

Two assumptions generally acceptable in these problems are retained:

(1) That aerothermoelastic problems may be satisfactorily solved assuming constant speed.

(2) That vibration and flutter problems may be satisfactorily solved at constant speed and mass flow rate about mean steady state properties.

The present capability has been formulated within NASA constraints and guidelines principally related to:

(1) Use of state-of-the-art techniques.

(2) Linearized two-dimensional steady and unsteady cascade theories (the steady theory implemented is actually three-dimensional).

(3) Use of substructuring techniques (as contrained by NASTRAN Level 16).

(4) Unconstrained bladed disc modal spectra.

(5) Perturbations in blade dynamic properties.

(6) Simplified thermal considerations.

(7) Initial operational capability within the NASA/Lewis NASTRAN Level 16 Program on the UNIVAC 1100/40 Computer.

In the main text of this report, details of the problem spectrum and formulation are given. The integration of current features of NASTRAN with available steady and unsteady cascade aerodynamic theories for application to aeroelastic, flutter and forced vibration problems is discussed. Developments in mistuned modal analyses are outlined with details in Appendix E.

Results of some specific applications to a NASA rotor example are described although the rotor is too stiff to exhibit large aeroelastic effects. Finally, the current status of the program is related to desirable additional capabilities and recommendations for further work are made.

General Approach

The principal objective of this work was to provide a coherent computational capability for the solution of practical bladed disc aeroelastic ("static") and dynamic problems. NASA recognized particularly flutter and engine order forced vibration, but required that aerodynamic, structural and thermal technologies be integrated into a practical computer program for general aeroelastic problems. State-of-the-art aerodynamics and structures analytical techniques were to be implemented. The program was to be delivered for operation on the NASA UNIVAC 1100/40.

In particular, the following guidelines were suggested:

- Aerodynamic steady and unsteady pressures would be based on existing linearized two-dimensional cascade theories used in a strip theory manner
- The "mistuned" nature of real bladed discs was to be recognized, in that the dynamic properties, sector to sector, might vary because of minor geometric and material randomness
- The program would include automatic finite element mesh generation
- No boundary layer heat transfer was to be considered (equal local flow and blade surface temperatures could be assumed)

- Comprehensive input data including mesh, material, element types, temperatures and connections would be possible
- Various permitted boundary conditions of shroud and blade root should be considered
- Gravity, inertial, centrifugal, pressure and temperature (equivalent) loading was possible
- Comprehensive numerical and pictorial output was required;
- The program would be applied to a NASA specified rotor example
- Comprehensive documentation and demonstration of the program at a NASA three day seminar were specified.

Subsequent to proposal submission, it was determined that the program would be accomplished by the development of appropriate updates to the NASTRAN Level 16 Program. Relevant items listed in the guidelines above such as element definitions and output options were constrained to that version.

Problem Spectrum

In solving the range of problems including static aeroelastic, modal, stability and forced vibration of tuned and mistuned systems it was recognized that certain interdependencies existed. These led to the definition of a logical progression of problems and a related sequence of computational algorithms.

Figure 1 illustrates the problem spectrum in terms of three major groups of subproblems and the main thread of interdependence.

Group A, the Aerothermoelastic problems, consists of three problems in which structural dynamics and mistuning play no part.

The first problem A1, is that of designing a blade which, under load, will exhibit a specified performance at a single design point on the compressor map under equilibrium thermal conditions.

The second problem A2, is "off-design" analysis of the performance in terms of pressure ratio (PR) and mass flow rate ($\dot{m}$) of the elastic blade along constant speed characteristics.

Strictly, two "elastic" maps are definable, one for a "cold" blade and one for a thermally equilibrated blade. These will generally be very similar.

In cases where they are not, a third problem, A3, may be of significance in defining the transient performance during thermal equilibration.

FIGURE 1. MAIN PROBLEM SPECTRUM

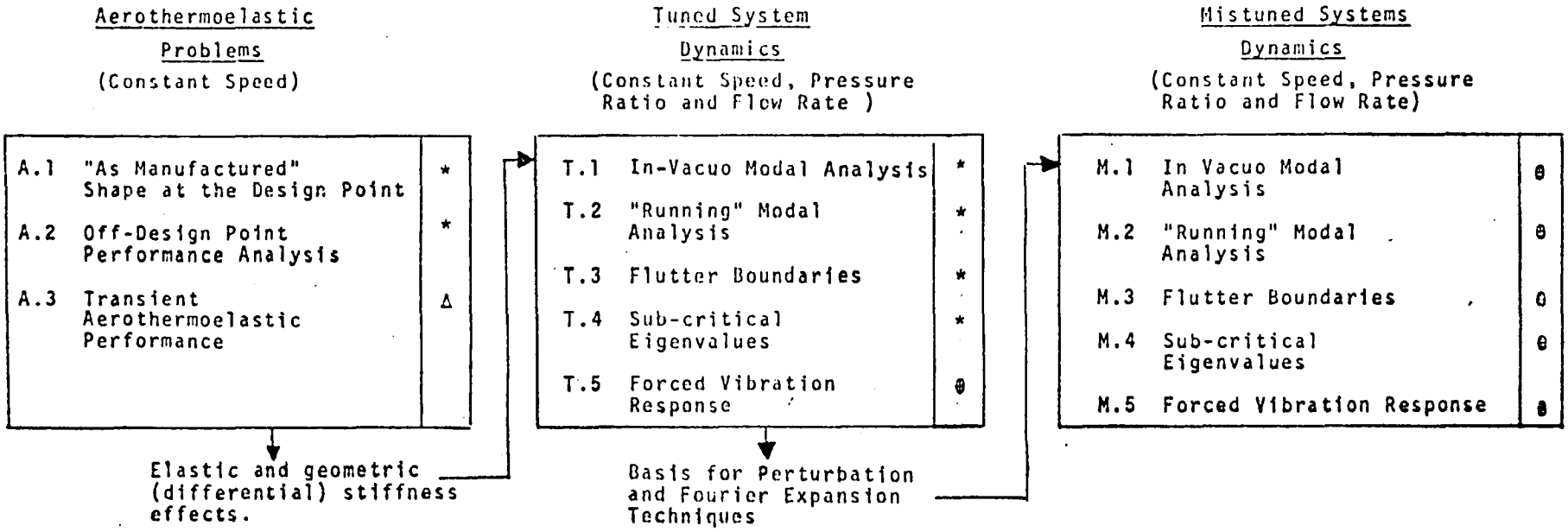

NOTES:

1. After design point A.1, A.2 gives the elastic system "Map" within aerodynamic program limitations
2. T.1, T.2, are functions of selected operating points on the Compressor Map.
3. T.3 uses modes from T.2.
4. T.4 uses harmonic aerodynamics from T.3.
5. T.5 uses complex eigenvalues from T.4.
6. M.1, M.2 use the modal information from T.1, T.2,
7. M.3, M.4 use T.3 harmonic aerodynamics and Fourier expansion techniques. (Cascade theories limit validity)
8. M.5 uses complex eigenvalues from M.4.
9. * - Operational
   θ - Methods Formulated
   Δ - Approach Conceptualized.

This transient aerothermoelastic problem capability is not currently operational and is of uncertain practical significance.

The second major group (T) of subproblems, contains the dynamics problems of perfectly tuned cyclic bladed disc assemblies. Elastic and differential stiffness properties developed from Group A problems are utilized in this group.

The first problem T1, relates to in-vacuo modal analysis requiring the consideration of vibrational inertia terms and centrifugal stiffening effects (the latter from Group A). The second problem, T2, the "running" modal analysis involves a set of "pseudo-modes" and frequencies which form a suitable basis for subsequent problems T3-5. In these "running" modes, the stiffness effects of thermal and differential pressure loads are included in the eigenvalue problem. Unsteady aerodynamic terms are omitted.

The modes from T2 are used as a basis for problem T3, in which unstalled flutter boundaries are determined. This involves the use of existing unsteady cascade theories for the compilation of generalized air forces as a function of reference reduced frequencies, Mach numbers and interblade phase angles. Actual flutter boundary determination involves an interpolation process on output results. The complexity of this process is dependent on the mass ratio of blade to air. For "high mass ratio" compressor stages, little interpolation is necessary since the modal frequencies change little over

the map. Flutter of "low mass ratio" stages (e.g. large high by-pass fans) may resemble wing flutter and require significant interpolation.

A limitation on the validity of most two-dimensional cascade theories must be mentioned here. They are usually developed in terms of spacing, stagger, Mach number, and reduced frequency and interblade phase angle for various chord "modes". These modes generally include rigid body heave and pitch, and flexible chordwise motions. However, the theories generally assume that all chords perform equal amplitudes of motion. This, however, is only true for bladed disc modes of zero circumferential harmonic number. Their use for flutter of modes of non-zero harmonic number is not strictly justified. However, in Appendix E, a plausible argument is given for extending the applicability of current theories in a simple manner to account approximately for non-zero harmonic number. This approximation could be adequate until studies show the necessity or otherwise of formal extensions of the theories.

At subcritical conditions, cascade theories may be used to find subcritical eigenvalues (T4) and define complex aerodynamic transfer functions for use in periodic or random forced vibration problems.

The postulation of external forcing functions and the generalization to the tuned system modes is a prerequisite to the forced vibration response problem T5. For periodic or random forcing,valid subcritical eigenvalue bases may be deduced from T4. For transient forcing, such eigenvalues

are not strictly valid but may be used as a reasonable approximation. (The strictly correct approach, not programmed, is to determine the complete subcritical transfer function in the frequency domain and then use Fourier Integral Transformation and Convolution or Duhamel integral techniques.)

The proper posing, development, solution and understanding of tuned system problems is regarded as a prerequisite to the posing of the same problems for mistuned systems. Any real bladed disc assembly is a "perturbed" tuned assembly. By "perturbed" is meant a state in which the characteristics of individual sections of the real assembly vary by a "small magnitude" from the mean characteristics of all sections. In the mathematical sense, this means that characteristics of the tuned system are a good basis for estimating the characteristics of the mistuned system. Such an approach has very large advantages, some of which are as follows:

- Standard mathematical techniques of spectral analysis and Fourier expansion may be used for structural and aerodynamic features
- Standard cascade aerodynamic theories may be exploited (within limits - see Appendix E)
- Smaller and more economical modal and flutter analyses may be posed
- Possible advantages of specific types of mistuning arrangement can be more easily explored and exploited

from flutter and forced vibration points of view.

With this basis in mind, the third group of subproblems (Group M, that of the dynamics of mistuned systems) is the same as that of the tuned system problems (Group T).

Figure 2-A-C gives a qualitative description of the relationship of tuned problems to mistuned problems of modes, flutter and forced vibration.

The tuned system modes consist of families of distinct harmonic number "k". (The $k = o$ modes are simple, the $k \neq o$ modes are double roots.)

The modal frequencies are asymptotically related to "disc alone" and "blade alone" frequencies as sketched in Figure 2-A. (See Reference 14.) The distribution of a particular aspect of mistuning (e.g. a local blade mass or stiffness coefficient) may itself be expressed as a circumferential harmonic series.

Ewins, (Reference 14) has shown that any component of such a series is capable of splitting the roots of two associated harmonic families of the tuned system. Figure 2-A gives an example of the root splitting of a 30 blade disc by mistuning orders of 2, 4, 6.....14. Each mistuned mode will be closely expressible as some combination of tuned modes of similar frequency. While this is useful explanatory knowledge, it is of limited practical significance because in a real mistuned system, the multiplicity of mistuning aspects (i.e.sector local masses and/or sector local stiffnesses) will all have their own spectral distribution.

a. MODES

TUNED SYSTEMS

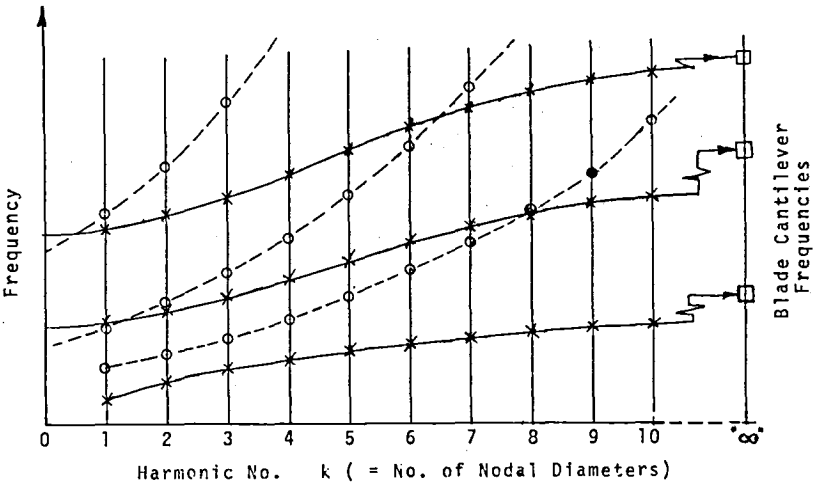

□ Blade alone

o Disc alone

x Bladed Disc

Tuned Bladed Disc

Frequency Spectrum

Harmonic Number $k = o$ Simple Roots

Harmonic Number $k \neq o$ Double Roots

MISTUNED SYSTEMS

Mistuning:

1. Couples modes of similar frequency and different harmonic numbers.
2. Splits double roots ($k \neq o$) into distinct roots.

For modest mistuning, each mode can be described as a vector (or spectrum) of the tuned system modes.

Reference 14 shows cos 2kθ mistunig splits harmonic orders, k and $\frac{N}{2} - k$;

e.g. - 30 bladed disc:

Mistuned Order		cos 2θ	cos 4θ	cos 6θ	cos 8θ	cos 10θ	cos 12θ	cos 14θ
Splits	k = 1	✓						
	2		✓					
	3			✓	- - -			
	7,8						- - -	- - ✓
	13		✓					
	14	✓						

FIGURE 2 QUALITATIVE RELATIONS - TUNED/MISTUNED DYNAMICS

b. FLUTTER & SUBCRITICAL ROOTS

TUNED SYSTEMS

1. Only modes of the same harmonic number can couple to cause flutter.
2. High harmonic number flutter is probably less significant than low harmonic number? (See Appendix E)
3. Current unsteady aero theories (cascade) are valid only for $k = 0$.
4. Current theories are probably reasonable provided $\frac{k}{N} << 1$. (Adjacent blade motions are of approximately the same amplitude.)
5. A plausible approach to extending the use of current theories to general $k \neq 0$ is given in Appendix E.
6. The plausibility of subcritical dampings depends on the proximity of the roots to the flutter boundary.

MISTUNED SYSTEMS

1. Generalized aerodynamic force coupling can only arise from like harmonic components (k) in each mode, i.e. takes the form

$$Q_{ij} = \sum_{\text{Blades}} \sum_{k} \int_{\text{Blade}} z_{ki}\, p_{kj}\, dS$$

Terms from $z_{k_1 i}\, p_{k_2 j} = 0$ by orthogonality.

2. Valid only for harmonic components such that $\frac{k}{N} << 1$. (but see Appendix E)
3. Subsequent flutter solution is of same form as for tuned systems.
4. Should aeros be developed for $k \neq 0$ - see general discussion.

FIGURE 2 - CONTINUED

c. FORCED RESPONSE

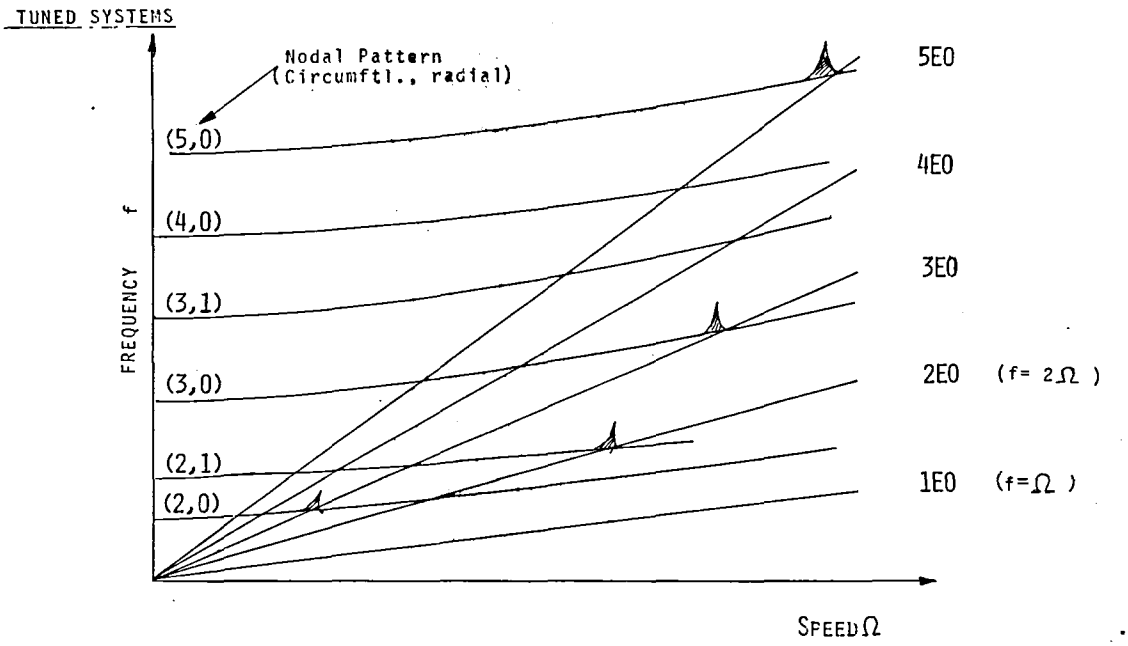

Conventional "Interference Diagram" highlights potential forced vibration occurrence when engine orders and harmonic numbers coincide at the same frequency. Magnitude of response will be conditioned by generalized excitation level and subcritical modal damping.

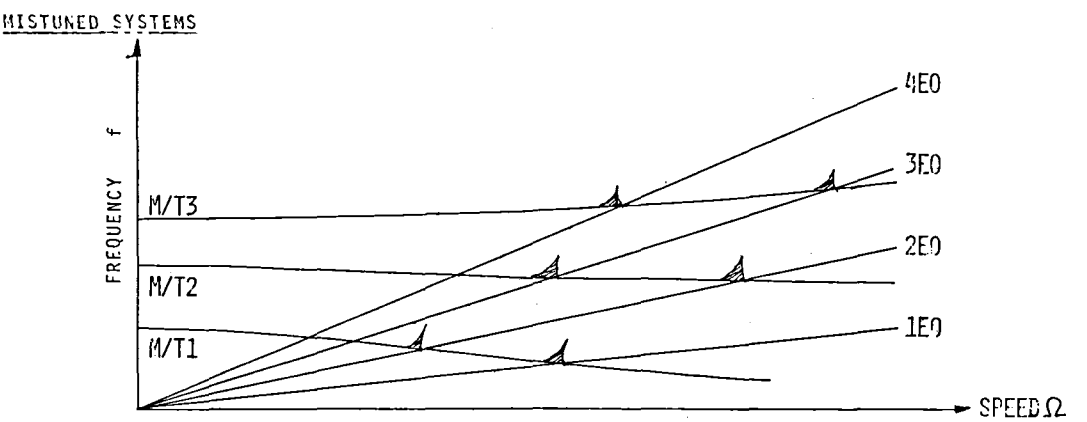

Each speed-dependent mode contains components of various harmonic numbers and, therefore, may be forced by engine order disturbances of more than one number as speed varies.

FIGURE 2 (Concluded)

Thus, in general, all tuned modes will be split by the cumulative effects of the many different mistuning distributions.

Further discussion of the exploitation of these characteristics is reserved for Appendix F , in which the mathematical formulation of the mistuned modal problem is posed.

Thus mistuned modes problems M1 and 2, are developable in terms of tuned mode combinations. The flutter problem for mistuned modes M3 may now exploit generalized aerodynamic forces calculated for tuned system flutter using the superposition principle on the unsteady aerodynamic coefficients for various harmonic numbers. (Limitations on the validity of such non-zero harmonic number aerodynamics were mentioned earlier.) (Figure 2B)

Again, for periodic and random forcing, valid subcritical eigenvalues (M4) may be determined as a basis for forced vibration estimates (M5). Transient forcing response could be approximately determined assuming such subcritical eigenvalues were valid, or much more complex Fourier Integral/Duhamel techniques would have to be developed (as mentioned earlier for tuned systems).

The more complex characteristic of mistuned disc forced vibration is illustrated in Figure 2c. Since each mistuned mode may contain many harmonic orders of motion, any mode may be excited effectively by more than a single engine order of harmonic excitation. (Reference 14.) Again, however, the use of superposition principles are admissible.

In summary, a logical sequence of aeroelastic, and tuned and mistuned dynamics problems, and approaches to their solution has been qualitatively described.

The relation of structural, aerodynamic and program ingredients to NASTRAN is related in the next section.

Program Basis

The essential ingredients for the required capability are:

*o An established finite element structural program capable of modification and expansion

o A steady-state compressor stage analysis program

o Aeroelastic solution algorithms.

o Subsonic and supersonic two-dimensional cascade theories

*o Modal, flutter, and forced vibration algorithms

o A practical "mistuning" problem formulation.

NASTRAN offered the (*) capabilities with the additional advantage of a cyclic structure analysis capability. It was, therefore, proposed and approved as a basis at Level 16, which was the current NASA Lewis operational version.

Reviews of available compressor stage and cascade analysis programs were made (Table 1). (References 19-25.)

	NAME	TYPE	ORIGINATOR	SOURCE	REMARKS/REF.
1.	NASTRAN Level 16	General Purpose Structural Analysis	R. H. MacNeal R. G. Schwendler et.al.	COSMIC	NASA Lewis Level 16. Implemented at Bell Ref. 7.
2.	-	Axial Compressor Design	R. M. Hearsey A. J. Wennerstrom	N.T.I.S.	Reference 19.
3.	MERIDL, TSONIC	Axial Flow Calculations	T. Katsanis W. D. McNally	NASA/Lewis	No Pressures. NASA-TN D-7343 Ref. 20.
4.	ROTOR	Blade Transonic Flow Analysis	J. W. Kurzrock and A. S. Novick	WPAFB & DDAD of G.M.	AFAPL-TR-73-69 V.I&II Ref. 21
5.	JONES MRULE	Unsteady Subsonic 2-D Cascade	B. M. Rao W. P. Jones	Texas A&M U.	Completed concurrently with this work. Ref. 22
6.	UCAS	Unsteady Supersonic 2-D Cascade	J. J. Adamczyk	NASA/Lewis	Completed concurrently with this work. Ref. 23.
7.	-	Unsteady Characteristics	R. A. Delaney P. Kavanogh	D.D.A. of Gen. Motors	Cascade Research Program. Ref. 24. See Trans ASME, July 1976. Volume 98,Series
8.	-	Unsteady Supersonic 2-D Cascade	J. M. Verdon	P & W	AIAA Journal, V. 12, No. 2, Feb. 1975. Ref. 25.

Table 1. Extant Technology Programs

In attempting to select suitable approaches/programs it became obvious that a number of candidates in the literature were of a proprietary nature, others suffered from inadequate documentation problems or were likely to be incompatible with the constraints imposed. Those finally selected and approved were Reference 19 for steady aerodynamics and References 22 and 23 respectively for unsteady subsonic and supersonic cascade aerodynamics.

General literature reviews of tuned and mistuned system dynamics were conducted (References 8-18.) No Satisfactory general development for mistuned problems existed. It was, therefore, developed and is described both quantitatively and in detail in Appendix F.

Finally, a mesh generation capability suitable for interfacing with the front of the program was selected from the "Analytic Meanline Section" of the program of Reference 19.

The basic structure of the overall program was now definable in terms of these elements and the problem spectrum previously described.

The general features are indicated in Figure 3. Blade mesh generation and steady state analysis are abstracted from Reference 19. When these capabilities are combined with the NASTRAN Rigid Format No. 4,"Statics with Differential Stiffness", a modified Rigid Format to conduct aeroelastic design and analysis is constructed. This contributes a differential stiffness matrix to the NASTRAN cyclic modal analysis capability, which becomes part of a second Rigid Format covering Modes & Flutter. The two cascade theories are

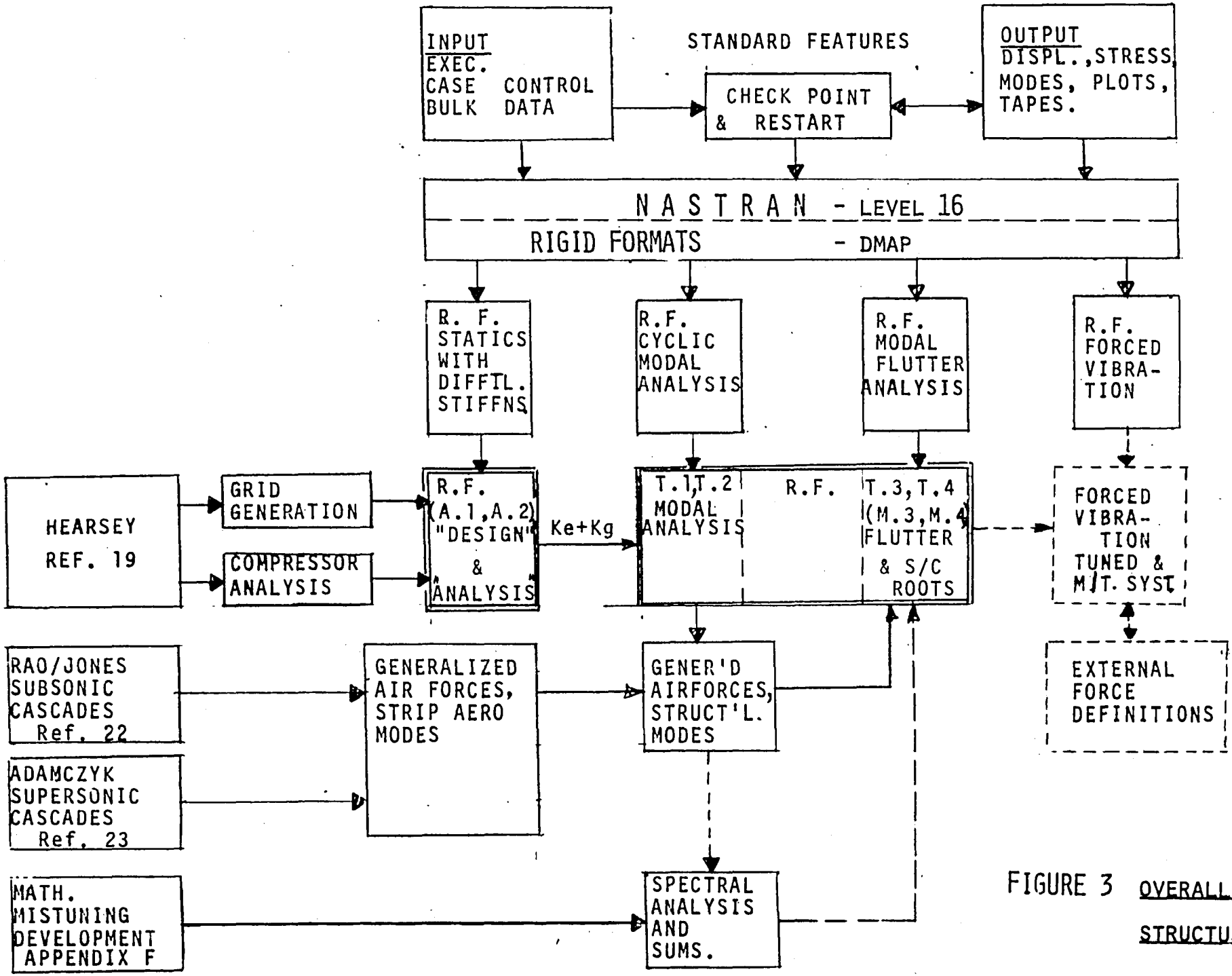

FIGURE 3 OVERALL PROGRAM STRUCTURE

used to determine chordwise "Strip Theory" generalized matrices for heave, pitch and Fourier series modes. These are transformed appropriately at each spanwise station to local mode chordwise forces which are then integrated spanwise for structural mode generalized aerodynamic forces. The tuned flutter problem is now formulated and solved using modifications to the existing NASTRAN Flutter Rigid Format.

External to this Rigid Format, subcritical modes can be used with suitably developed generalized forcing functions in the existing NASTRAN forced vibration Rigid Format.

Mathematical development of mistuned system modes is presented in Appendix F based on tuned mode expansions of different harmonic numbers. Appropriate quadratic transformations of tuned system mode unsteady aerodynamics may then be used to determine generalized forces for mistuned flutter calculations. These can use the same algorithm used for tuned flutter. Similarly, external forces generalized for tuned modes can be transformed for mistuned modes and the forced vibration problem similarly attacked.

It will be recalled that aeroelastic analysis and tuned dynamics are all operational, transient aeroelastic in abeyance, and mistuned dynamics generally developed but not programmed.

With respect to the guidelines listed earlier, the following observations are made:

- A more sophisticated steady analysis program than cascade theory has been incorporated.
- The required ranges of input and output options and loading and boundary conditions are accommodated.

- All necessary mistuning analyses have been developed.
- A plausible approach to using current cascade theories for non-zero harmonic modes and mistuned dynamics has been proposed.
- Documentation and demonstration have been accomplished.

TUNED SYSTEMS

General

Bladed discs of axial flow compressors and turbines in which geometry, mass, stiffness and damping properties repeat exactly from representative sector to sector are defined as tuned systems. The problem/solution formulation for the static and dynamic (natural and forced) response of these tuned structures is greatly simplified by this "cyclic symmetry" (see Appendix B), from both aspects of finite element idealization and computational efforts.

As discussed previously, the solution of tuned system problems forms a good basis for the solution and understanding of similar problems of real (mistuned) systems.
The discussion that follows is devoted to the problems of tuned bladed discs, and deals specifically with;

1. Static aerothermoelastic 'design/analysis' of compressors
2. Cyclic normal modes analysis of compressors and turbines
3. Flutter and subcritical roots analysis of compressors and turbines
4. Forced vibration analysis of compressor and turbines, and
5. Transient aerothermoelastic analysis of compressors.

Static Aerothermoelastic Design/Analysis

The bladed discs of axial flow compressors, under steady operating conditions, are subjected to centrifugal, thermal and aerodynamic loads. These loads depend on the operating conditions and the shape of the bladed disc, and cause deformation of the elastic structure. This interdependence of geometry and loads defines a (non-linear) problem of determining the equilibrium deformation and operating conditions of the flexible bladed disc.

Two distinct problems can be stated:

1. The problem of arriving at an "as manufactured" blade shape to produce a desired, design pressure ratio at given design point flow rate and rotational speed. This will be called the 'design' problem. (It is not strictly "well-posed".)

2. The subsequent problem of analyzing the performance of the "as manufactured" geometry at off-design operating conditions of flow rate and speed. This will be called the 'analysis' problem.

An operating point on a compressor map defines a distribution of centrifugal and aerodynamic pressure and temperature loads on the bladed disc. Under the action of these non-aerodynamic and aerodynamic loads, an iterative approach to the bladed disc 'design' and 'analysis' problems can be expressed by

$$[K^e + i_1 K^d(u)]\{u\} = \{P^{NA}\} + \{P^A(u)\}, \qquad (1)$$

where $i_1 = \mp 1$ represents the 'design' and 'analysis' problems respectively.

The non-linear dependence of aerodynamic loads $\{P^A\}$ and differential stiffness $[K^d]$ on the elastic deformation in equation (1) requires an iterative solution procedure with the differential stiffness matrix $[K^d]$ and the aerodynamic load vector $\{P^A\}$ being redefined as functions of the preceding solution step.

A solution procedure closest to the one required has been the basis of the NASTRAN Level 16 Displacement Approach Rigid Format 4, "Static Analysis with Differential Stiffness" (Ref. 7), with the express limitations being,

$$\begin{aligned} &1. \quad i_1 \equiv +1, \text{ and} \\ &2. \quad \{P^A(u)\} \equiv \{0\} \end{aligned} \tag{2}$$

These limitations have been removed in designing and developing a new Displacement Approach Rigid Format 16 (see Section 3.21, Ref. 27). A user-determined parameter (SIGN) has been defined based on the value of i_1, thus selecting the 'design' or 'analysis' problem.

The computation of the aerodynamic pressure and temperature loads has been accomplished by adapting and implementing the computer code of Reference 19 in the NASTRAN Functional Module ALG. A detailed description of the module ALG is given in Section 4.149 of Reference 28, while aerodynamic data pertaining to the blade geometry and operating conditions for the generation of airloads are described in Section 1.15 of Reference 27.

The overall (and simplified) solution flow for both 'design' and 'analysis' problems is outlined in Figure 4 while the salient steps in the associated algorithm are shown in Figure 5.

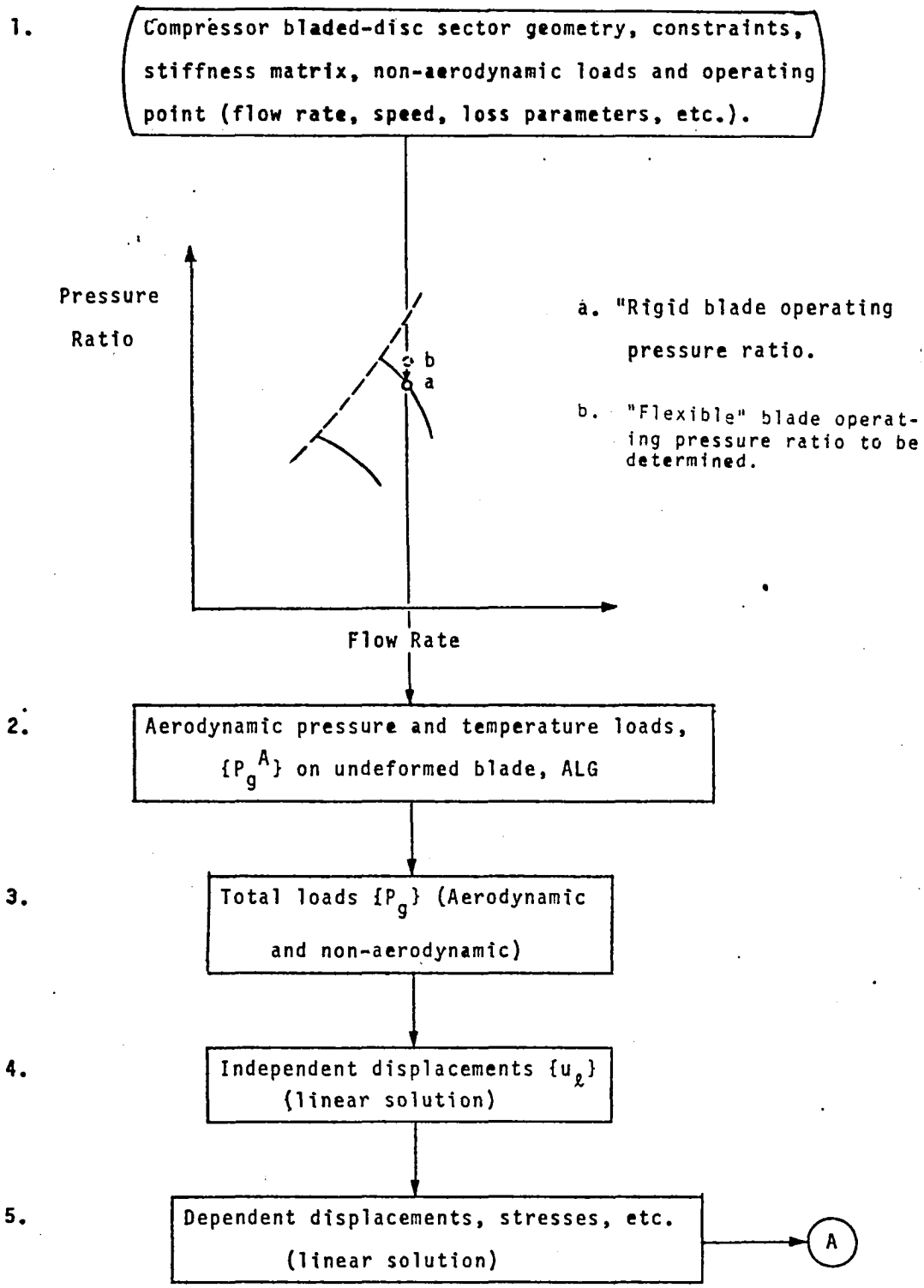

Figure 4. Simplified Solution Flow for Static Aerothermoelastic "Design/Analysis" Rigid Format for Axial Flow Compressors including Differential Stiffness Effects. (continued)

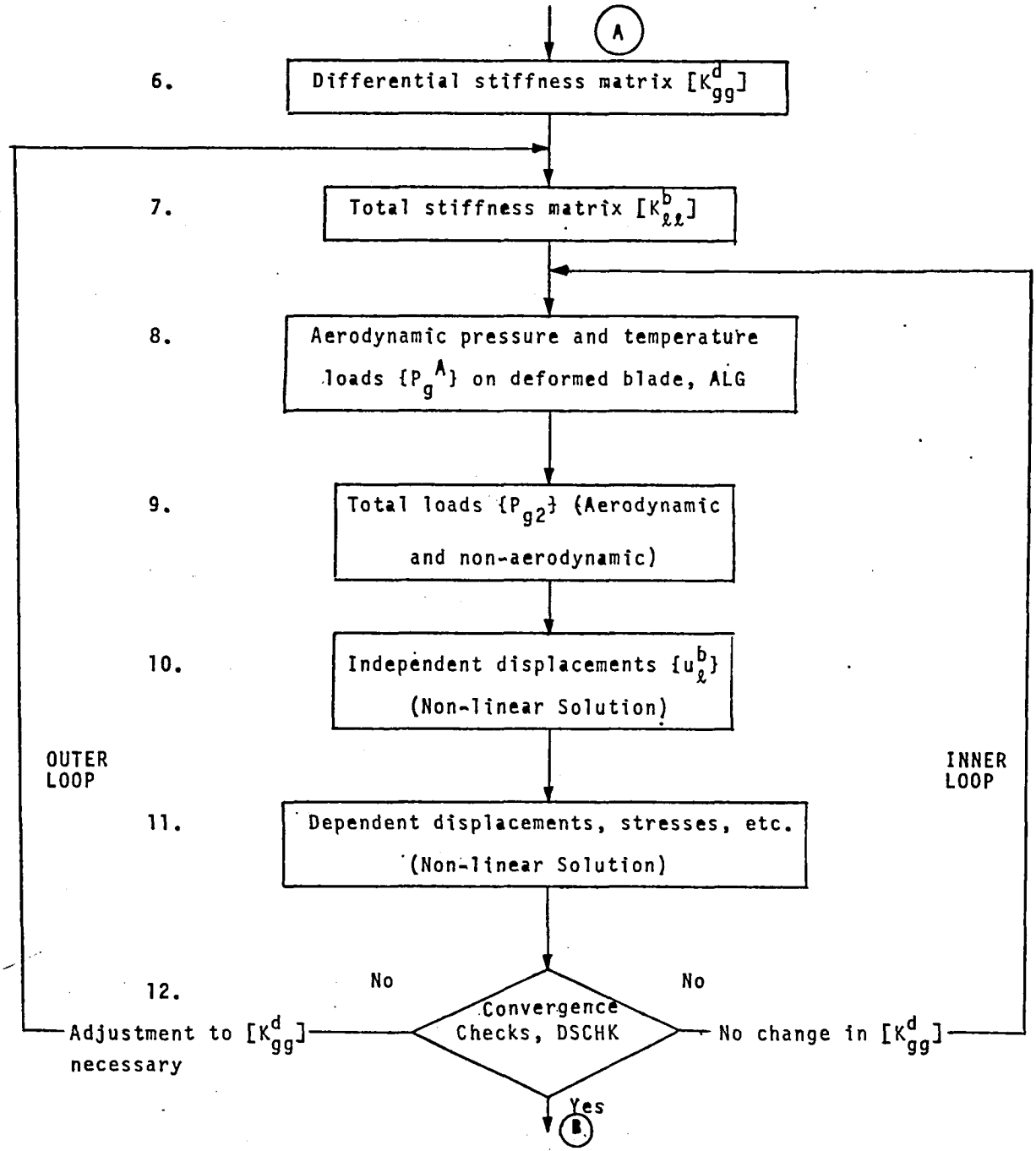

Figure 4. Simplified Solution Flow for Static Aerothermoelastic "Design/Analysis" Rigid Format for Axial Flow Compressors including Differential Stiffness Effects. (continued)

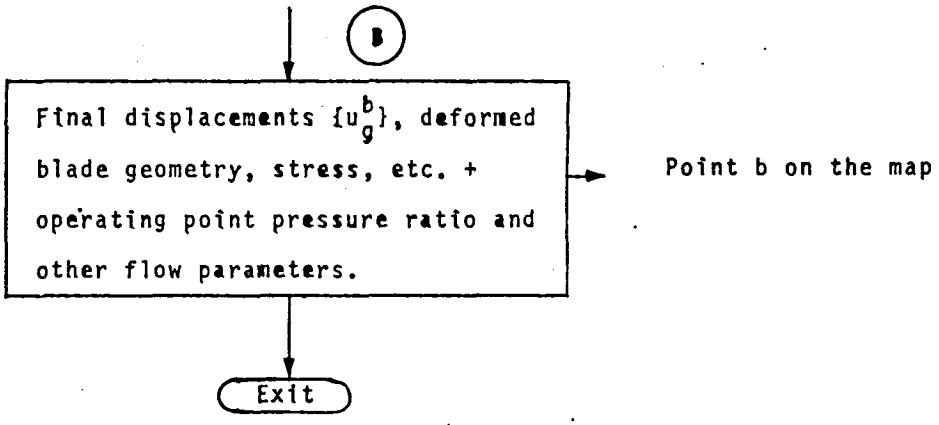

Figure 4. Simplified Solution Algorithm for Static Aerothermoelastic "Design/Analysis" Rigid Format for Axial Flow Compressors including Differential Stiffness Effects. (concluded)

1. Enter, after the application of constraints and partitioning to the stiffness matrix and the generation and transformation of the non-aerodynamic load vectors (centrifugal, etc.), with K_{aa}, P_g^{NA}, G_m, G_o, etc.

2. $\{P_g^A\} \leftarrow$ (ALG) $\leftarrow$ Undeformed blade geometry + operating point (flow rate, speed, loss parameters, etc.)

   Aerodynamic Load Generator (pressure and temperature)

3. $\{P_g\} = \{P_g^{NA}\} + \{P_g^A\}$

   $\{P_\ell\} \xleftarrow[\text{partition}]{\text{constrain}} \{P_g\}$

4. $\{u_\ell\} = [K_{aa}]^{-1} \{P_\ell\}$

5. $\{u_g\} \xleftarrow{\text{recover}} \{u_\ell\}$
   $[G_m]$, $[G_o]$, etc.

6. $[K_{gg}^d] \xleftarrow{\text{generate}} [K_{gg}^d (\{u_g\})]$

   $\{P_g\} = \{P_g^{NA}\}$ ——— (A) OUTER LOOP begins

   $\{P_{g1}\} = \{P_g\}$

   $[K_{aa}^d] \xleftarrow[\text{partition}]{\text{constrain}} [K_{gg}^d]$

7. $[K_{\ell\ell}^b] = [K_{aa}] \pm [K_{aa}^d]$, (+) for "analysi" mode of the rigid format
   (-) for "design" mode of the rigid format

   $\{P_{go}\} = \{P_{g1}\} + \{o\}$

   $\{u_g^A\} = \{u_g\}$

Figure 5. Simplified Solution Algorithm for Static Aerothermoelastic "Desing/Analysis" Rigid Format for Axial Flow Compressors including Differential Stiffness Effects. (continued)

(B) Inner Loop begins

8. $\{P_g^A\}$ ← (ALG) ← Deformed blade geometry, revised with $\{u_g^A\}$, + operating point.

9. $\{P_{g2}\} = \{P_{g1}\} + \{P_g^A\}$

$\{P_\ell^b\} \xleftarrow[\text{partition}]{\text{constrain}} \{P_{g2}\}$

10. $\{u_\ell^b\} = [K_{\ell\ell}^b]^{-1} \{P_\ell^b\}$

11. $\{u_g^b\} \xleftarrow{\text{recover}} \{u_\ell^b\}$
$[G_m]$, $[G_o]$, etc.

$\{u_g^A\} = \{u_g^b\}$

$\{u_g^d\} = \{u_g\} - \{u_g^b\}$

$[\delta K_{gg}^d] \xleftarrow{\text{generate}} [\delta K_{gg}^d (\{u_g^d\})]$

$\{P_{gI1}\} = [\delta K_{gg}^d] \{u_g^b\} + \{P_{go}\}$

$\{P_{gI2}\} = \{P_{gI1}\} + \{P_g^A\}$

12. Convergence checks ← (DSCHK) ← $\{P_{g2}\}$, $\{P_{gI2}\}$, $\{u_g^b\}$

Differential Stiffness Checks

1. $\varepsilon \leq \varepsilon_o$:

Exit with

a. $\{u_g^b\}$, stresses, etc.

Figure 5. Simplified Solution Algorithm for Static Aerothermoelastic "Design/Analysis" Rigid Format for Axial Flow Compressors including Differential Stiffness Effects. (continued)

b. Final deformed blade geometry → ALG → $\{P_g^A\}$ + operating pressure ratio and other flow parameters.
+ operating point (flow rate, speed, loss parameters, etc.).

OR 2. $\varepsilon > \varepsilon_o$ and adjustment to K_{gg}^d not necessary.

Shift to the beginning of Inner Loop with

a. $\{P_{g1}\} = \{P_{gI1}\}$ ——— To B

OR 3. $\varepsilon > \varepsilon_o$ and adjustment to K_{gg}^d necessary.

Shift to the beginning of Outer Loop with

a. $\{u_g\} = \{u_g^b\}$

b. $[K_{gg}^d] = [K_{gg}^d] - [\delta K_{gg}^d]$ ——— To A

Figure 5. Simplified Solution Algorithm for Static Aerothermoelastic "Design/Analysis" Rigid Format for Axial Flow Compressors including Differential Stiffness Effects. (concluded)

Solution flow (Figure 4) involves the following steps:

1. The geometry of the compressor bladed-disc sector, its material properties and the applied constraints are used to generate and partition the elastic stiffness matrix. Non-aerodynamic load vectors are formed and operating point flow rate, speed, loss parameters, etc. are selected.

2. Based on the undeformed blade geometry and the operating point aerodynamic parameters, the functional module ALG generates the aerodynamic load vector.

3. Total loads are defined as a combination of aerodynamic and non-aerodynamic loads.

4. A linear solution for independent displacements is obtained based on the elastic stiffness and the total loads.

5. Omitted and constrained displacements are recovered, and stresses, reactions, etc., are obtained.

6. A differential stiffness matrix is derived as a function of the grid point displacements.

7. A total stiffness matrix is now defined as a sum (or difference) of the elastic and geometric (differential) stiffness matrices for the 'analysis' (or 'design) problem.

8. The linear displacements obtained earlier are used to revise the blade geometry and a revised aerodynamic load vector is obtained.

9. Again, the aerodynamic and non-aerodynamic load vectors are combined to define the total load vector.

10. A non-linear solution for independent displacements is obtained based on the total stiffness and the total loads.

11. Dependent displacements are obtained and data such as stresses, reactions, etc., are recovered.

12. Convergence of the solution is based on the parameter ε defined by

$$\varepsilon = \frac{u_g^b \{P_{gI2} - P_{g2}\}}{u_g^b \{P_{g2}\}} \leq \varepsilon_o \qquad (3)$$

Upon convergence, the final displacements, loads, and deformed blade geometry, etc., are output. Otherwise, further iterations are performed.

A decision to update the differential stiffness matrix requires a shift to the outer loop. Only the load vector is revised in the inner loop iterations.

13. The final pass, upon convergence, through the functional module ALG yields the "flexible" operating point pressure ratio (among other aerodynamic data), which can be relocated on the compressor map.

In the solution algorithm (Figure 5), based on the updated blade geometry, the aerodynamic loads are computed before, within, and after the differential stiffness loops. The revision of the blade geometry, necessitated by the elastic deformations due to applied loads, is carried out by updating a selected set of variables that form a list of partial aerodynamic input used to define the blade geometry. The variables and their revisions are described in Appendix D.

It should be noted that the 'design' problem is defined only at the design operating point of the compressor. It is

a two-step procedure in that having 'designed' the blade shape, i.e., the 'as manufactured' shape, it should be 'analyzed' at the same operating point to confirm the design point pressure ratio. The 'analysis' problem is a one-step procedure. The 'designed' blade is 'analyzed' at selected operating points over the compressor map, one at a time, to generate the 'flexible' performance characteristics of the compressor.

For very stiff compressors, the difference in the 'rigid' and the 'flexible' performances and the contributions of the differential stiffness matrix to the total stiffness matrix may not be appreciable. However, for low pressure ratio high flow rate machines such as high bypass fans the aeroelastic effects are important enough to alter the performance significantly. The differential stiffness may also significantly affect the natural frequencies (and mode shapes) and, hence, the forced response of such flexible structures. Accordingly, provision has been made in the new Rigid Format 16 to save the total stiffness matrix, including the differential stiffness matrix, for subsequent use in dynamic analyses.

Examples illustrating the 'design/analysis' problem and the solution using the newly developed capability are presented and the results discussed in a later section.

Cyclic Modal Analysis

The normal modes of cyclically symmetric structures are grouped into harmonic subsets of uncoupled modes. The tuned bladed discs of turbomachines, due to their cyclic symmetry, exhibit such modal characteristics. The normal modes analysis of such structures is discussed in Section 4.5 of Reference 7, and hence, only a summary of cyclic modal analysis, with emphasis on specific application to bladed discs, is presented here.

The degrees of freedom in any cyclic segment n of the bladed disc, Figure 6 , may be expanded in a finite Fourier series as

$$\{u\}^n = \{\bar{u}\}^0 + \sum_{k=1}^{k_L} \{\bar{u}\}^{kc} \cos\left(\overline{n-1}\, ka\right) + \{\bar{u}\}^{ks} \sin\left(\overline{n-1}\, ka\right) + (-1)^{n-1} \bar{u}^{N/2} \quad (4)$$

These degrees of freedom can be further classified as being either <u>within</u> the cyclic sector boundaries, or <u>on</u> the boundaries. The displacements on the two sides of the sector are related, in pairs, by the intersegment continuity/compatibility conditions. An independent set of degrees of freedom $\{\bar{u}\}^K$, is, therefore, defined which, for a given harmonic number analysis, consists of both the cosine and the sine symmetric components, $\{\bar{u}\}$, of the internal and the "side 1-only" degrees of freedom in the sector. The equations of motion in terms of the $\{\bar{u}\}^K$ set are derived in Appendix B. The cyclic modal analysis problem of the bladed disc is then addressed via the real eigenvalue problem,

$$\left[-\omega^2 [\bar{M}]^K + [\bar{K}]^K\right] \{\bar{u}\}^K = \{0\} \quad (5)$$

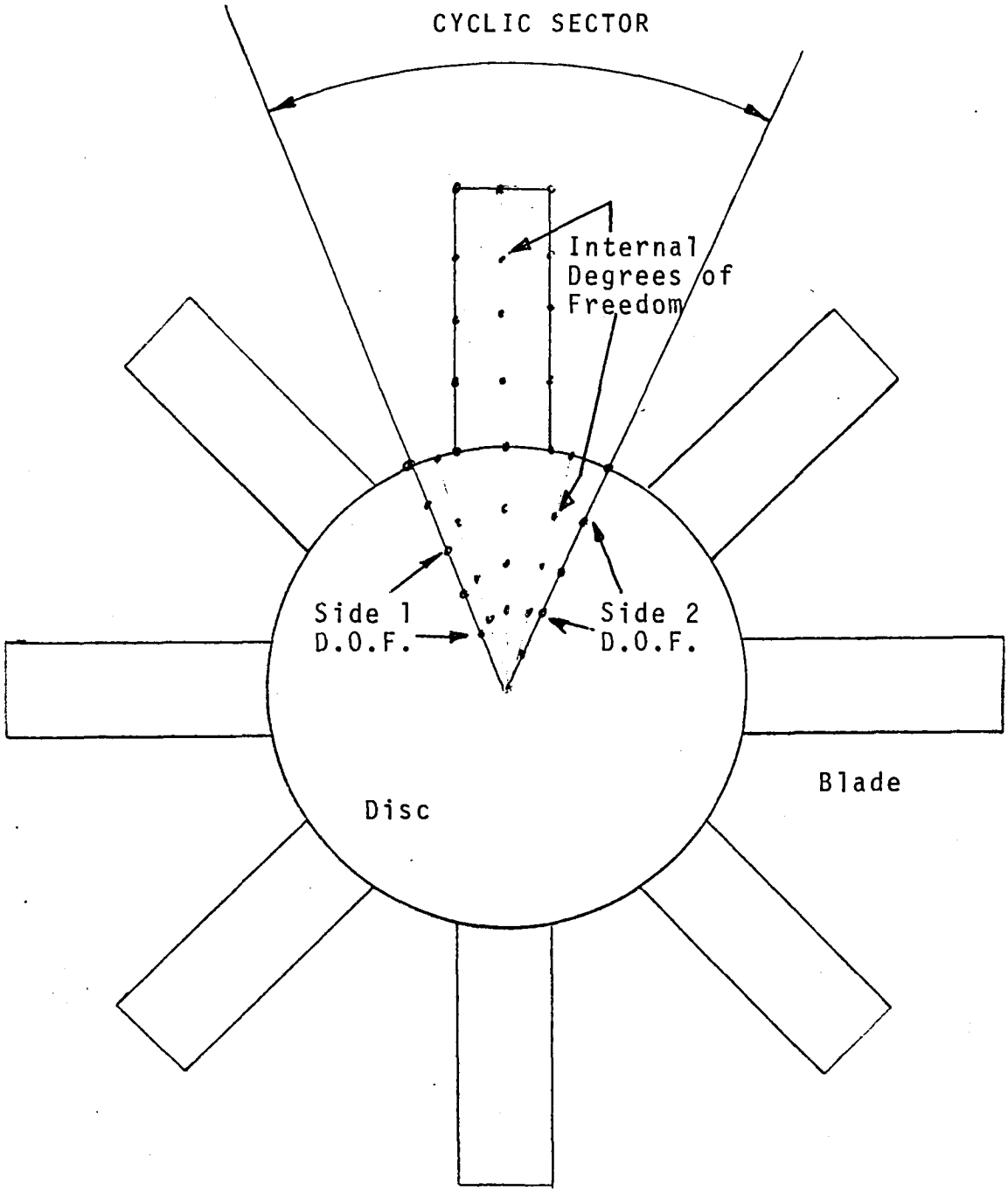

FIGURE 6: CYCLIC SECTOR -INTERNAL AND BOUNDARY FREEDOMS

where the mass $[\bar{M}]^K$ and the stiffness $[\bar{K}]^K$ matrices are as defined in Appendix B. For non-zero harmonic numbers, repeated eigenvalues of multiplicity two are obtained, and the corresponding mode shapes expressed by the cosine and the sine modal matrices, $[\bar{\phi}]^{kc}$, and $[\bar{\phi}]^{ks}$ (see Appendix B).

The modal columns of $[\bar{\phi}]^{kc}$, and $[\bar{\phi}]^{ks}$ are self and jointly orthogonal and can be combined to describe the 'physical' mode shape of any segment n in the k^{th} harmonic motion as

$$[\bar{\phi}]^n = [\bar{\phi}]^{kc} \cos(\overline{n-1}\, ka) + [\bar{\phi}]^{ks} \sin(\overline{n-1}\, ka) \qquad (6)$$

The bladed disc of a turbomachine normally operates under significant centrifugal and aerodynamic pressure and thermal loads. The total stiffness of such structures, including the elastic and geometric stiffness, therefore, changes with the operating point. A more representative set of modal characteristics is, therefore, obtained with the inclusion of the differential stiffness (based on the operating point loads) in the cyclic modal analysis of the bladed discs.

In the present development, this is accomplished by saving the (operating point) total stiffness matrix at the end of a static aerothermoelastic analysis.
The saved stiffness matrix is used in the cyclic modal analysis of the bladed disc at the same operating point.

The effects of the (operating point dependent) differential stiffness on the natural frequencies and mode shapes of a very stiff, high pressure ratio compressor or turbine disc may not be

appreciable. However, they do assume significance in the case of flexible, low pressure ratio, high-flow bypass fans.

Cyclic Flutter Analyses

The problem of determining the complete, unstalled flutter boundaries of a cyclically symmetric compressor or turbine bladed disc involves each member set of the series of harmonic families of its modes, and the effects of permissible interblade phase angle, over an adequate set of operating points (flow rates, speeds, pressure ratios, implied Mach numbers, etc.) of the performance map. In view of the large number of variables influencing the definition of the flutter boundaries, a thorough parametric study requires a systematic effective solution procedure.

A capability, therefore, has been introduced in NASTRAN which, with repeated exercises over the range of variables involved, will enable determination of the flutter boundaries. The existing features of NASTRAN for Normal Modes Analysis using Cyclic Symmetry (Section 3.16, Reference 7) and Modal Flutter Analysis (Section 3.20, Reference 7) have been suitably combined for the cyclic modal, flutter and subcritical roots analyses in a new Rigid Format 9, Approach AERØ. Provision is also made to include the differential stiffness effects by using the total stiffness matrix saved from the Static Aero-thermoelastic Analysis.

In a compressor or turbine, an operating point implies an equilibrium of flow properties such as density, velocity, Mach number, flow angle, etc., that vary across the blade span. Blade properties such as the blade angle, stagger angle, chord, etc., also, in general, change from the blade root to the tip. The resulting spanwise variation in the local reduced frequency and the relative Mach number must be accounted for in estimating the chordwise generalized aerodynamic forces per unit span at each streamline. Integration of these forces over the blade span yields the blade generalized aerodynamic force matrix. Since the relative Mach number varies along the blade span, two two-dimensional, linearized, harmonic cascade theories (Ref. 22 & 23) one each for subsonic and supersonic flow have been implemented in a strip theory manner along the blade span. The chordwise aerodynamic matrices for streamlines with transonic inflow are derived by linear interpolation between those on adjacent (subsonic and supersonic) streamlines.

The generation of the generalized air force matrices is an expensive operation and should be judiciously controlled. In the present development, the aerodynamic matrices are computed at a few reduced frequencies and interblade phase angles, and interpolated for others. Additionally, the chordwise generalized air force matrices are first computed for "aerodynamic modes" (see Appendix A). The matrices for chordwise structural modes are then determined from bilinear transformations along each streamline prior to the spanwise integration to obtain the complete blade generalized aerodynamic matrix. This permits

a change in the structural mode shapes of the same or a different harmonic number to be included in the flutter analysis without having to recompute the modal aerodynamic matrices for aerodynamic modes.

The following remarks apply to the simplified problem flow shown in Figure 7. In this figure, a compressor bladed disc performance map is shown, although the analysis is equally applicable to both compressors and turbines.

1. The geometry and the material properties of the bladed disc sector are defined along with the applicable constraints. An operating point is selected near the expected location of the flutter boundary. The solution procedure examines if this operating point is a flutter point.

2. Flutter parameters such as densities, interblade phase angles and reduced frequencies are selected.

3. The chosen operating point implies a certain spanwise variation of blade and flow properties.

4. A harmonic number is selected for the cyclic modal analysis. Grid point mass and stiffness matrices are generated. The stiffness matrix saved from a previous Static Aerothermoelastic Analysis can be used instead, and would include the differential stiffness effects at the steady state operating point under consideration.

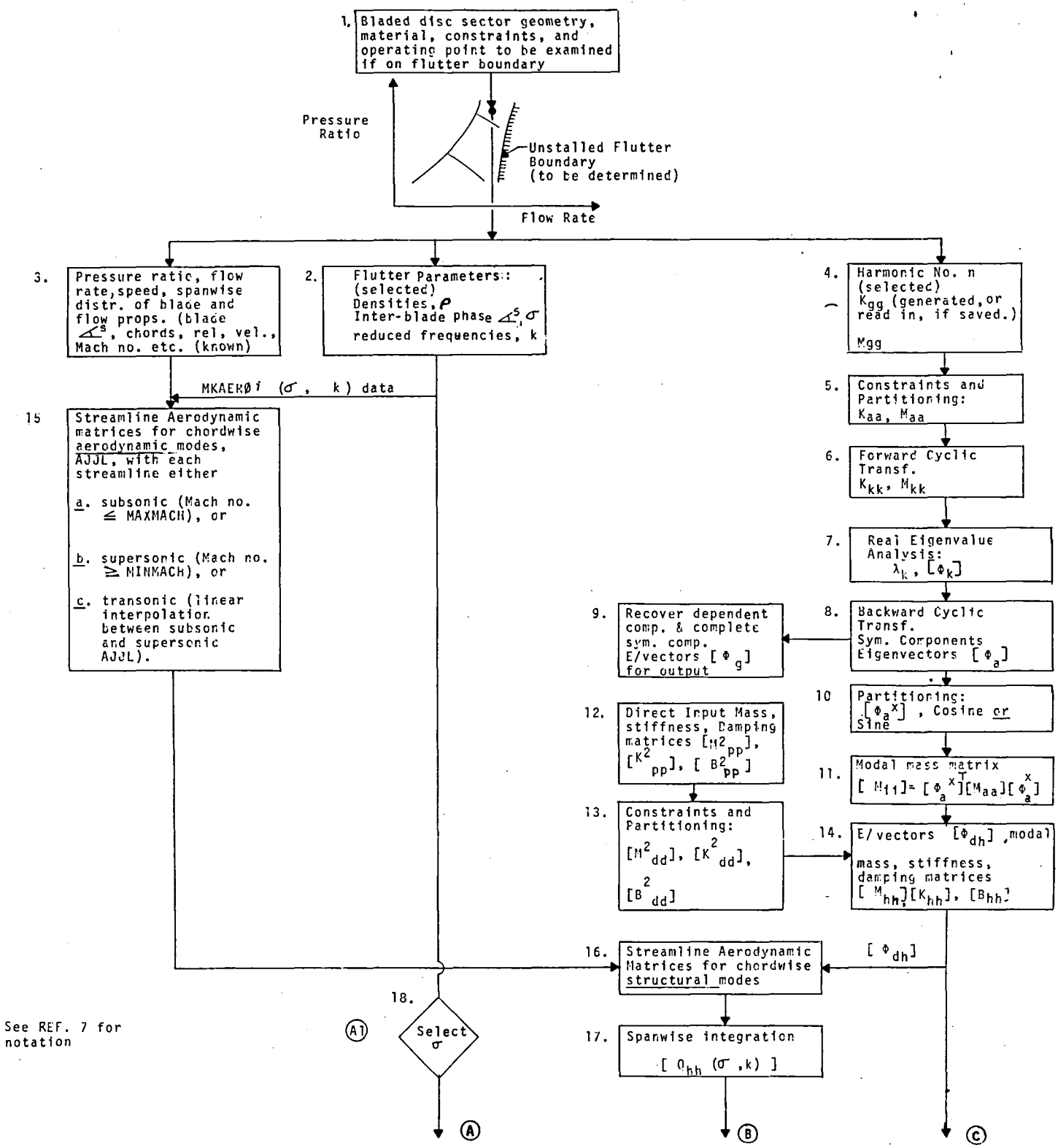

FIGURE 7 SIMPLIFIED PROBLEM FLOW: CYCLIC MODAL FLUTTER ANALYSIS OF BLADED DISCS (continued).

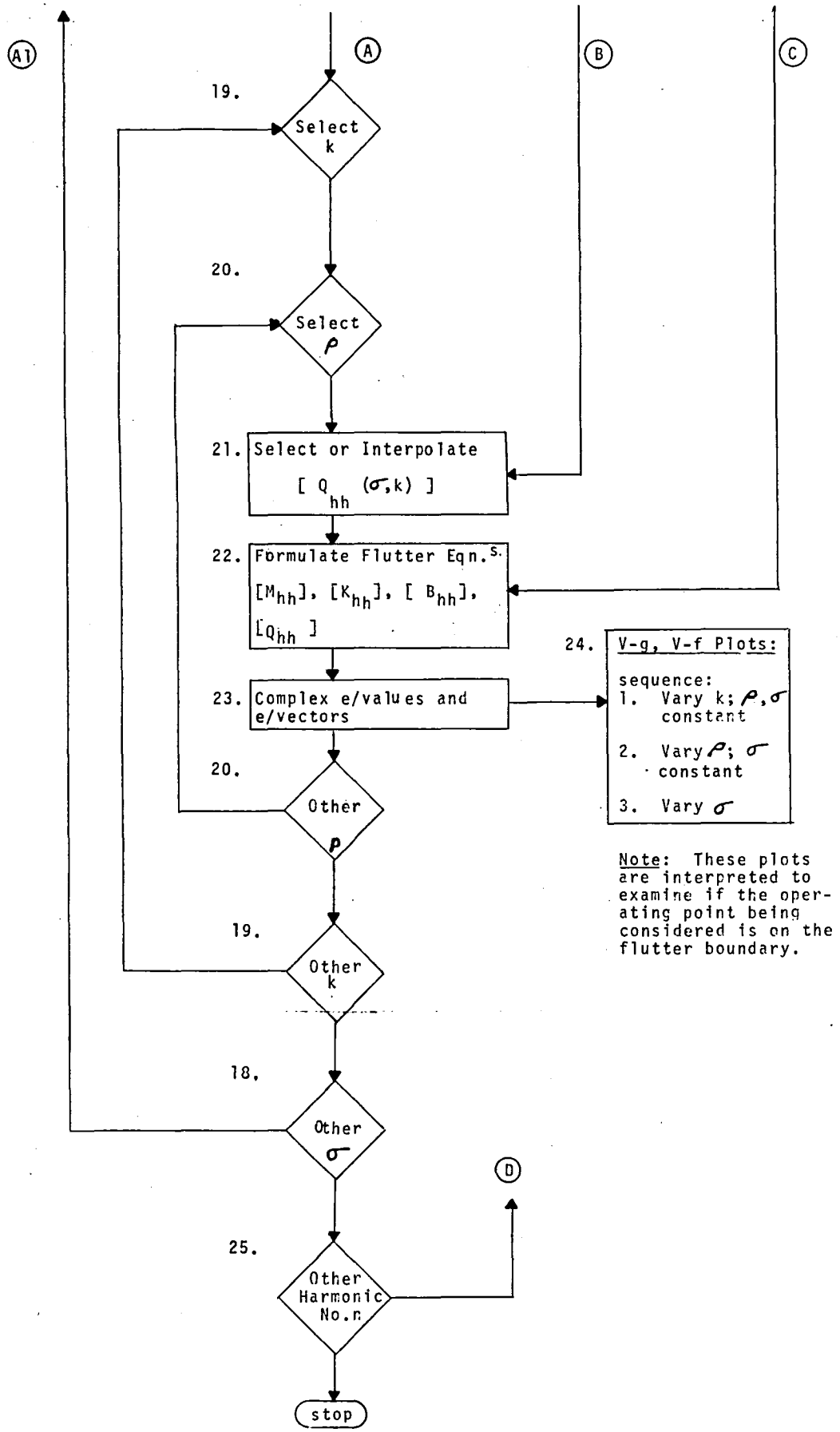

FIGURE 7. SIMPLIFIED PROBLEM FLOW: CYCLIC MODAL FLUTTER ANALYSIS OF BLADED DISCS (CONCLUDED).

5. Constraints and partitioning yield the analysis set mass and stiffness matrices.

6. Forward cyclic transformation results in the solution set mass and stiffness matrices for the cyclic eigenvalue problem.

7. Eigenvalues and eigenvectors in the solution set are obtained.

8. Symmetric components eigenvectors are derived by a backward cyclic transformation.

9. Symmetric components eigenvectors are augmented by recovering the dependent components, and are prepared for output if desired.

10. For a non-zero harmonic number, the symmetric component eigenvectors are partitioned to separate the cosine and sine components.

11. Based on the number of modes selected for flutter analysis the modal mass matrix is computed.

12,13. Direct input mass, stiffness and damping matrices, if necessary, and the constraints thereon define these matrices for further analysis.

14. The augmented eigenvectors, including any extra (or scalar) points introduced for dynamic analysis, are formed and used to define the new generalized mass, stiffness and

damping matrices.

15. The streamline generalized aerodynamic matrices for chordwise aerodynamic modes are generated. The variation of the relative Mach number from streamline to streamline dictates the use of either of the subsonic and supersonic harmonic cascade theories. Such matrices for the streamlines with transonic inflow are interpolated. No transonic flow theory has been currently included.

16. The structural modes are introduced via bilinear transformations along each streamline to define the chordwise generalized air force matrices.

17. The blade generalized aerodynamic matrix is derived by a spanwise integration of the chordwise aerodynamic matrices for structural modes.

18 - 20. The analysis loops through the user-selected combinations of density, interblade phase angle and reduced frequency.

21. Based on the (σ,k) combination, the appropriate blade aerodynamic matrix is chosen for the flutter equation. Linear or surface interpolation, at user's option, is used if necessary.

22. The generalized mass, stiffness and damping matrices of Step 14 and the generalized air force matrix of Step 21 are used to define the modal flutter equations.

23. The solution to the flutter equations is sought in the form of complex eigenvalues and eigenvectors.

24. The velocity-damping and velocity-frequency curves output for each (ρ,σ,k) group are interpreted to identify flutter points.

25. Based on the relative stiffnesses of the blade and the hub of the bladed disc sector, a series of harmonic numbers are investigated before arriving at the flutter boundaries. Presently, the solution rigid format is designed to accept one harmonic number at a time.

Forced Vibration Response

Having solved for the complex eigenvalues of the dynamic system at some stable operating point, the forced vibration equations of motion may be expressed as

$$M\ddot{\xi} + D\dot{\xi} + K\xi = F(t) \tag{7}$$

where the D matrix represents some form of assumed structural damping.

A complete formulation of the solution approach will depend on the source of F(t) which could arise from

- Specified distributed pressures on the blade and disc
- Specified inflow velocity perturbations
- Mechanical forcing of the disc by specified forces or displacements.

In addition, the form of any of these sources may be

- transient
- periodic
- random (and here assumed stationary and ergodic)

The solutions of the equations for all such forms of input are well established and commonly practiced in such areas as aircraft gust response and are outlined in Table 2. See for example Ref. 30.

The most significant additional requirement to current computations is the need for the "sinusoidal" gust function over the complete range of "gust" reduced frequency, or the equivalent

"Kussner function"for the step gust transient induced aerodynamics for subsonic and supersonic cascades. Such a capability already exists in the UCAS subroutine, but not in the CASCADES subroutine. The latter would have to be extended.

Some related solution algorithms for the transient problem exist in NASTRAN Level 17.5 although when indicial effects are present the current capabilities are somewhat limited. The Fourier Transform approach, an alternative to direct numerical integration, is also available with limitations in Level 17.5.

Although equation forms and solution approaches are well formulated, specific sources of excitation must be put into appropriate form. No programming for forced vibration has so far been incorporated.

TABLE 2. EQUATION FORMULATION - FORCED RESPONSE

Nature \ Source	Pressure (space, t)	Velocities (space, t)	Forces or Displacements as f(space, time)	Solution Technique
Periodic	p(t) is weighted with mode shapes. Response is periodic so that complex subcritical roots are valid.	Appropriate Harmonic "Gust" Functions are weighted with mode shapes. Otherwise, same as pressure source.	Forces - same as pressures Displacements - must derive equivalent forces, then generalize similarly.	Periodic Output is product of Transfer Function and Input, over input spectrum.
Random	Disturbance spatial correlation characteristics are used to generalize forcing fields with respect to mode shapes. Appropriate Transfer functions must be determined. Solution then follows - see right.			Output Spectral Density is product of $\|T.F.\|^2$ and Input Spectral Density
Transient	p(t)is weighted with mode shapes. Indicial response integral necessary. (Inverse Fourier Transform of Unsteady Aerodynamic Matrix)	Indicial Gust Function is weighted with velocities and mode shapes. Otherwise, same as pressure source.	Forces - same as pressures Displacements - must derive equivalent forces including indicial terms where appropriate.	a) Numerical Integration of Integro-Differential Equations, or b) Via Laplace Transform and Inverse Transform Techniques, numerically handled.

Transient Aerothermoelasticity

This effect is relevant, for example, to very high temperature flexible turbine stages, although the practical significance is not clear. If static aeroelastic analyses of bladed discs at the beginning and the end of thermal equilibration showed significantly different results, then the equilibration process itself (an aero-thermo-elastic transient event) could be worthy of solution.

Although this capability has not been programmed, a conceptual process is outlined, and an annotated flow diagram of the transient aerothermoelastic analysis is presented in Figure 8.

1. The auxiliary aerodynamic data and blade mesh generator can be used to generate element connection (CTRIA2), element property (PTRIA2), and coordinate (GRID) bulk data cards defining the blade geometry. It would also generate aerodynamic streamline data on STREAML cards and aerodynamic data that can be incorporated into the input for the aerodynamic load generator (ALG) module in NASTRAN. (References 26-29.)

2. A steady aerothermoelastic analysis, would initially be executed and aerodynamic temperature loads would be punched on TEMP bulk data cards. These temperatures would represent the surface temperatures on the blade.

3. The aerodynamic blade surface temperatures must be used as prescribed temperatures for the transient heat transfer analysis. To do this a large scalar conductor element, K_0, would be connected to the blade surface grid point to be enforced and a thermal load $P=TK_0$ applied to the grid point, where T is the desired temperature.

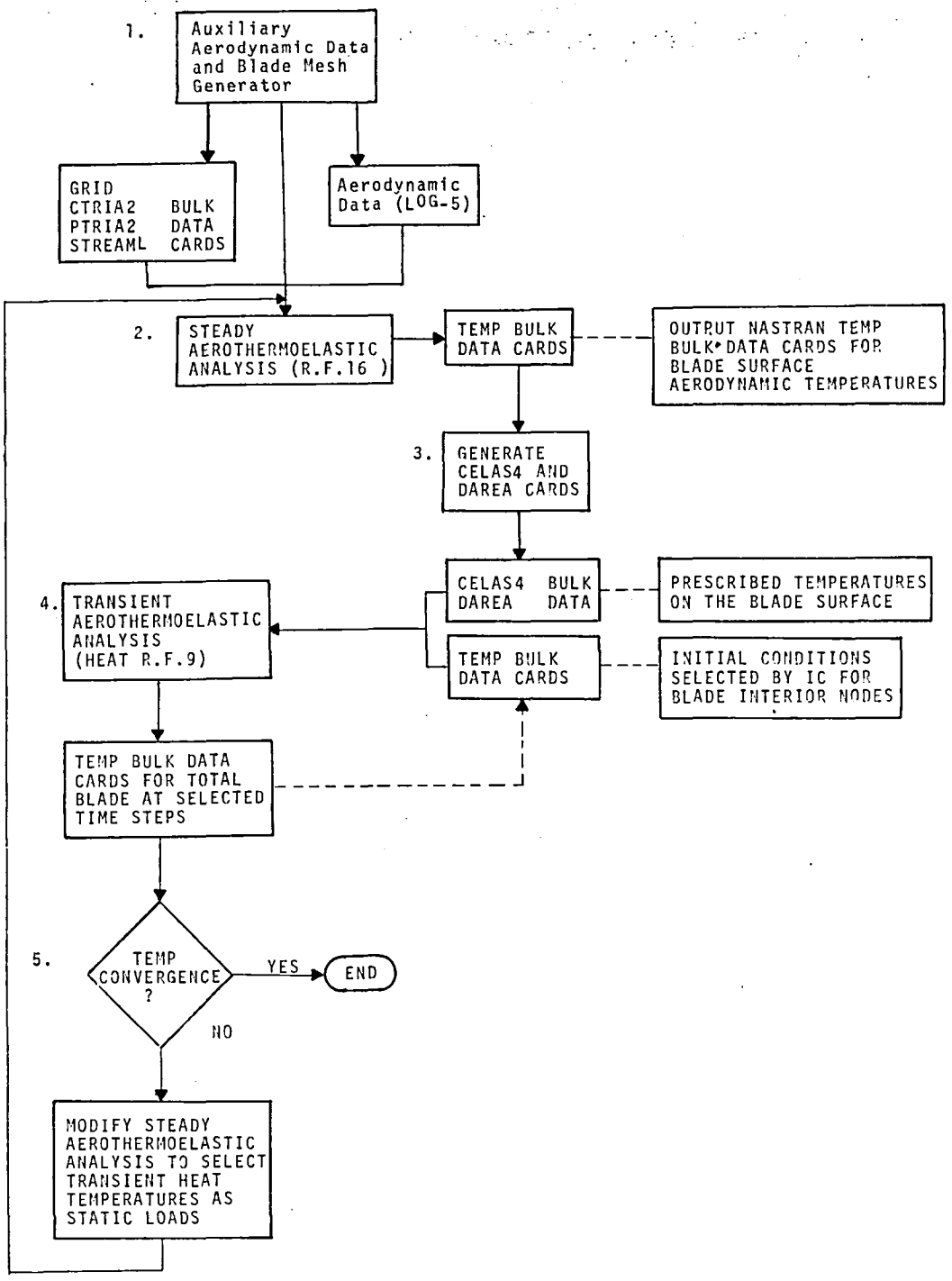

FIGURE 8 Conceptual Approach to Transient Aerothermoelasticity

The scalar elements would be modeled with CELAS4 elements and the prescribed temperature would be generated on DAREA cards.

4. A transient heat transfer analysis, using HEAT rigid format 9 would then be performed. Input would consist of the enforced blade surface temperatures via CELAS4 and DAREA bulk data cards as generated in paragraph 3 and a set of initial conditions selected by IC on TEMP bulk data cards. The initial condition temperatures would be on TEMP cards punched from the last iteration through the transient heat transfer analyses. Only temperature data for nodes not on the blade surface would be specified since surface temperatures would be prescribed.

Output from the transient analyses would be total temperatures on the bladed shrouded disk for a set of user selected time points. These temperatures would be punched on TEMP bulk data cards by requesting THERMAL (PRINT, PUNCH) in the case control deck.

5. If the temperatures have converged then the transient aerothermoelastic analysis is complete.

6. If the temperatures have not converged then a new steady aerothermoelastic analysis would be executed. The user would decide which time step temperatures, from the transient heat analyses, he wants to use and input them into the steady aerothermoelastic analysis and select them in the first static subcase.

MISTUNED SYSTEMS

General Discussion

The cyclic structural nature of a tuned bladed disc considerably simplifies problem formulation and solution, enables many existing NASTRAN features to be used, reduces computational effort and gives basic insight into the characteristics of such discs in operation.

No practical bladed disc is perfectly cyclic, due mainly to manufacturing tolerances in blades and their attachments. This can strongly affect dynamic stability and forced response, particularly when isolated disc and blade frequencies are similar.

The analysis of mistuned systems is, therefore, necessary because such systems typify practical assemblies. Their dynamic, stability and response characteristics must be formulated, analyzed and understood. Mistuning may be even exploited through selective installation to achieve "optimum" stability or forced vibration.

Before discussing potential approaches to mistuned system analysis, a qualitative discussion of mistuning effects on modes, flutter and forced vibration is desirable.

A tuned (cyclic) system possesses families of modes distinguished by harmonic number "k" (the number of nodal diameters) see Figure 2(A)Modes. Such modes occur in pairs of equal frequency for $k \neq 0$ (double eigenvalues). As the harmonic number increases, the frequencies tend asymptotically

to the blade root-fixed frequencies.

Mistuning destroys the cyclic dynamics character of the assembly and its modes, by coupling together the harmonic families of the tuned system. The detailed effect depends on the specific mistuning distribution. For modest mistuning levels the effect is to couple together modes of similar frequency and different harmonic number into distinct modes and frequencies. The double eigenvalues of the tuned assembly are, in general, separated by mistuning.

For mistuning circumferential distributions of a single harmonic component, it has been shown (Ref. 14) that mistuning of the form cos $2k\theta$ will split double eigenvalues only of order k and $\frac{N}{2}$ - k where N (or N+1) is the number of blades. An example of this is given in Figure 2(A) Modes. For a general multiparameter mistuning all mistuned harmonic components are likely to be present, and all double roots are likely to be split. Each mistuned mode may still be characterized as a vector or "spectrum" of harmonic components, the sum of which represents the complete mistuned mode shape. Note that very flexible mistuned blades on a stiff disc will tend to act almost independently. Very stiff mistuned blades on a very flexible disc (unusual?) would show little mistuning effect for some lower range of modal frequencies.

The notions of tuned harmonic families, mistuning harmonic spectra, double root splitting, and mistuned modes spectra are valuable as an aid to understanding and formulation of mistuning problems and effects, and the interpretation of laboratory modal test results of real assemblies.

In a tuned system with harmonic families of modes, only modes of the same harmonic family can couple aerodynamically to give a flutter problem. Modes of different harmonic number cannot couple because of circular function orthogonality. Flutter aerodynamics is generally formulated using cascade theories, some limitations of which are noted in Appendix E. We assume that, until proved otherwise, the suggestions of Appendix E for the determination of non-zero harmonic number cascade aerodynamics are acceptable.

As discussed earlier, mistuned modes can be expressed as a vector consisting of modal components of various harmonic numbers. The generalized unsteady aerodynamic forces for mistuned mode sets may now be determined using this vector and the assumptions of Appendix E .

In the total generalized aerodynamic force expression

$$Q_{ij} = \sum_{\text{blades}} \cdot \int_{\text{blade}} u_i p_j \, dS$$

in which u = displacement, p = pressure, only like harmonic components of u and p will contribute non-zero terms.

Thus, the decomposition of mistuned modes into harmonic components will enable the use of all tuned system analyses to contribute to mistuned system flutter analysis. The mistuned flutter problem solution is the same in principle as for tuned systems.

The flutter stability and subcritical roots of a mistuned assembly having been determined, the forced vibration problem can be properly posed. Note that for harmonic or periodic forcing which results in harmonic or periodic response, cascade theories are valid for the determination of aerodynamic damping and stiffness coefficients of mistuned systems (within limitations discussed above).

Subcritical damping coefficients determined during flutter calculations could also be used for transient response calculations with the same qualifications already mentioned for tuned systems.

Tuned system response studies are frequently guided by the usual "interference diagram". Adequate descriptions of external forcing functions are necessary to predict quantitative response features (amplitude, stress, etc.); see Figure 2(C).

Each mistuned system mode will contain several circumferential harmonic displacement components, so that different engine order excitations may produce vibration in that mode as speed varies. Vibration intensity will depend on the spectral distribution of the mistuned modal decomposition and the effectiveness of engine forcing term components in doing work in the corresponding mode shape component. Figure 2(C).

Potential approaches to mistuned dynamics problems should solve practical problems, build on the knowledge of tuned system dynamics, and exploit current computer program features in the mode, flutter and response problem area as much as possible.

Mistuned Dynamics Approach

The stability, strength and life of a real mistuned assembly are the ends to be assured in the analyses under discussion. The modes of a mistuned assembly are significant but still only a means to understanding the behavior of the system and the attainment of the ends.

Mistuning must be adequately described to enable analyses to proceed. The form of this definition is important. The method of solving for the mode shapes of a mistuned assembly must obviously be compatible with the form of definition of the mistuning.

The modal analysis results can be used for various purposes:

1. As a basis for subsequent flutter and forced response calculations.
2. As an aid to the interpretation of experimental studies of modes of blades, discs, and mistuned assemblies. (Note: Experimental blade characteristics give a "measured" mistuning characteristic - a "sample" of a large set of possibilities.)
3. For mathematical studies of the influence of prescribed mistuning distributions on the modal results and subsequent flutter and response results.

How mistuning is characterized can affect the approach to the modal analysis. Four plausible characterizations are as follows:

1. Simple measures such as differences in blade mass, and overall bending and torsional stiffness parameters.

2. Dynamic properties such as the measurement of the "root-fixed" blade modal frequencies and generalized masses, (and perhaps, mode shapes as well).

3. Some measure of blade dimensional differences.

4. Some prescribed mistuning distribution (very valuable for analytical studies of mistuning effects).

Note that 1-3 are basically samples of a random process, 4 could be of a 'deterministic' or random nature.

The eigenvalue formulation itself for the mistuning problem can also take various forms which should be considered in relation to the mistuning characterizations listed above.

A. Finite element idealizations of disc and blade.

B. Mixed idealization of disc finite elements and blade individual normal modes.

C. Substructure and normal modal idealization for disc and individual blades.

In Table 3, eigenvalue formulations and mistuning characterizations are related in terms of the compatibility of various combinations in promising practical computational approaches.

It is obvious that two formulations are desirable:

1. A formulation (2B, 4B) which uses (measured) blade modes directly. This would be particularly applicable to studies paralleling actual tests of discs, blades and assemblies.

2. A formulation (4A, B) using prescribed forms of mistuning either as blade properties or analytical distributions of mistuning. This would be particularly applicable to theoretical studies of the effects of mistuning distributions and of ways to ameliorate flutter and forced response characteristics by selective blade installation.

In both methods, the potential should be studied for reducing the eigenvalue problem to one involving expansion of the mistuned eigenfunctions in terms of the eigenfunctions (harmonic families) of the "averaged tuned" system. This can reduce the problem to manageable proportions and more clearly illustrate cause-effect relations of specific mistuned types.

Mathematical developments of these two formulations are described in Appendix F.

	EIGENVALUE FORMULATION		
	A. All Finite Elements	B. Disc Finite Elements & Blade Mode Sets -OR- C. Disc Modes & Blade Mode Sets	Comments
1. Blade Mass, plus overall bending & torsional stiffness	No reliable way of apportioning mass mistune. Could crudely factor stiffness matrices but might lead to conditioning problems.	N/A	Characterization not helpful. Basically inadequate.
2. All blade mode sets. (At least frequencies & generalized mass & stiffness.) All Mode shapes?	Difficult system identification problem to relate M, K for grid points. Conditioning problems certain. NOT COMPATIBLE.	Feasible provided experimental data is accurate. Couple disc to blade modes using cyclic structure method with blade modes represented as "scalar points". (See NASTRAN Theory 14.1, Reference 7.) Can further use perturbation theory and cyclic mode.	Information usable at two levels of completeness. 1. ω's, M's, K's 2. ω, M's, K's and all mode shape variations. Use of 2 complicated & possibly unnecessary.
3. Detailed geometry measurements of all blades.	Could roughly modify element densities & moduli for each blade to approximate mass & stiffness variations. Feasible but not very practical.	Requires calculation of all blade mode sets with variations dependent on measurement accuracy - Not practical.	Measurement adequacy doubtful as a practical proposition.
4. Prescribed mistuning in mass and/or stiffness.	Incorporate directly into element properties. See Appendix F for theoretical development.	Use directly for blade and/or disc modes. See Appendix F for method.	Valuable for studying the effects of known or controlled mistuning. Can be a guide to the advantages of selective mistuning arrangements in minimizing response.

Table 3. APPROACHES TO MISTUNED MODES

NUMERICAL RESULTS AND DISCUSSION

Demonstrations of the current program capability are of two types:

- o The usual "demonstration" examples included for completeness in the documentation of NASTRAN capabilities. (Ref. 29)
- o Specific examples on a research rotor known as Rotor 12 at NASA/Lewis, (Dwg. CF 848322).

This section will not discuss the former examples which are adequately covered in Program Documentation (Ref. 29). For the latter examples, NASA required that the first five resonant frequencies of the rotor would be determined at three specified operating conditions.

The actual results obtained have exceeded this requirement in that the progressive analysis of Rotor 12 through the aeroelastic, modal and flutter algorithm has yielded both performance and dynamics data. Specifically, NASA requested aeroelastic analysis of the "rigid" Rotor 12 characteristics at the three operating points shown on Figure 9, of which point 310 is the design point.

Finite Element Model

The finite element model/grid used for Rotor 12 analyses is illustrated in Figures 10 & 11, and is based on 8 streamlines and 5 computing stations on the bladed sector. This, with the shroud and hub modeling results in a total of 68 plate elements

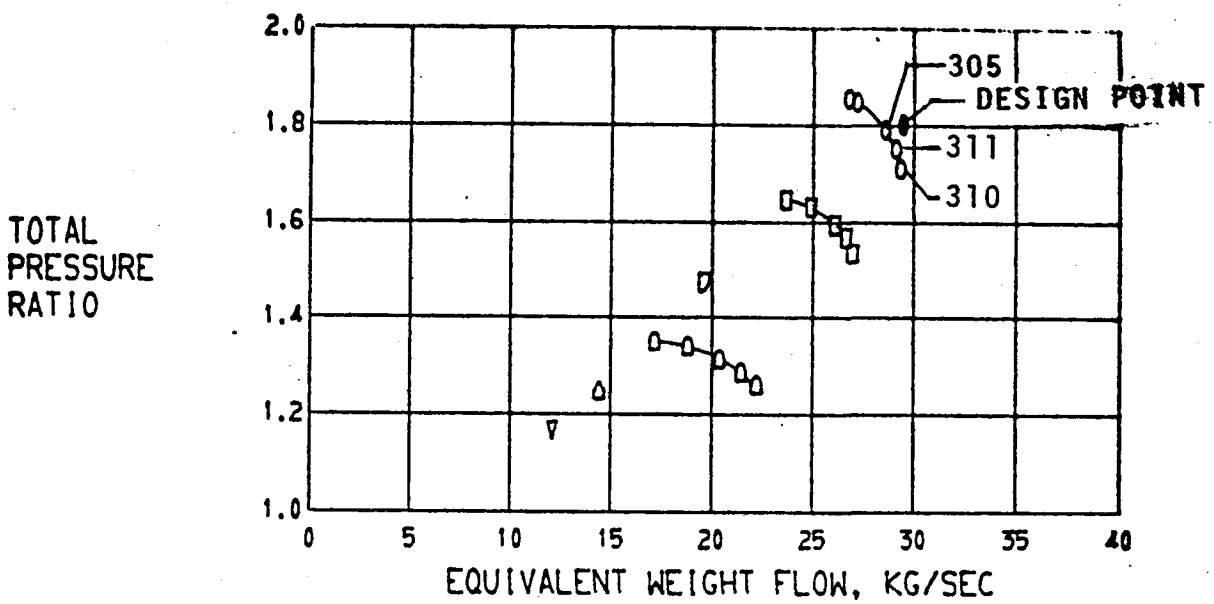

FIGURE 9 - OVERALL PERFORMANCE FOR ROTOR 12.

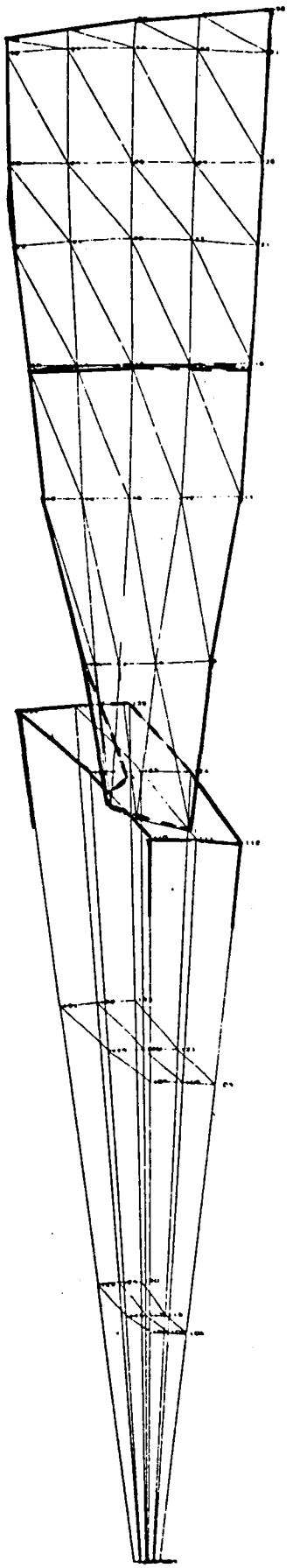

BLADE - 64 PLATE ELS.

SHROUD - 4 PLATE ELS.

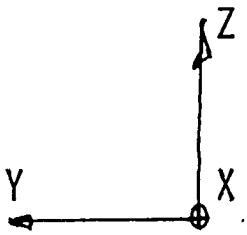

DISK - 12 SOLID ELS.

NASA LEWIS ROTOR 12
FINITE ELEMENT MODEL
FOR AEROELASTIC &
MODAL ANALYSIS

Figure 10

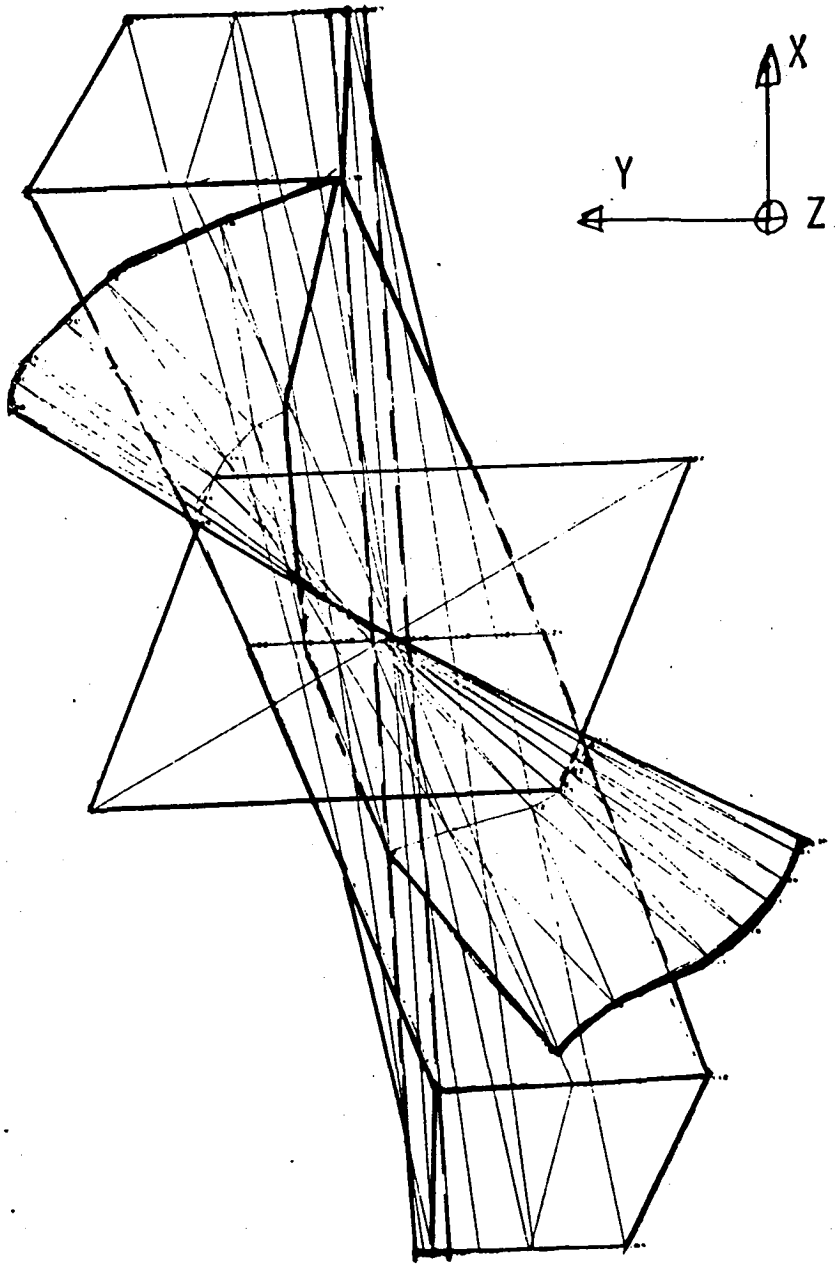

Figure 11. NASA LEWIS ROTOR 12
FINITE ELEMENT MODEL FOR AEROELASTIC &
MODAL ANALYSIS

(blade, 64; shroud, 4) and 12 solid elements (hub).

Aeroelastic "DESIGN" And "ANALYSIS"

The values of parameters to be input to the ALG (Hearsey) analyses have not been supplied by NASA but guessed by Bell at this writing. It was intended to rerun these analyses with NASA -determined input at the final program seminar at NASA/Lewis, but this was not possible.

The basic aeroelastic results are presented on Figure 12, (computer tabulations of flow details are not included here), and compared with "rigid" rotor and test results. Note, that since Rotor 12 already exists, Point 310 was actually "analyzed".

Point 310

Rigid rotor "ALG" P.R. of 1.725 compares with test P.R. of 1.705 and aeroelastic P.R. of 1.810.

Point 311

Rigid P.R. of 1.745 agrees with test value, and aeroelastic analysis value.

Point 305

Rigid P.R. of 1.785 agrees with test value but aeroelastic value is 1.910.

It is obvious that these results are not satisfactory because of the "out-of-sequence" order of the ΔP increments. This is currently attributed to inappropriate values of input parameters selected by Bell. Repeated analyses at NASA with more representative inputs are intended to see the effect on these results.

Figure 12. NASA ROTOR 12 AEROELASTIC ANALYSIS

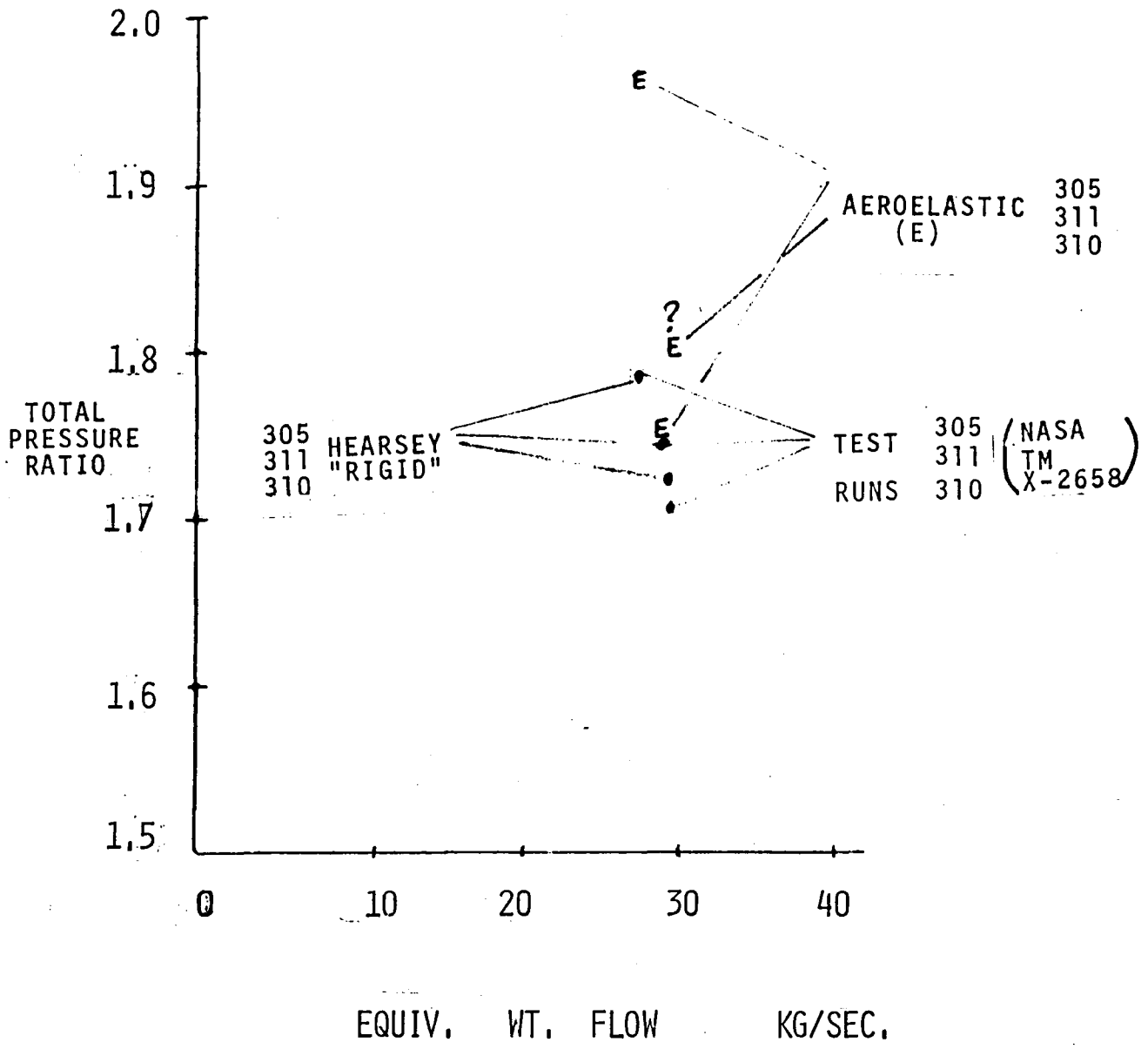

Modal Analyses

Results for the first five tuned modes at the three operating points for zero harmonic number, and the first four modes for point 310 for the 28th harmonic number are presented in Table 4 . The effects of operating point are quite small as expected since Rotor 12 is quite stiff. Hence, modal plots for point 310 only are presented for harmonic numbers zero and 28 in Figures 13 to 15 . Results at harmonic number 28 for point 310 do not vary significantly from the zeroth harmonic number results for the first three modes indicating that hub stiffness is relatively great.

It is obvious that the modes of 2113 Hz and 2214 Hz for point 310 are not orthogonal and represent the same mode. The NASTRAN eigenvalue algorithm used here was the FEER Method . Similarly Mode 3 for Harmonic Number 28 of 2303 Hz appears very similar to mode 5 of H.N. zero at 2534 Hz. Suppression of Modes 3 and 4 as harmonic number increases may account for the appearance of an apparent double value at zero harmonic number and its non-appearance for H.N. 28.

Flutter Analyses

These have only been carried out for one operating point 310 and zero harmonic number in terms of the "pseudo" flutter roots at that point. This is because the disc is very stiff and the effects of operating point and harmonic number on modes and frequencies are small. Actual compressor map flutter boundaries have not been determined.

TABLE 4 - MODAL RESULTS ROTOR 12

FREQUENCIES IN HERTZ

OPERATING CONDITIONS	310 (DESIGN POINT)		311	305
HARMONIC NO.	0	28	0	0
MODE 1	785	799	786	780
MODE 2	1830	1981	1831	1826
MODE 3	2113 ?	2303	2114 ?	2112 ?
MODE 4	2214	3406	2214	2214
MODE 5	2534	-	2535	2530

ROTOR 12

HARMONIC NUMBER ZERO

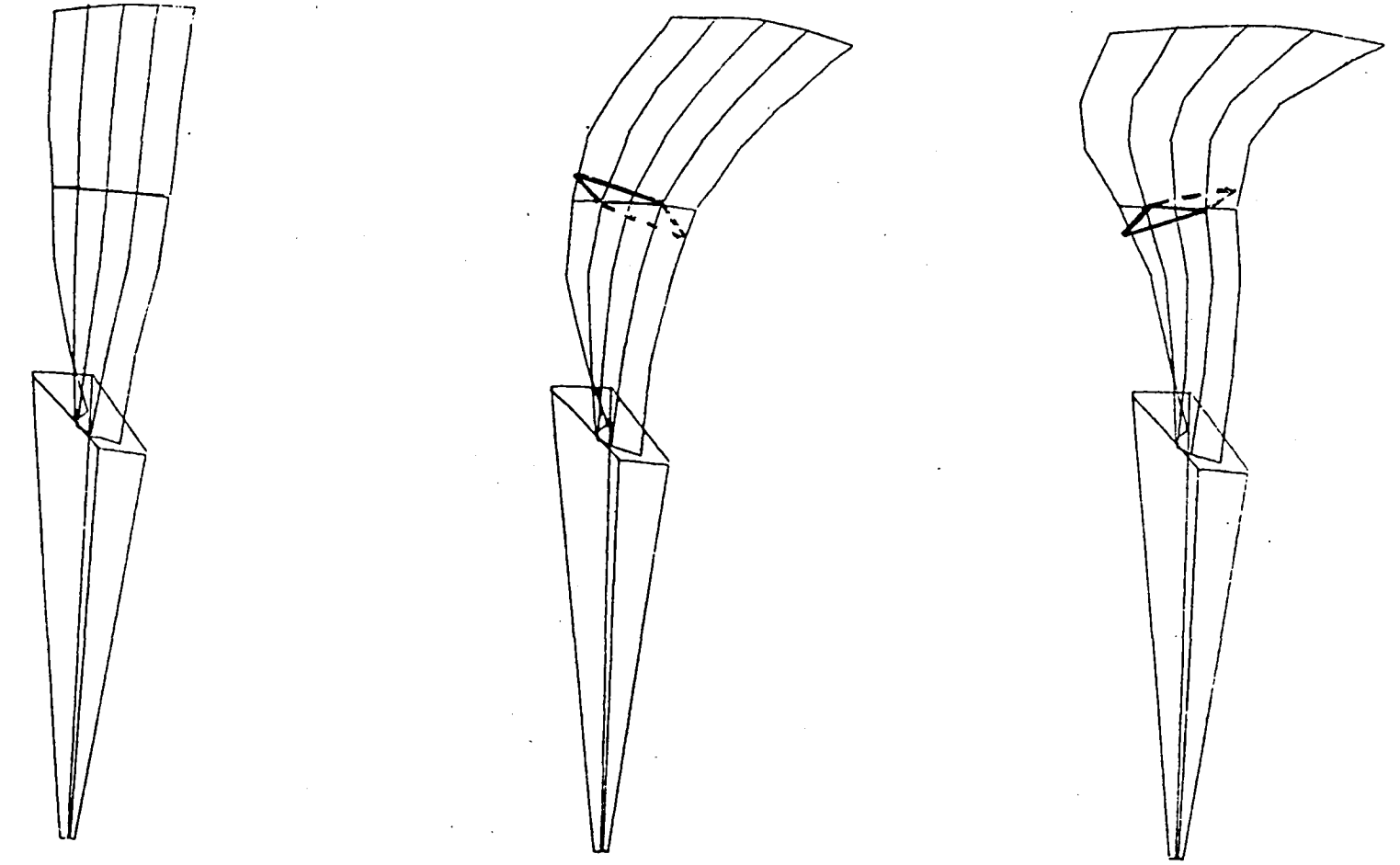

Figure 13. NASA LEWIS ROTOR 12 MODES AT DESIGN POINT (310)

ROTOR 12

HARMONIC NUMBER ZERO

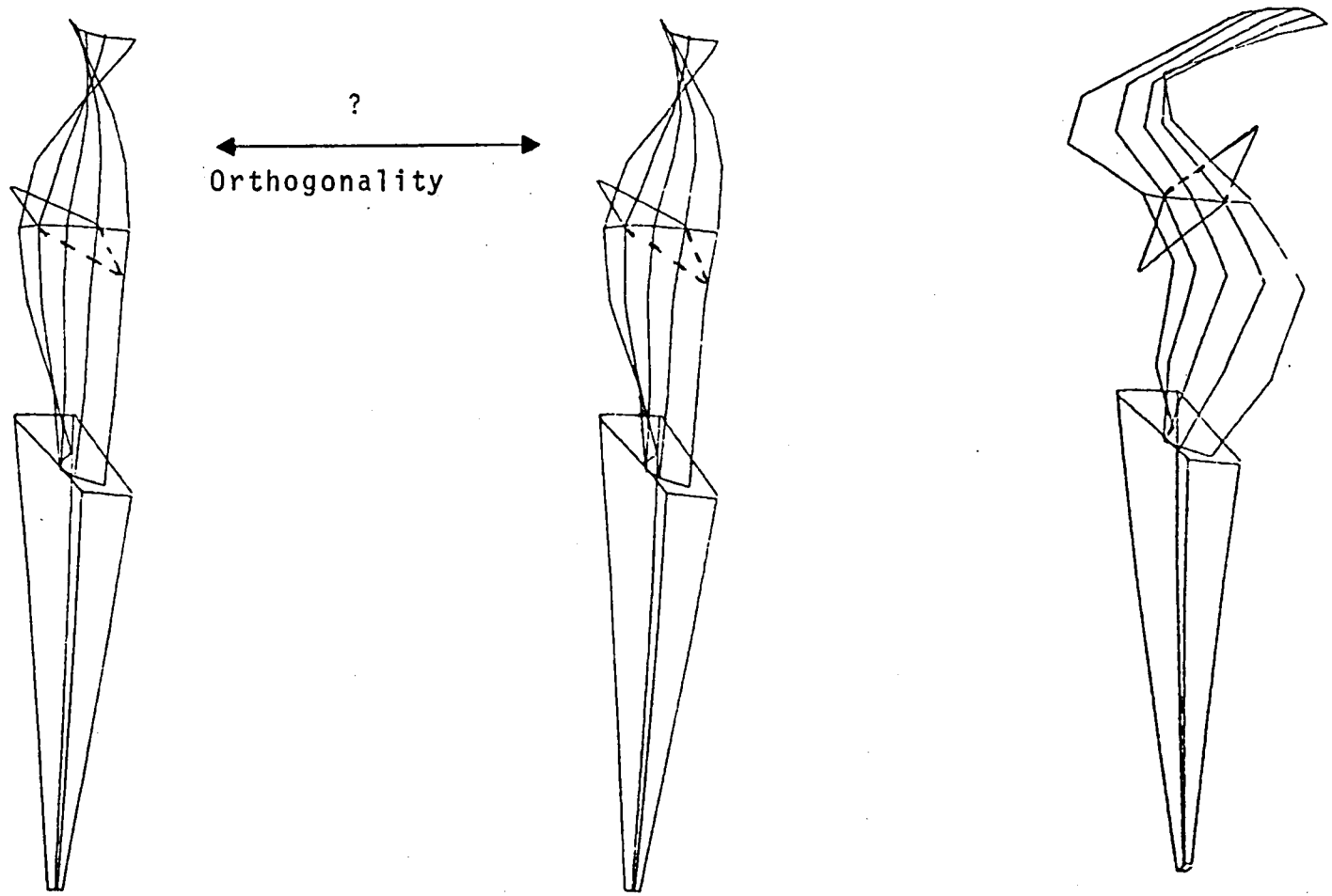

MODE 3
2113 Hz

MODE 4
2214 Hz

MODE 5
2534 Hz

Figure 13 (continued)

ROTOR 12

HARMONIC NUMBER 28

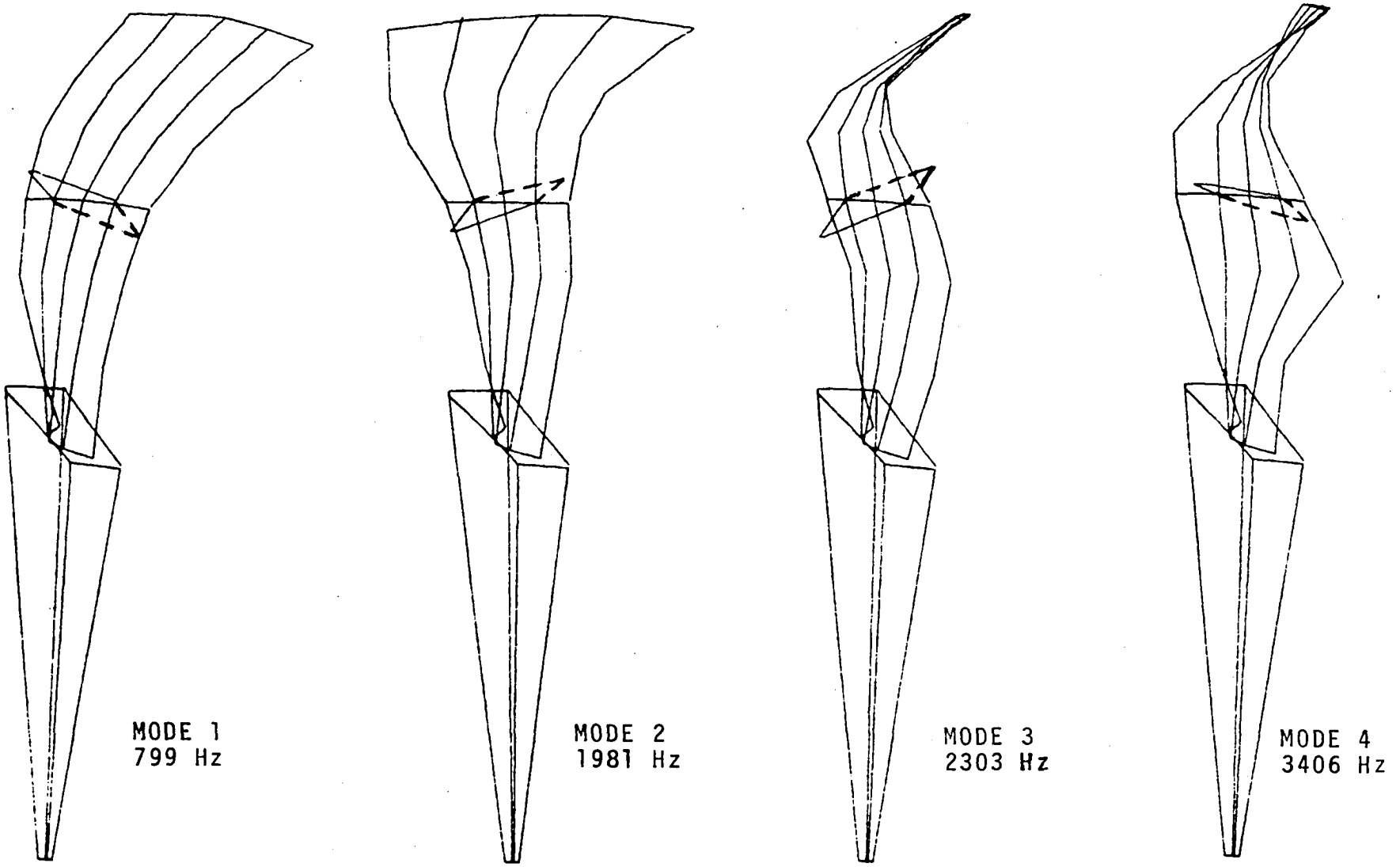

Figure 14. NASA LEWIS ROTOR 12 MODES AT DESIGN POINT (310)

Flutter loops were conducted for a single interblade phase angle of 180°, five reduced frequencies based on reference tip chord, tip speed and modal frequency spread, and actual, X2 and X3 reference density.

Complex eigenvalue plots are presented in Figure 16.

The high blade/air density ratio means that results are dominated by aerodynamic damping effects. Thus, mode frequencies are almost unchanged and all modal dampings are roughly proportional to the input air density. Note that no structural damping was included.

Bending modes 1, 2 are reasonably well damped, while torsional mode 4 exhibits negative damping (only -.002 at the correct density).

A complete exercise, of course, requires coverage of the compressor map for permissible sets of interblade phase angle and harmonic number, each analysis including adequate ranges of reduced frequency in the standard NASTRAN flutter algorithm.

In the course of rerunning the analysis at NASA/Lewis with changed aeroelastic input, it is not expected that modal and flutter results will change significantly.

It may be noted that CPU time on the IBM370/3031 at Bell for all flutter results was 1785 seconds, of which 1440 seconds were absorbed by unsteady aerodynamic calculations, of which 1400 seconds were for the four out of five streamlines requiring supersonic cascade calculations by the UCAS subroutines.

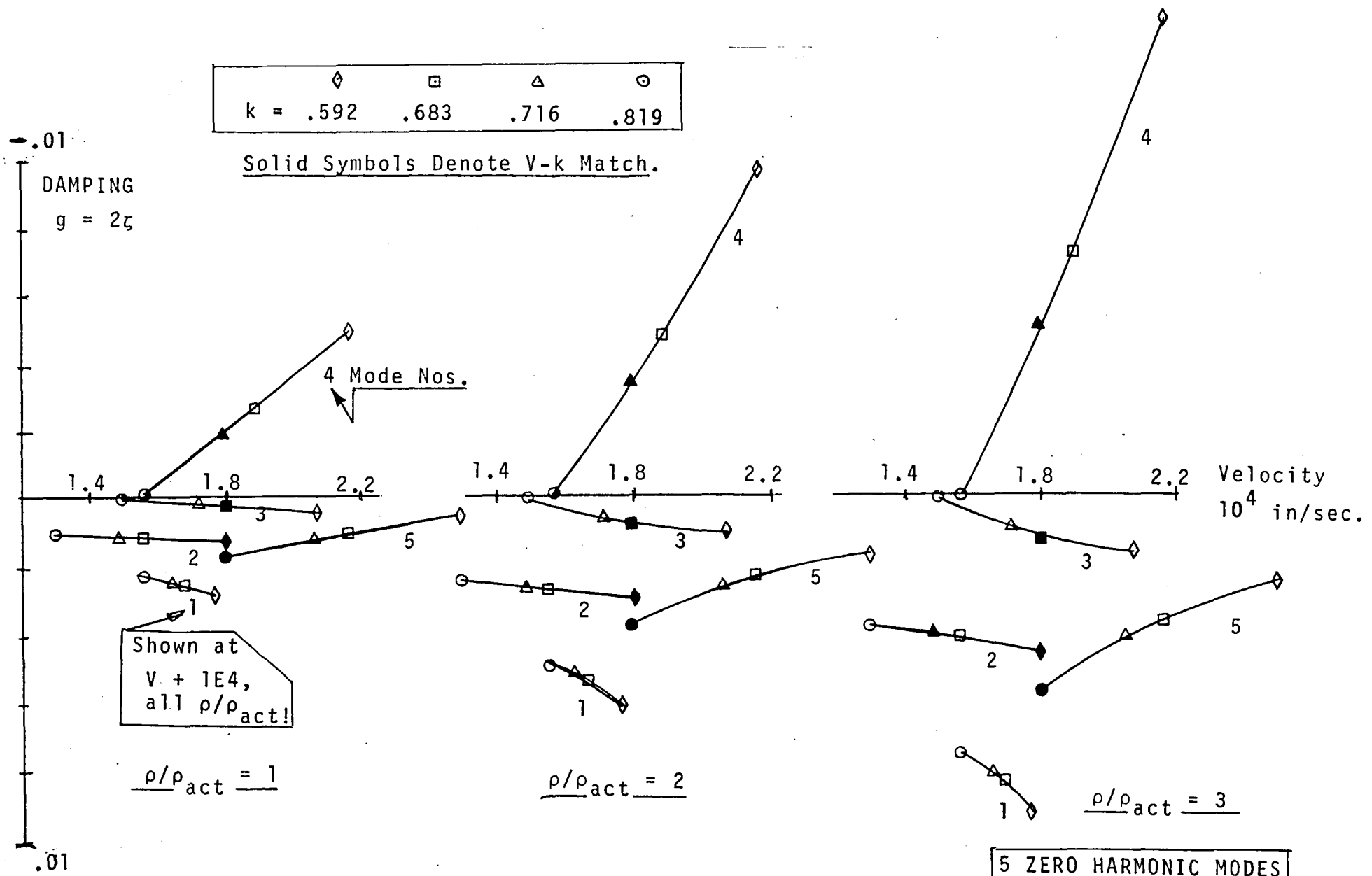

Figure 15. "FLUTTER" ROOT RESULTS - ROTOR 12
DESIGN POINT - 310

CONCLUSIONS

The complete objectives of the original program which principally required the ability to predict the forced response of mistuned ("real") bladed discs have not yet been reached.

However, a formal basis for reaching those objectives has been fully defined and largely established. This basis itself rests on two theses:

- That "mistuned" analyses should be based on the view of a mistuned system as a perturbed tuned system, and that complete understanding of and the ability to analyze tuned systems is a prerequisite .
- That analysis of tuned and mistuned systems must be approached through a logical progression of aeroelastic, modal, flutter (stability) and forced response for genuine results to be achieved.

The capability for tuned systems to the stability step has been created, with a final forced vibration stage still to be fully defined. Mathematical formulations for mistuned modes have been defined together with the bases for using these in stability and forced response calculations.

There is a need for continuing improvement and utilization of steady and unsteady aerodynamic theories from physical, mathematical and computer programming viewpoints.

RECOMMENDATIONS

These can be divided into use, improvement and extension of the current capability.

Use

The delivered program must be thoroughly exercised to prove and appreciate its value. Not only must the assumptions relating to its logical format be validated, but its technical value should be established by applying to problems in which aeroelastic and stability effects are expected to be really significant. This is not the case with the current examples on Rotor 12. Thus application to, say, a large by-pass fan will be more valuable in demonstrating the technical/design feedback potential.

It is, therefore, strongly recommended that the program be put to an extensive test by broad-band coverage of the map of a relatively flexible stage or a large by-pass fan.

Improvements

See Table 5.

From a structural point of view, the current program is strong, and can easily take advantages of NASTRAN finite element improvements as they develop. Likewise it is felt that the solution algorithms are more than adequate at this stage. However, the steady and unsteady aerodynamic subroutines will probably always be capable of improvement and the modular design of the program will facilitate updating to better methods.

It may be recalled that the actual list of unsteady cascade theories available to Bell was somewhat limited by

proprietary and other considerations. Thus, if establishments other than NASA make use of the program, there is potential for its improvement if they have superior in-house subroutines.

In particular (Ref. 23) for unsteady supersonic cascades was originally coded as a research tool for the comparison and evaluation of the results of other cascade programs which were unavailable to Bell. See Table 5 . The method should be recoded as a production program to reduce the very large running time. The program is run very many times in a flutter evaluation, for sets of cascade stagger and spacings, Mach numbers, reduced frequencies, interblade phase angles and mode shapes.

Many improvements can be made such as the following:

(1) It was noted that computations of several expressions are recalculated hundreds of times in the program. These expressions may instead be calculated once, stored, and then used wherever required from the single storage.

(2) Many variables were typed as complex when in reality, they were real. These expressions not only required more storage than necessary but also required the use of complex arithmetic when real arithmetic would have sufficed.

(3) The present coding has instances where expressions which were constant within a Fortran loop were calculated within the loop rather than just computed once.

(4) Criteria of error and convergence used in this program should be analyzed in order to determine the minimum values necessary to maintain a sufficient degree of accuracy in the final answers.

Alternatively, the whole theoretical basis of the UCAS method could be recoded from scratch with the intention of producing an "optimum production" program.

The program was delivered in NASTRAN Level 16, and it is recommended that it be periodically updated to later, more versatile Levels. To begin with, this level could be Level 17 or Level 17.5. We understand that NASTRAN Level 17.5 has been changed to work under the new UNIVAC loader and, therefore, recommend Level 17.5. The additional substructure capability in Level 17.5 should be a further advantage.

Extensions

See Table 5.

These may be classified as essential, desirable, and possible and are "priority rated" respectively 1, 2 or 3 in Table 5,

Tuned Forced Vibration.

Given a set of mode shapes, current NASTRAN capabilities can determine the forced vibration resulting from a variety of forcing function types. However, the current format takes no advantage of cyclic structural geometry. Such advantage should be developed, programmed and exercised in a suitably modified Rigid Format for specific types of forcing function of interest to NASA. Such forcing functions may include transient, periodic or random force distributions arising from incident pressure or velocity fluctuations, or from resonance or unbalance testing.

Mistuned Modes

Engineering definition of approaches to mistuned modes for research ("analysis") and test purposes has been presented. See Appendix F. These should be coded, exercised and incorporated as additional Rigid Formats.

Mistuned Flutter & Subcritical Roots

An approach has been outlined for a plausible use of current unsteady cascade theories to enable the estimation of aerodynamic coefficients for arbitrary circumferential harmonic number (Appendix E). This will enable tuned non-zero harmonic flutter to be studied. Fourier expansion techniques may then be used for the estimation of unsteady aerodynamics of mistuned modes and their flutter stability.

These capabilities should be coded, exercised and incorporated as additional Rigid Formats.

Mistuned Forced Vibration

Forced vibration arising from defined external pressure-or velocity- related forcing functions, implied in resonance testing, or arising from unbalance should be developed taking maximum advantage of the cyclic geometry and previous developments. Beating phenomena such as may arise on forced unbalanced rotating discs should be treatable.

Transonic Unsteady Aerodynamics

If a suitable cascade theory emerges, its use should be considered in order to improve the interpolation of unsteady aerodynamics along the blade. This would improve flutter,

subcritical root and forced vibration estimates for tuned and mistuned systems.

It is not necessary for current operations.

Replace Compressor Code

Some 'discomfort' has been expressed by NASA personnel from time to time with the use of the Hearsey Code (Ref. 19) as an aerodynamic tool in the aeroelastic analyses.

If NASA has a preferred code, this could be substituted for the Hearsey Code.

Automate Transient Aerothermoelasticity (TATE)

Full TATE automation was not accomplished. It is not regarded as a serious shortcoming. Indeed practical results using initial and final blade temperatures migh show sufficiently small differences that the transient capability could be delayed (indefinitely?).

If required, it would be necessary to knit together features of the SATE Design/Analysis and Heat Transfer Rigid Formats and cycle between these two in terms of deformation/flow and temperature iterations.

Non-Zero Harmonic Cascade Theory (k>o)

In the strict sense this is necessary for:

a. Correct definition and study of tuned system non-zero harmonic flutter.

b. Correct formulation of overall unsteady generalized airforces for mistuned flutter problems.

It can be argued that the use of current cascade theories is reasonable for $\frac{\text{Harmonic No.}}{\text{No. of Blades}} \ll 1$ and conservative otherwise.

If studies show that tuned non-zero harmonic flutter is of practical design significance, such developments should then be undertaken since the implication is that mistuned flutter would be inadequately evaluated by current cascade theories.

However, a decision on this should await the results of tuned non-zero harmonic and mistuned flutter studies using the suggestions of Appendix E.

TABLE 5

ITEM	COMMENT	PRIORITY
1. Change NASTRAN Level	To 17 or 17.5? (Level 17.5 is UNIVAC Compatible.)	1
2. Recode "UCAS"	(a) Improve coding of existing program. (b) Recode theory entirely for use as a production program.	1 1,2
3. Tuned Forced Vibration	Current NASTRAN capability should be formally extended to take advantage of cyclic structure.	1
4. Mistuned Modes	Finalize and code existing developments. See Appendix F.	1
5. Mistuned Flutter and Subcritical Roots	Incorporate Fourier Expansion Technique to Modal and (Harmonic number, inter-blade phase), Aerodynamic definitions.	1
6. Mistuned Forced Vibration	Include capability for In-Vacuo & Operating "Resonance Tests" and unbalance effect. NASA to define other specific types of forcing functions to be considered.	1
7. Transonic Unsteady Aeros	Review literature for possible improvement to current approximation.	2
8. Replace Hearsey Steady Aeros	Would be based on a NASA preference for an existing or commonly used method.	2
9. Automate Transient Aerothermoelasticity	Current status requires manual intervention between aeroelastic and Heat Transfer Rigid Formats.	3
10. Develop Unsteady Cascade Theories for $k \neq 0$	Should follow flutter studies using suggestions of Appendix E.	3

Table 5 POTENTIAL PROGRAM IMPROVEMENTS & EXTENSIONS

APPENDIX A.

BLADE MODAL AIRFORCE MATRIX [Q]

The generalized aerodynamic force matrix $[Q_{ij}]$ for the blade modes, (i,j = 1, 2, ..,I) is derived. The blade motion is described in terms of the displacements at streamline-computing station intersections shown in Figure A-1. The blade aerodynamic forces are determined by spanwise integration of the forces per unit span on each streamline. Based on the relative flow at the leading edge, two-dimensional subsonic or supersonic aerodynamic cascade theory for harmonic oscillations is used to calculate the pressure distribution on each streamline.

In the process of locating the flutter boundaries on a compressor map, a series of operating points is investigated. At each of these candidate flutter operating points, a range of combinations of flutter parameters such as interblade phase angle and reduced frequency is considered. A substantial portion of this extensive effort is expended towards computing the generalized airforce matrices for ranges of Mach number, reduced frequency, interblade phase angle and chordwise mode shape.

In the present development, therefore, modal generalized airforce matrices are first defined for prescribed aerodynamic mode shapes (see Section A.2) for each streamline. These matrices are independent of the structural mode shapes which are subsequently introduced through Fourier matching for each streamline. An added advantage of this procedure is reflected in the flexibility of the flutter computational algorithm (Figure 7) to supplement

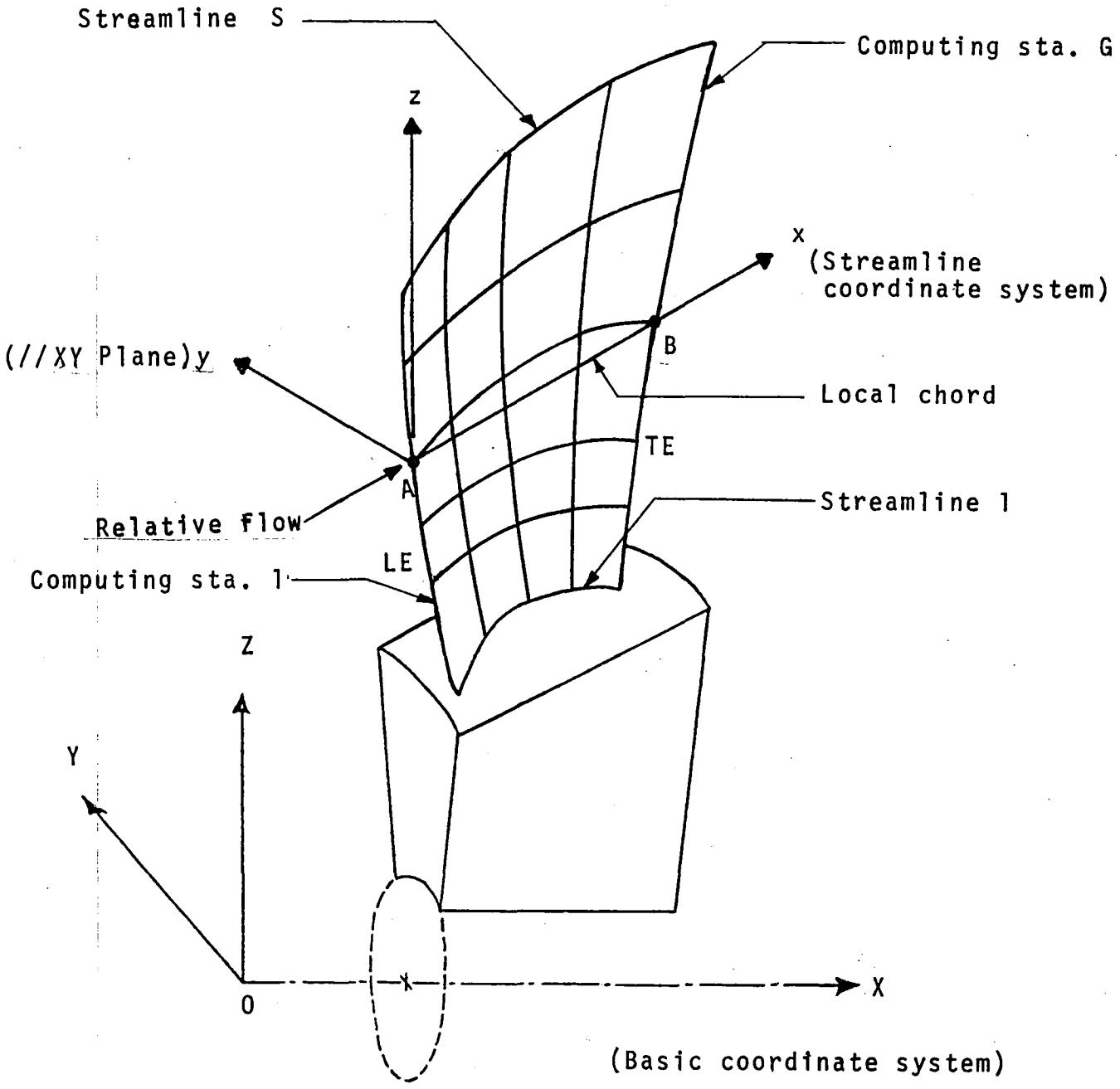

FIGURE A-1 BASIC AND STREAMLINE COORDINATE SYSTEMS

or replace the existing aerodynamic cascade theories and the use of the same Fourier series aerodynamics for different mode shapes or sets.

A.1 Blade Degrees Of Freedom

Let {u} represent the total degrees of freedom in any cyclic sector of the bladed-shrouded disc (Figure A-3). The degrees of freedom on the blade and the rest of sector structure (disc, shroud, etc.) can be partitioned and written as

$$\{u\} = \begin{Bmatrix} u_b \\ \hline u_c \end{Bmatrix} \qquad A\,(1)$$

The blade is spanned by S streamlines with G structural grid points on each streamline (Figure A-1). Therefore, the blade degrees of freedom can be further partitioned as

$$\{u_b\} = \begin{Bmatrix} u_{b1} \\ \hline u_{b2} \\ \hline \vdots \\ \hline u_{bs} \\ \hline \vdots \\ \hline u_{bS} \end{Bmatrix}, \qquad A\,(2)$$

where

$$\{u_{bs}\} = \begin{Bmatrix} u_{bs1} \\ \hline u_{bs2} \\ \hline \vdots \\ \hline u_{bsg} \\ \hline \vdots \\ \hline u_{bsG} \end{Bmatrix}. \qquad A\,(3)$$

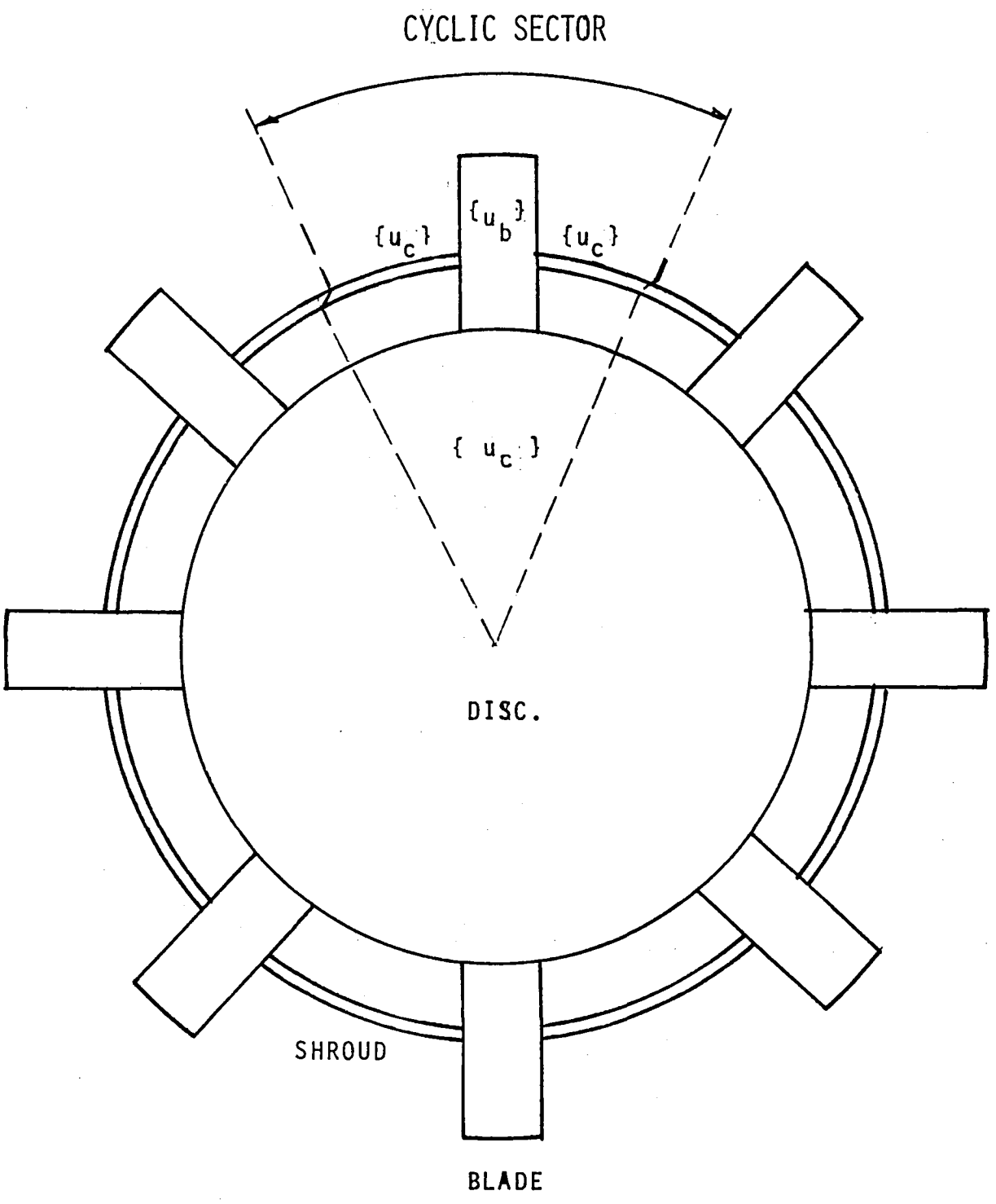

SECTOR DEGREES OF FREEDOM, $\{u\} = \begin{Bmatrix} u_b \\ u_c \end{Bmatrix}$

FIGURE A2. CYCLIC SECTOR DEGREES OF FREEDOM

$\{u\}_{bsg}$ represents the degrees of freedom at grid point g on streamline s on the blade.

In order to define the blade motion normal to a local chord, a rectangular streamline coordinate system is located at each streamline (Figure A-1). With the origin at the leading edge, the x-axis passes through the trailing edge, and the y-axis lies parallel to the basic XY-plane. Displacements in the y-direction, therefore, represent the local motion.

A.2 Chordwise Aerodynamic Modes and Pressure Distribution

The normal displacement at any point x on the streamline s can be expressed as a linear combination of the aerodynamic mode shapes shown in Figure A-3. In the local streamline coordinate system, this can be written as

$$u_{sn}(x) = \ell_s \sum_{g=1}^{G} \Phi_{sg}(x) \cdot \eta_{sg} = \ell_s \lfloor \Phi_{sg}(x) \rfloor \{\eta_{sg}\} \quad , \qquad \text{A (4)}$$

where

$$\lfloor \Phi_{sg}(x) \rfloor = \left\lfloor 1 \; , \; \frac{x}{\ell_s} \; , \; \sin\left(\frac{\overline{3-2}\,\pi x}{2\ell_s}\right), \cdots, \sin\left(\frac{\overline{G-2}\,\pi x}{2\ell_s}\right) \right\rfloor , \text{and} \qquad \text{A (5)}$$

the aerodynamic modal participation vector is given by

$$\{\eta_{sg}\} = \frac{1}{\ell_s} \begin{Bmatrix} a_1 \\ a_2 \\ a_3 \\ \vdots \\ a_g \\ \vdots \\ a_G \end{Bmatrix} . \qquad \text{A (6)}$$

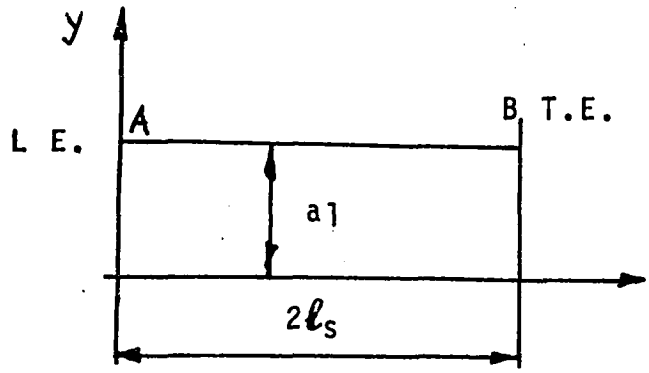

MODE 1

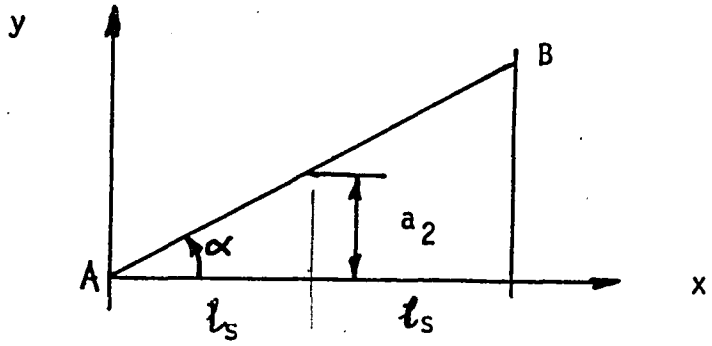

MODE 2

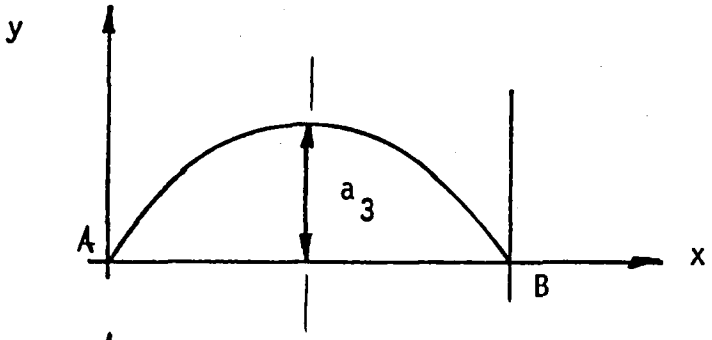

MODE 3

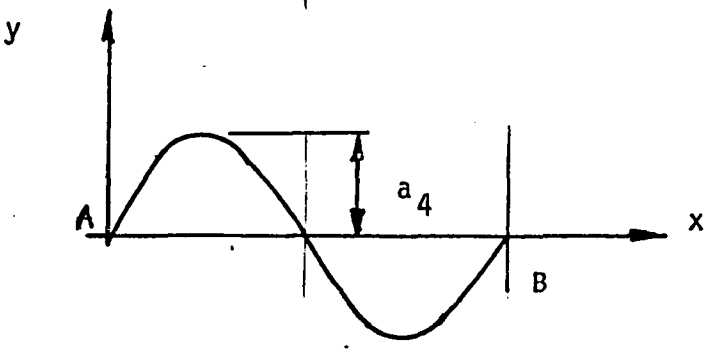

MODE 4

FIGURE A-3 CHORDWISE AERODYNAMIC MODE SHAPES

It should be noted that the total number of aerodynamic modes considered on a streamline is equal to the number of structural grid points on the streamline enabling transformation between the aerodynamic and the structural degrees of freedom (see Section A-4).

In a similar manner, the chordwise aerodynamic pressure differential across the blade at any point x on the streamline s can be derived from an appropriate theory as

$$p_{sn}(x) = \tfrac{1}{2}\rho_s V_s^2 \sum_{g=1}^{G} \Psi_{sg}(x)\cdot\eta_{sg} = \tfrac{1}{2}\rho_s V_s^2 \left[\Psi_{sg}(x)\right]\{\eta_{sg}\}, \qquad \text{A (7)}$$

where $\{\eta_{sg}\}$ is given by equation A(6). The differential pressure, Ψ_{sg}, at the point $\underline{x}$ in the mode $\underline{g}$ is further expanded in series form in order to properly account for the leading edge singularity while integrating the pressure forces along the bladed chord in subsonic flow, i.e.,

$$\Psi_{sg}(x) = \left[C_{g1}\ C_{g2} \cdots C_{gp} \cdots C_{gP}\right]\{\Pi_{p,sub.}(x)\}, \qquad \text{A (8)}$$

where

$$\{\Pi_{p,sub.}(x)\} = \begin{Bmatrix} \sqrt{\frac{2\ell_s - x}{x}} \\ \sin\left(\frac{2-1\,\pi x}{2\ell_s}\right) \\ \vdots \\ \sin\left(\frac{\overline{p-1}\,\pi x}{2\ell_s}\right) \\ \vdots \\ \sin\left(\frac{\overline{P-1}\,\pi x}{2\ell_s}\right) \end{Bmatrix} \qquad \text{A (9)}$$

In a given mode, the subsonic theory determines the aerodynamic differential pressures at P locations along the blade chord.

For similarity, and hence, computational efficiency, a similar distribution is defined for supersonic flow also, with

$$\left\{ \underset{p,sup.}{\Pi(x)} \right\} = \begin{Bmatrix} 1 \\ x/\ell_s \\ \sin\left(\frac{\overline{3-2}\,\pi x}{2\ell_s}\right) \\ \vdots \\ \sin\left(\frac{\overline{p-2}\,\pi x}{2\ell_s}\right) \\ \vdots \\ \sin\left(\frac{\overline{P-2}\,\pi x}{2\ell_s}\right) \end{Bmatrix} . \qquad \text{A (10)}$$

The number of locations, P, at which differential pressures are calculated on the blade chord in supersonic flow may, in general, differ from that in the subsonic case.

Now, equation A(8) written for all modes at the point $\underline{x}$ yields

$$\left\{ \underset{sg}{\Psi(x)} \right\} = \left[C_{gp} \right] \left\{ \underset{\substack{p,\,sub. \\ \underline{or}\ sup.}}{\Pi(x)} \right\} . \qquad \text{A (11)}$$

The chordwise differential pressure distribution can, therefore, be repeated as

$$p_{sn}(x) = \tfrac{1}{2} \rho_s V_s^2 \left[\Pi_p(x) \right] \left[C_{gp} \right]^T \left\{ \eta_{sg} \right\} . \qquad \text{A (12)}$$

A.3 Generalized Airforce Matrix For Chordwise Aerodynamic Modes

In a virtual displacement $\delta u_{sn}(x)$, the total virtual work done on the blade chord per unit span is given by

$$\delta W_s/\text{span} = \int_{x=0}^{2\ell_s} p_{sn}(x)\,\delta u_{sn}(x)\,dx \qquad \text{A (13)}$$

$$= \tfrac{1}{2}\rho_s V_s^2 \ell_s^2 \int_0^2 \delta[\eta]_{sg}\,\{\Phi_{sg}(x)\}[\Pi_p(x)]\,[C_{gp}]^T\{\eta_{sg}\}\,d\left(\frac{x}{\ell_s}\right)$$

$$= \tfrac{1}{2}\rho_s V_s^2 \ell_s^2\,\delta[\eta_{sg}] \int_0^2 \{\Phi_{sg}\}[\Pi_p]\,d\left(\frac{x}{\ell_s}\right)[C_{gp}]^T\{\eta_{sg}\}$$

$$= \tfrac{1}{2}\rho_s V_s^2 \ell_s^2\,\delta[\eta_{sg}]\,[I_{gp}][C_{gp}]^T\{\eta_{sg}\} \qquad \text{A (14)}$$

The integrals defining the elements of the matrix $[I_{gp}]$ for both subsonic and supersonic flow are discussed in Appendix C.

The aerodynamic generalized force per unit span for streamline s is, therefore, given by

$$\{A_{sg}\} = \frac{\delta W_s/\text{span}}{\delta \eta_{sg}}$$

$$= \tfrac{1}{2}\rho_s V_s^2 \ell_s^2\,[I_{gp}][C_{gp}]^T\{\eta_{sg}\}$$

$$= [A_{sgg}]\{\eta_{sg}\} \qquad \text{A (15)}$$

whereby the generalized airforce matrix per unit span for chordwise aerodynamic modes is expressed by

$$[A_{sgg}] = \tfrac{1}{2}\rho_s V_s^2 \ell_s^2 [I_{gp}][C_{gp}]^T . \qquad A(16)$$

The matrix $[C_{gp}]^T$ in the above equation is evaluated from equationA11 as follows. Transposing both sides of equationA11,

$$[\Psi_{sg}(x)] = [\Pi_p(x)][C_{gp}]^T ,$$

and for all points P on the blade chord at which aerodynamic differential pressures are estimated, we have

$$[\Psi_{spg}] = [\Pi_{pp}][C_{gp}]^T$$

and, therefore,

$$[C_{gp}]^T = [\Pi_{pp}]^{-1}[\Psi_{spg}] . \qquad A(17)$$

A.4 Transformation Between Aerodynamic & Structural Modal Coordinates

Referring to Figure A.1, if $\{u^{\ell}_{bsg}\}$ represents the 3 translational dofs at any grid point g along the streamline s, expressed in the local streamline coordinate system, we can write the normal displacement

$$u^{\ell}_{bsgn} = [0 \quad 1 \quad 0]\{u^{\ell}_{bsg}\} \qquad A(18)$$

i.e.,

$$u^{\ell}_{bsgn} = \begin{bmatrix} 0 & 1 & 0 \end{bmatrix} [T_s^{b\ell}] \{u^{b}_{bsg}\}$$

$$= \begin{bmatrix} 0 & 1 & 0 \end{bmatrix} [T_s^{b\ell}] [T_g^{bg}]^{T} \{u^{g}_{bsg}\} \,, \quad \left([T_g^{bg}]^{-1} = [T_g^{bg}]^{T} \right)$$

For all the grid points on the streamline s, therefore,

$$\{u^{\ell}_{bsgn}\} = \begin{bmatrix} 0 & 1 & 0 \\ 0 & 1 & 0 \\ & \vdots & \\ 0 & 1 & 0 \end{bmatrix} \left[T_s^{b\ell} \mid T_s^{b\ell} \mid \cdots \mid T_s^{b\ell} \right] \begin{bmatrix} [T_1^{bg}]^{T} & & & \\ & [T_2^{bg}]^{T} & & 0 \\ & & \ddots & \\ & & & [T_G^{bg}]^{T} \end{bmatrix} \{u^{g}_{bsg}\} \qquad A(19)$$

OR

$$\{u^{\ell}_{bsgn}\} = [G_n] \{u^{g}_{bsg}\} \,. \qquad A(20)$$

The normal displacements $\{u^{\ell}_{bsgn}\}$ can also be expressed as linear combinations of structural and aerodynamic mode shapes. (See Figure A.2)

$$\{u^{\ell}_{bsgn}\} = \underset{\text{(i structural modes)}}{[\phi^{\ell}_{bsgni}]} \{\}_i\} = \ell_s \underset{\text{(g aerodynamic modes)}}{[\Phi_{sgg}]} \{\eta_{sg}\} \,, \qquad A(21)$$

where

$$[\phi^{\ell}_{bsgni}] = [G_n][\phi^{g}_{bsgi}] \quad , \qquad A(22)$$

$$[\Phi_{sgg}] = \begin{bmatrix} 1 & \frac{x_1}{\ell_s} & \sin\left(\frac{\overline{3-2}\,\pi x_1}{2\ell_s}\right) & \cdots & \sin\left(\frac{\overline{G-2}\,\pi x_1}{2\ell_s}\right) \\ 1 & \frac{x_2}{\ell_s} & \sin\left(\frac{\overline{3-2}\,\pi x_2}{2\ell_s}\right) & \cdots & \sin\left(\frac{\overline{G-2}\,\pi x_2}{2\ell_s}\right) \\ \vdots & \vdots & \vdots & \vdots & \vdots \\ 1 & \frac{x_g}{\ell_s} & \sin\left(\frac{\overline{3-2}\,\pi x_g}{2\ell_s}\right) & \cdots & \sin\left(\frac{\overline{G-2}\,\pi x_g}{2\ell_s}\right) \\ \vdots & \vdots & \vdots & \vdots & \vdots \\ 1 & \frac{x_G}{\ell_s} & \sin\left(\frac{\overline{3-2}\,\pi x_G}{2\ell_s}\right) & \cdots & \sin\left(\frac{\overline{G-2}\,\pi x_G}{2\ell_s}\right) \end{bmatrix} , \qquad A(23)$$

and $\{\eta_{sg}\}$ is given by equation A(6).

From equation A(21), therefore, we have

$$\{\eta_{sg}\} = \frac{1}{\ell_s}[\Phi_{sgg}]^{-1}[\phi^{\ell}_{bsgni}]\{\}_i\}$$

$$= \frac{1}{\ell_s}[G_{gi}]\{\}_i\} \quad , \qquad A(24)$$

where

$$[G_{gi}] = [\Phi_{sgg}]^{-1}[\phi^{\ell}_{bsgni}] \qquad A(25)$$

defines the transformation from the aerodynamic to the structural modes.

A.5 Generalized Airforce Matrix for Chordwise Structural Modes

In a virtual displacement $\delta u_{sn}(x)$, the total virtual work done on the blade chord s per unit span is expressed by equation A(14). Substituting for η_{sg} from equation A(24), the virtual work becomes

$$\delta W_s/\text{span} = \tfrac{1}{2}\rho_s V_s^2 \ell_s^2 \cdot \frac{1}{\ell_s^2} \delta L\}_i \,] [G_{gi}]^T [I_{gp}][C_{gp}]^T [G_{gi}] \{\}_i\},$$

which, by equation A(16), can be written as

$$= \delta L\}_i \,] [G_{gi}]^T \left(\frac{1}{\ell_s^2} [A_{sgg}] \right) [G_{gi}] \{\}_i\} \quad . \qquad \text{A(26)}$$

The generalized aerodynamic force per unit span for streamline s is, therefore given as

$$\{Q_{si}\} = \frac{\delta W_s/\text{span}}{\delta \}_i}$$

$$= [G_{gi}]^T \left(\frac{1}{\ell_s^2} [A_{sgg}] \right) [G_{gi}] \{\}_i\} \quad , \qquad \text{A(27)}$$

and the generalized airforce matrix, per unit span, for chordwise structural modes on streamline s is given by

$$[Q_{sii}] = [G_{gi}]^T \left(\frac{1}{\ell_s^2} [A_{sgg}] \right) [G_{gi}] \quad . \qquad \text{A(28)}$$

These chordwise aerodynamic matrices are calculated for streamlines with subsonic or supersonic inflow, and interpolated for other streamlines with transonic inflow.

A.6 Blade Generalized Airforce Matrix

The virtual work done by the airforces on the entire blade is the integral of the virtual work done on all the streamlines across the blade span, i.e.,

$$\delta W_{blade} = \int_{R_r}^{R_t} \delta W_s / span \cdot dr$$

$$= \delta \{\xi\}_i^T \int_{R_r}^{R_t} [Q_{sii}]\, dr\, \{\xi\}_i \,, \qquad \text{(By equations A(26) and A(28))}$$

whence the aerodynamic force vector for the blade becomes

$$\{Q_i\} = \delta W_{blade} / \delta \{\xi\}_i$$

$$= \int_{R_r}^{R_t} [Q_{sii}]\, dr\, \{\xi\}_i$$

$$= [Q_{ii}]\{\xi\}_i \,. \qquad \text{A (29)}$$

The generalized airforce matrix for the entire blade is, therefore, given by

$$[Q_{ii}] = \int_{R_r}^{R_t} [Q_{sii}]\, dr = \sum_{s=1}^{S} [Q_{sii}]\, \Delta r \,,$$

or,

$$[Q_{ii}] = \begin{bmatrix} \sum_s LQ_{s11}\rfloor \{W(r)\} & \sum_s LQ_{s12}\rfloor \{W\} & \cdots & \sum_s LQ_{s1I}\rfloor \{W\} \\ \sum_s LQ_{s21}\rfloor \{W\} & \sum_s LQ_{s22}\rfloor \{W\} & \cdots & \sum_s LQ_{s1I}\rfloor \{W\} \\ \vdots & \vdots & \vdots & \vdots \\ \sum_s LQ_{sI1}\rfloor \{W\} & \sum_s LQ_{sI2}\rfloor \{W\} & \cdots & \sum_s LQ_{sII}\rfloor \{W\} \end{bmatrix} \,, \qquad \text{A (30)}$$

where, for the trapezoidal rule of integration across the blade span, the integration matrix $\{W(r)\}$ is given by

$$\{W(r)\} = \frac{1}{2} \begin{Bmatrix} R_2 - R_1 \\ R_3 - R_1 \\ R_4 - R_2 \\ \vdots \\ R_{s+1} - R_{s-1} \\ \vdots \\ R_S - R_{S-2} \\ R_S - R_{S-1} \end{Bmatrix} \qquad A(31)$$

APPENDIX B.

EQUATIONS OF MOTION FOR CYCLIC MODAL AND FLUTTER ANALYSES

The equations of motion of a bladed-shrouded disc for cyclic modal and flutter analyses are derived via the Lagrange formulation,

$$\frac{d}{dt}\left(\frac{\partial T}{\partial \dot{q}_i}\right) + \frac{\partial U}{\partial q_i} = \frac{\partial W}{\partial q_i} \quad , \; i = 1, 2, \cdots, K \; , \qquad \text{B(1)}$$

where the q_i represent the total degrees of freedom considered in the problem. This form and notation of the equations developed is compatible with that described in Section 4.5 of Reference 7

B.1 Independent Solution Degrees of Freedom

Consider a bladed-shrouded disc with N cyclically symmetric segments as shown in Figure A-3, Appendix A. In any segment n, the physical displacements are given by

$$\{u\}^n = \{\bar{u}\}^0 + \sum_{k=1}^{k_L} \{\bar{u}\}^{kc} \cos\left(\overline{n-1}\, k\alpha\right) + \{\bar{u}\}^{ks} \sin\left(\overline{n-1}\, k\alpha\right) + (-1)^{n-1} \{\bar{u}\}^{N/2} \; , \qquad \text{B(2)}$$

where k is the harmonic number, n the segment being considered, and $\alpha = 2\pi/N$. The last term of equation B(2) exists only when N is even. The upper limit of the harmonic numbers considered, k_L, is given by

$$k_L = (N-2)/2 \quad , \text{ for } N \text{ even} \; ,$$

and

$$= (N-1)/2 \quad , \text{ for } N \text{ odd} \; . \qquad \text{B(3)}$$

For a given harmonic number k, equation B(2) can be written as .

$$\{u\}^{n,k} = \{\bar{u}\}^{kc} \cos\left(\overline{n-1}\, k\alpha\right) + \{\bar{u}\}^{ks} \sin\left(\overline{n-1}\, k\alpha\right) \; . \qquad \text{B(4)}$$

In a cyclic sector, each of the total degrees of freedom can be described as being on either of the two boundaries of the sector, or within the sector. The degrees of freedom on the sector boundaries are also required to observe the inter-segment compatibility constraints (see Section 4.5, Ref. 7). An independent solution set, $\{\bar{u}\}^K$, comprising the degrees of freedom within, and on one of the boundaries of the sector, therefore, is defined as

$$\{\bar{u}\}^{kc} = [G_{ck}(k)]\{\bar{u}\}^K, \qquad \text{B (5)}$$

and

$$\{\bar{u}\}^{ks} = [G_{sk}(k)]\{\bar{u}\}^K,$$

where each row of the transformation matrices G_{ck} or G_{sk} contains only one or two non-zero terms (see Section 4.5, Ref. 7).

In terms of the independent solution degrees of freedom, equation (4), therefore, can be restated as

$$\{u\}^{n,k} = \left[[G_{ck}]\cos(\overline{n-1}\,ka) + [G_{sk}]\sin(\overline{n-1}\,ka)\right]\{\bar{u}\}^K. \qquad \text{B (6)}$$

B.2 Bladed Disc Kinetic Energy

The kinetic energy in segment n for harmonic k motion can be written as

$$T^{n,k} = \tfrac{1}{2}\{\dot{u}\}^{n,k}[M]\{\dot{u}\}^{n,k}, \qquad \text{B (7)}$$

which, by equation B(6), becomes

$$T^{n,k} = \tfrac{1}{2}\{\dot{\bar{u}}\}^K\Big[[G_{ck}]^T[M][G_{ck}]\cos^2(\overline{n-1}\,ka) + [G_{sk}]^T[M][G_{sk}]\sin^2(\overline{n-1}\,ka) + [G_{ck}]^T[M][G_{sk}]\cos(\overline{n-1}\,ka)\cdot\sin(\overline{n-1}\,ka) + [G_{sk}]^T[M][G_{ck}]\cos(\overline{n-1}\,ka)\cdot\sin(\overline{n-1}\,ka)\Big]\{\dot{\bar{u}}\}^K. \qquad \text{B (8)}$$

Summing over all the segments, the bladed-disc kinetic energy in the kth harmonic motion can be expressed as

$$T^k = \sum_{n=1}^{N} T^{n,k}$$

$$= \tfrac{1}{2} \left\lfloor \dot{\bar{u}} \right\rfloor^K \Big[[G_{ck}]^T [M] [G_{ck}] \sum_n \cos^2\left(\overline{n-1}\, ka\right) + [G_{sk}]^T [M] [G_{sk}] \sum_n \sin^2\left(\overline{n-1}\, ka\right)$$

$$+ [G_{ck}]^T [M] [G_{sk}] \sum_n \cos\left(\overline{n-1}\, ka\right) \cdot \sin\left(\overline{n-1}\, ka\right)$$

$$+ [G_{sk}]^T [M] [G_{ck}] \sum_n \cos\left(\overline{n-1}\, ka\right) \cdot \sin\left(\overline{n-1}\, ka\right) \Big] \{\dot{\bar{u}}\}^K .$$

By the orthogonality relation between the sine and the cosine functions, this simplifies to

$$T^k = \frac{N}{4} \left\lfloor \dot{\bar{u}} \right\rfloor^K [\bar{M}]^K \{\dot{\bar{u}}\}^K , \qquad B(9)$$

where

$$[\bar{M}]^K = [G_{ck}]^T [M] [G_{ck}] + [G_{sk}]^T [M] [G_{sk}] . \qquad B(10)$$

B.3 Bladed Disc Strain Energy

The sum total of strain energy in all the cyclic segments N of the bladed-disc represents the total strain energy in the bladed-disc. Therefore, by reasoning on lines similar to those used for the kinetic energy term, the strain energy is expressed as

$$U^k = \frac{N}{4} \left\lfloor \bar{u} \right\rfloor^K [\bar{K}]^K \{\bar{u}\}^K \qquad B(11)$$

with

$$[\bar{K}]^K = [G_{ck}]^T [K] [G_{ck}] + [G_{sk}]^T [K] [G_{sk}] . \qquad B(12)$$

B.4 Virtual Work Done On The Bladed-Disc

The oscillatory external forces acting on the blades of a bladed-disc of an axial flow turbomachine are those due to the compressible airflow past the oscillating blades. These aerodynamic forces per unit generalized displacement, [Q], depend upon the operating point of the turbomachine (flowrate, rotational speed, etc.) and the flow parameters (Mach No., inter-blade phase angle, reduced frequency, etc.).

The virtual work done by the airforces in any segment n and harmonic k motion, in a virtual displacement $\delta u^{n,k}$ is, therefore, given by

$$\delta W^{n,k} = \delta \{u\}^{n,k} [Q] \{u\}^{n,k}$$

$$= \left(\tfrac{1}{2}\rho V^2\right)_{ref.} \delta \{u\}^{n,k} [Q'] \{u\}^{n,k} . \qquad B(13)$$

The virtual work done on the entire bladed-disc, therefore, becomes

$$\delta W^{k} = \sum_{n=1}^{N} \delta W^{n,k}$$

$$= \left(\tfrac{1}{2}\rho V^2\right)_{ref.} \frac{N}{2} \delta \{\bar{u}\}^{K} [\bar{Q}']^{K} \{\bar{u}\}^{K} , \qquad B(14)$$

where

$$[\bar{Q}']^{K} = [G_{ck}]^{T} [Q'] [G_{ck}] + [G_{sk}]^{T} [Q'] [G_{sk}] . \qquad B(15)$$

B.5 Equations Of Motion

Substitution of the expressions for the kinetic energy (equation B9), strain energy (equation B11) and the virtual work (equation B14) in the Lagrange formulation (equation B1) with $q \equiv \bar{u}^{K}$ results in the equations of motion as

$$\frac{N}{2} [\bar{M}]^{K} \{\ddot{\bar{u}}\}^{K} + \frac{N}{2} [\bar{K}]^{K} \{\bar{u}\}^{K} = \frac{N}{2} \left(\tfrac{1}{2}\rho V^2\right)_{ref} [\bar{Q}']^{K} \{\bar{u}\}^{K} , \qquad B(16)$$

or

$$[\bar{M}]^K\{\ddot{\bar{u}}\}^K + [\bar{K}]^K\{\bar{u}\}^K - \left(\tfrac{1}{2}\rho V^2\right)_{ref}[\bar{Q}']^K\{\bar{u}\}^K = \{0\} \qquad B(17)$$

B.6 Cyclic Modal Analysis

For the k^{th} harmonic motion of the bladed-disc, the equations of motion, equation B17, are reduced to the eigenvalue problem ,

$$\left[-\omega^2[\bar{M}]^K + [\bar{K}]^K\right]\{\bar{u}\}^K = \{0\} \qquad B(18)$$

The K eigenvalues $\lambda^K(-\omega^2{}'s)$ and the associated eigenvectors $[\bar{\phi}]^K$ represent the modal characteristics of the bladed-disc in the k^{th} harmonic. The cosine and sine components of the eigenvectors $[\bar{\phi}]^K$ are recovered as

$$[\bar{\phi}]^{kc} = [G_{ck}(k)][\bar{\phi}]^K , \qquad B(19)$$

and

$$[\bar{\phi}]^{ks} = [G_{sk}(k)][\bar{\phi}]^K .$$

B.7 Cyclic Modal Flutter Analysis

As a result of the cyclic modal analysis (Section B.6 above), the independent solution degrees of freedom $\{\bar{u}\}^K$ can be expressed as

$$\{\bar{u}\}^K = [\bar{\phi}]^K\{\bar{\bar{\xi}}\}^K \qquad B(20)$$

Substituting for $\{\bar{u}\}^K$ in equation B(17), and premultiplying by $[\bar{\phi}^K]^T$, results in

$$\left[-\omega^2[\bar{\phi}^K]^T[\bar{M}]^K[\bar{\phi}]^K + [\bar{\phi}^K]^T[\bar{K}]^K[\bar{\phi}]^K - \left(\tfrac{1}{2}\rho V^2\right)_{ref}[\bar{\phi}^K]^T[\bar{Q}']^K[\bar{\phi}]^K\right]\{\bar{\bar{\xi}}\}^K = \{0\} \qquad B(21)$$

If the expressions for $[\bar{M}]^K$ (equation B10), $[\bar{K}]^K$ (equation B12) and $[\bar{Q}']^K$ (equation B15) are now introduced into equation B(21) above, the result is

$$\Big[-\omega^2[\bar{\phi}^K]^T[G_{ck}]^T[M][G_{ck}][\bar{\phi}]^K + [\bar{\phi}^K]^T[G_{ck}]^T[K][G_{ck}][\bar{\phi}]^K - (\tfrac{1}{2}\rho V^2)_{ref}[\bar{\phi}^K]^T[G_{ck}]^T[Q'][G_{ck}][\bar{\phi}]^K$$
$$-\omega^2[\bar{\phi}^K]^T[G_{sk}]^T[M][G_{sk}][\bar{\phi}]^K + [\bar{\phi}^K]^T[G_{sk}]^T[K][G_{sk}][\bar{\phi}]^K$$
$$-(\tfrac{1}{2}\rho V^2)_{ref}[\bar{\phi}^K]^T[G_{sk}]^T[Q'][G_{sk}][\bar{\phi}]^K\Big]\{\bar{\xi}\}^K = \{0\}. \quad B(22)$$

By equation B(19), this can be restated as

$$\Big[-\omega^2[\bar{\phi}^{kc}]^T[M][\bar{\phi}]^{kc} + [\bar{\phi}^{kc}]^T[K][\bar{\phi}]^{kc} - (\tfrac{1}{2}\rho V^2)_{ref}[\bar{\phi}^{kc}]^T[Q'][\bar{\phi}]^{kc}\Big]\{\bar{\xi}\}^K$$
$$+\Big[-\omega^2[\bar{\phi}^{ks}]^T[M][\bar{\phi}]^{ks} + [\bar{\phi}^{ks}]^T[K][\bar{\phi}]^{ks} - (\tfrac{1}{2}\rho V^2)_{ref}[\bar{\phi}^{ks}]^T[Q'][\bar{\phi}]^{ks}\Big]\{\bar{\xi}\}^K = \{0\}. \quad B(23)$$

In equation B(23), the <u>cosine</u> eigenvectors $[\bar{\phi}]^{kc}$ and the <u>sine</u> eigenvectors $[\bar{\phi}]^{ks}$ are both self and jointly orthogonal and the mode <u>shapes</u> represented by $[\bar{\phi}]^{kc}$ and $[\bar{\phi}]^{ks}$ are identical up to a constant spatial phase difference between them. Therefore, either the sine or cosine parts of the equation B(23) can be independently used for cyclic modal flutter analysis. That is, a sufficient set of equations of motion for flutter analysis is

$$\Big[-\omega^2[\bar{\phi}^{kc}]^T[M][\bar{\phi}]^{kc} + [\bar{\phi}^{kc}]^T[K][\bar{\phi}]^{kc} - (\tfrac{1}{2}\rho V^2)_{ref}[\bar{\phi}^{kc}]^T[Q'][\bar{\phi}]^{kc}\Big]\{\bar{\xi}\}^K = \{0\}, \quad B(24)$$

<u>or</u>

$$\Big[-\omega^2[\bar{\phi}^{ks}]^T[M][\bar{\phi}]^{ks} + [\bar{\phi}^{ks}]^T[K][\bar{\phi}]^{ks} - (\tfrac{1}{2}\rho V^2)_{ref}[\bar{\phi}^{ks}]^T[Q'][\bar{\phi}]^{ks}\Big]\{\bar{\xi}\}^K = \{0\}. \quad B(25)$$

APPENDIX C.

CHORDWISE WEIGHTING FACTORS

The chordwise weighting matrix $[I_{gp}]$ (Appendix A) is defined as

$$[I_{gp}] = \int_0^2 \{\Phi_{sg}(x)\} \left[TT_{p,\substack{sub.\\ or\ sup.}}(x)\right] d(x/\ell_s) \qquad C(1)$$

where $\{\Phi_{sg}(x)\}$, $[TT_{p,sub.}(x)]$ and $[TT_{p,sup.}(x)]$ are given by equations (A-5), (A-9) and (A-10), respectively in Appendix A.

For subsonic flow, $[I_{gp}]$ can be expressed as

$$[I_{gp}]_{sub.} = \begin{bmatrix} I_{\sqrt{}} & I_{1.} & I_{2.} & \cdots & I_{(P-1).} \\ I_{x\sqrt{}} & I_{x.1} & I_{x.2} & \cdots & I_{x.(P-1).} \\ I_{1.\sqrt{}} & I_{1.1} & I_{1.2} & \cdots & I_{1.(P-1)} \\ I_{2.\sqrt{}} & I_{2.1} & I_{2.2} & \cdots & I_{2.(P-1)} \\ \vdots & \vdots & \vdots & \vdots & \vdots \\ I_{(G-2).\sqrt{}} & I_{(G-2).1} & I_{(G-2).2} & \cdots & I_{(G-2).(P-1)} \end{bmatrix} \qquad C(2)$$

and for supersonic flow, $[I_{gp}]$ is given by

$$[I_{gp}]_{sup.} = \begin{bmatrix} 2 & 2 & I_{1.} & I_{2.} & \cdots & I_{(P-2).} \\ 2 & 8/3 & I_{x.1} & I_{x.2} & \cdots & I_{x.(P-2)} \\ I_{1.} & I_{1.x} & I_{1.1} & I_{1.2} & \cdots & I_{1.(P-2)} \\ I_{2.} & I_{2.x} & I_{2.1} & I_{2.2} & \cdots & I_{2.(P-2)} \\ \vdots & \vdots & \vdots & \vdots & \vdots & \vdots \\ I_{(G-2).} & I_{(G-2).x} & I_{(G-2).1} & I_{(G-2).2} & \cdots & I_{(G-2).(P-2)} \end{bmatrix} , \qquad C\ (3)$$

where

$$\left.\begin{aligned} I_{\sqrt{\ }} &= \int_0^2 \sqrt{\frac{2\ell_s - x}{x}}\, d(x/\ell_s) , \\ I_{r.} &= \int_0^2 \sin\left(\frac{r.\pi.x}{2\ell_s}\right) d(x/\ell_s) , \quad r = 1, 2, \cdots , \\ I_{x\sqrt{\ }} &= \int_0^2 \left(\frac{x}{\ell_s}\right) \sqrt{\frac{2\ell_s - x}{x}}\, d(x/\ell_s) , \\ I_{x.r} &= \int_0^2 \left(\frac{x}{\ell_s}\right) \sin\left(\frac{r.\pi.x}{2\ell_s}\right) d(x/\ell_s) , \quad r = 1, 2, \cdots , \\ I_{r.\sqrt{\ }} &= \int_0^2 \sin\left(\frac{r.\pi.x}{2\ell_s}\right) . \sqrt{\frac{2\ell_s - x}{x}}\, d(x/\ell_s) , \quad r = 1, 2, \cdots , \\ I_{r.s} &= \int_0^2 \sin\left(\frac{r.\pi.x}{2\ell_s}\right) . \sin\left(\frac{s.\pi.x}{2\ell_s}\right) d(x/\ell_s) , \quad r, s = 1, 2, \cdots . \end{aligned}\right\} \qquad (C\text{-}4)$$

Each of the integrals of equation (4) is evaluated as follows:

1. $$I_{\sqrt{\ }} = \int_0^2 \sqrt{\frac{2\ell_s - x}{x}}\, d(x/\ell_s) .$$

Substituting $x = \ell_s(1+\cos\theta)$,

$$I_{\sqrt{}} = \pi \ .$$

2. $$I_{r.} = \int_0^2 \sin\left(\frac{r.\pi.x}{2\ell_s}\right) d(x/\ell_s) \ , \quad r=1,2,\ldots$$

$$= \frac{2}{\pi r}\left[1-(-1)^r\right] \ .$$

3. $$I_{x.\sqrt{}} = \int_0^2 \left(\frac{x}{\ell_s}\right)\sqrt{\frac{2\ell_s - x}{x}}\, d(x/\ell_s) \ .$$

Substituting $x = \ell_s(1+\cos\theta)$,

$$I_{x\sqrt{}} = \pi/2 \ .$$

4. $$I_{x.r} = \int_0^2 \left(\frac{x}{\ell_s}\right)\sin\left(\frac{r.\pi.x}{2\ell_s}\right) d(x/\ell_s) \ , \quad r=1,2,\ldots$$

Integrating by parts

$$I_{xr} = \frac{4}{r\pi}(-1)^{r+1}$$

5. $$I_{r.\sqrt{}} = \int_0^2 \sin\left(\frac{r.\pi.x}{2\ell_s}\right)\sqrt{\frac{2\ell_s - x}{x}}\, d(x/\ell_s) \ , \quad r=1,2,\ldots$$

Substituting $x = 2\ell_s(1-y)$,

$$I_{r.\sqrt{}} = -2\cos(r\pi)\int_0^1 \sqrt{\frac{y}{1-y}}\, \sin(r\pi y)\, dy$$

Ref.31, Section 3.768 gives

$$\frac{I}{r\sqrt{}} = \frac{2i\cos(r\pi)}{2} B\left(\tfrac{1}{2},\tfrac{3}{2}\right)\left[{}_1F_1\left(\tfrac{3}{2},2,i\pi r\right) - {}_1F_1\left(\tfrac{3}{2},2,-i\pi r\right)\right]$$

$$= \frac{i\pi\cos(r\pi)}{2}\left[{}_1F_1\left(\tfrac{3}{2},2,i\pi r\right) - {}_1F_1\left(\tfrac{3}{2},2,-i\pi r\right)\right] .$$

Ref. 31, Section 9.210 gives ${}_1F_1(\alpha,\gamma,\gamma) = \Phi(\alpha,\gamma,\gamma)$,

the degenerate hypergeometric function in series form

$$\Phi(\alpha,\gamma,\gamma) = 1 + \sum_{s=0}^{\infty} \frac{\alpha(\alpha+1)\ldots(\alpha+s)}{\gamma(\gamma+1)\ldots(\gamma+s)} \cdot \frac{\gamma^s}{s!}$$

Algebraic reduction results in

$$I_{r\sqrt{}} = \sum_{k=1}^{\infty} \frac{(-1)^{k+r}(4k-1)!\,(\pi r)^{2k-1}}{2^{4k-2}(2k-1)!\,(2k-1)!\,(2k)!}$$

which is rapidly convergent, having monotonically decreasing terms of alternating sign.

6. $$I_{r,s} = \int_0^2 \sin\left(\frac{r\cdot\pi\cdot x}{2\ell_s}\right)\cdot \sin\left(\frac{s\cdot\pi\cdot x}{2\ell_s}\right) d(x/\ell_s)\,, \quad r,s=1,2,\ldots$$

$$= 1 \quad , r=s$$

$$= 0 \quad , r\neq s \,.$$

These integrals completely define all the elements of both subsonic and supersonic $[I_{gp}]$ weighting matrices.

APPENDIX D.

REVISION OF BLADE GEOMETRY IN STATIC ANALYSIS

The blade geometry is constantly revised during the differential stiffness loops of the static Aerothermoelastic (SATE) Design/Analysis of the bladed-shrouded disc. The blade geometry is defined in terms of a set of variables including the blade mesh point coordinates (streamline-computing station intersections, Figure A-1), blade angles, blade chords etc. (See Analytic Meanline Blade Section of Ref. 19). The revision of the principal variables such as the blade mesh coordinates and the blade angles, as a result of the elastic deformation of the blade during the SATE design/analysis is described in this section.

With reference to Figure A-1, consider a blade mesh point defined by the intersection of the streamline s and the computing station g. Now, if the elastic deformations along the basic X, Y and Z directions are respectively given by u_{bsgX}, u_{bsgY} and u_{bsgZ}, the revised basic coordinates of the mesh point can be written as

$$\begin{Bmatrix} X \\ Y \\ Z \end{Bmatrix}_{revised} = \begin{Bmatrix} X \\ Y \\ Z \end{Bmatrix}_{previous} + i_1 \begin{Bmatrix} f_X \cdot u_{bsgX} \\ f_Y \cdot u_{bsgY} \\ f_Z \cdot u_{bsgZ} \end{Bmatrix} , \qquad D(1)$$

where, for 'analysis',

$$i_1 = +1$$

$$f_X, f_Y, f_Z = 1 ,$$

and for 'design'

$$i_1 = -1 ,$$

$$0 < f_X, f_Y, f_Z \leq 1 .$$

The factors f_i have been introduced to aid the SATE Design procedure by controlling the amount of "untwist" in the blade necessary to arrive at the "as manufactured" shape.

The X- and Z- rotations at the blade leading and trailing edges are used to revise the inlet and the exit blade angles as (see Figure A-1).

$$\begin{Bmatrix} \beta_{bs1} \\ \beta_{bsG} \end{Bmatrix}_{revised} = \begin{Bmatrix} \beta_{bs1} \\ \beta_{bsG} \end{Bmatrix}_{previous} - i_1 i_2 \begin{bmatrix} \theta_{bs1Z} & -\theta_{bs1X} & 0 & 0 \\ 0 & 0 & \theta_{bsGZ} & -\theta_{bsGX} \end{bmatrix} \begin{Bmatrix} \cos 2\nu_{bs1} \\ \sin 2\nu_{bs1} \\ \cos 2\nu_{bsG} \\ \sin 2\nu_{bsG} \end{Bmatrix} \quad D(2)$$

where i_1 = +1 for SATE analysis,

= -1 for SATE design,

i_2 = +1 for compressor disc rotation about +X axis, } Right

= -1 for compressor disc rotation about -X axis, } hand rule

and the meridional streamline angle at the blade leading and the trailing edge is given by

$$\begin{Bmatrix} \nu_{bs1} \\ \nu_{bsG} \end{Bmatrix} = \tan^{-1} \begin{Bmatrix} (Z_{bs2} - Z_{bs1})/(X_{bs2} - X_{bs1}) \\ (Z_{bsG} - Z_{bs(G-1)})/(X_{bsG} - X_{bs(G-1)}) \end{Bmatrix} \quad D(3)$$

APPENDIX E

ON CASCADE AERODYNAMICS FOR NON-ZERO HARMONIC AND MISTUNED FLUTTER STUDIES

Cascade aerodynamic theories exist for various Mach number regimes but are generally restricted to identical blade motions with inter-blade phase angle σ as a variable. Since blades undergo identical motion only in the case of zero circumferential harmonic number, ($k = 0$), existing cascade theories are not applicable to $k \neq 0$. Mistuned bladed-disc modes may be expanded in terms of a sum of a harmonic spectrum, and, therefore, appear to require the extension of cascade theories to non-zero harmonic number.

Consider a bladed-disc with N blades, with harmonic number denoted by k and interblade phase angle denoted by σ.

Suppose blades perform vibration denoted by a generalized coordinate u, then for the n'th blade,

$$u_n(k,\sigma) = u_1 \cos(\omega t + \overline{n-1}\,\sigma) \cdot \cos(n-1)\frac{2\pi k}{N} \qquad \text{(E-1)}$$

Thus for zero'th harmonic ($k = 0$) motion,

$$\frac{u_n(0,\sigma)}{u_1} = \cos(\omega t + \overline{n-1}\,\sigma) \qquad \text{(E-2)}$$

and for $\frac{N}{2}$'th harmonic motion,

$$\frac{u_n\left(\frac{N}{2},\sigma\right)}{u_1} = (-1)^{n-1}\cos(\omega t + \overline{n-1}\,\sigma) \qquad \text{(E-3)}$$

For all n, the following relations hold at the denoted values of k and σ for the motion u:

k \ σ	0	$\frac{\pi}{2}$	π	$\frac{3\pi}{2}$	2π	etc
0	$\cos \omega t$	$\cos(\omega t + n-1 \frac{\pi}{2})$	$(-)^{n-1} \cos \omega t$	$\cos(\omega t + n-1 \frac{3\pi}{2})$	$\cos \omega t$	
$\frac{N}{2}$	$(-)^{n-1} \cos \omega t$	$(-)^{n-1} \cos(\omega t + n-1 \frac{\pi}{2})$	$\cos \omega t$	$(-)^{n-1} \cos(\omega t + n-1 \frac{3\pi}{2})$	$(-)^{n-1} \cos \omega t$	

It is seen that motions u are the same for all blades at (k, σ) combinations of:

(1) $(0, 2\pi)$ and $(\frac{N}{2}, \pi)$

(2) $(0, \pi)$ and $(\frac{N}{2}, 2\pi)$

(3) $(0, \frac{\pi}{2})$ and $(\frac{N}{2}, \frac{3\pi}{2})$

(4) $(0, \frac{3\pi}{2})$ and $(\frac{N}{2}, \frac{\pi}{2})$

(3) and (4) may be found by expanding the corresponding expressions.

These relations may be illustrated as follows:

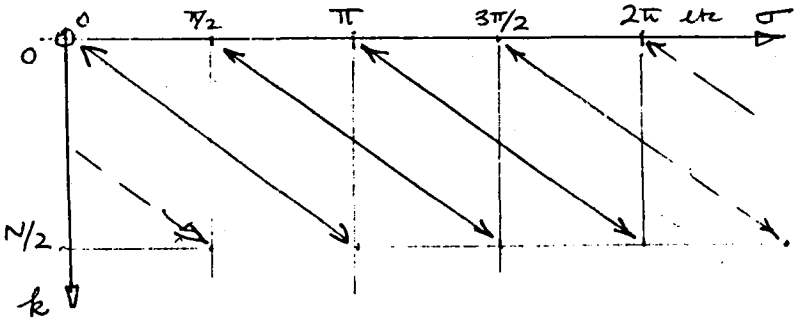

Indicates (k,σ) combinations at which blade motions are identical

It is seen that modes of harmonic number $\frac{N}{2}$ have the same motions as modes of harmonic number zero, when the interblade phase angle is increased by $\pm\pi$ compared with the interblade phase angle for k = 0.

Now the unsteady aerodynamic coefficients may be determined with existing theories along the k = 0 axis, and, therefore, we

may imply them along the $k = \frac{N}{2}$ line by translating the curve by π along the σ axis.

Furthermore for a given σ, we may expect that the variation of any coefficient with harmonic number will be monotonic and smooth from $k = 0$ to $\frac{N}{2}$ (and to tend to zero for k very large, though this is not very relevant).

Therefore, the variation with k may be assumed with reasonable justification to be linear. With this assumption, a plausible variation of cascade aerodynamics with both harmonic number and interblade angle becomes definable. This may be used as a tool for the study of the significance of non-zero harmonic number flutter, and the spectral composition of unsteady aerodynamics for mistuned modes. (See Figure E1)

These studies can then form a basis for a decision on the necessity of formally expanding cascade theories to non-zero harmonic number.

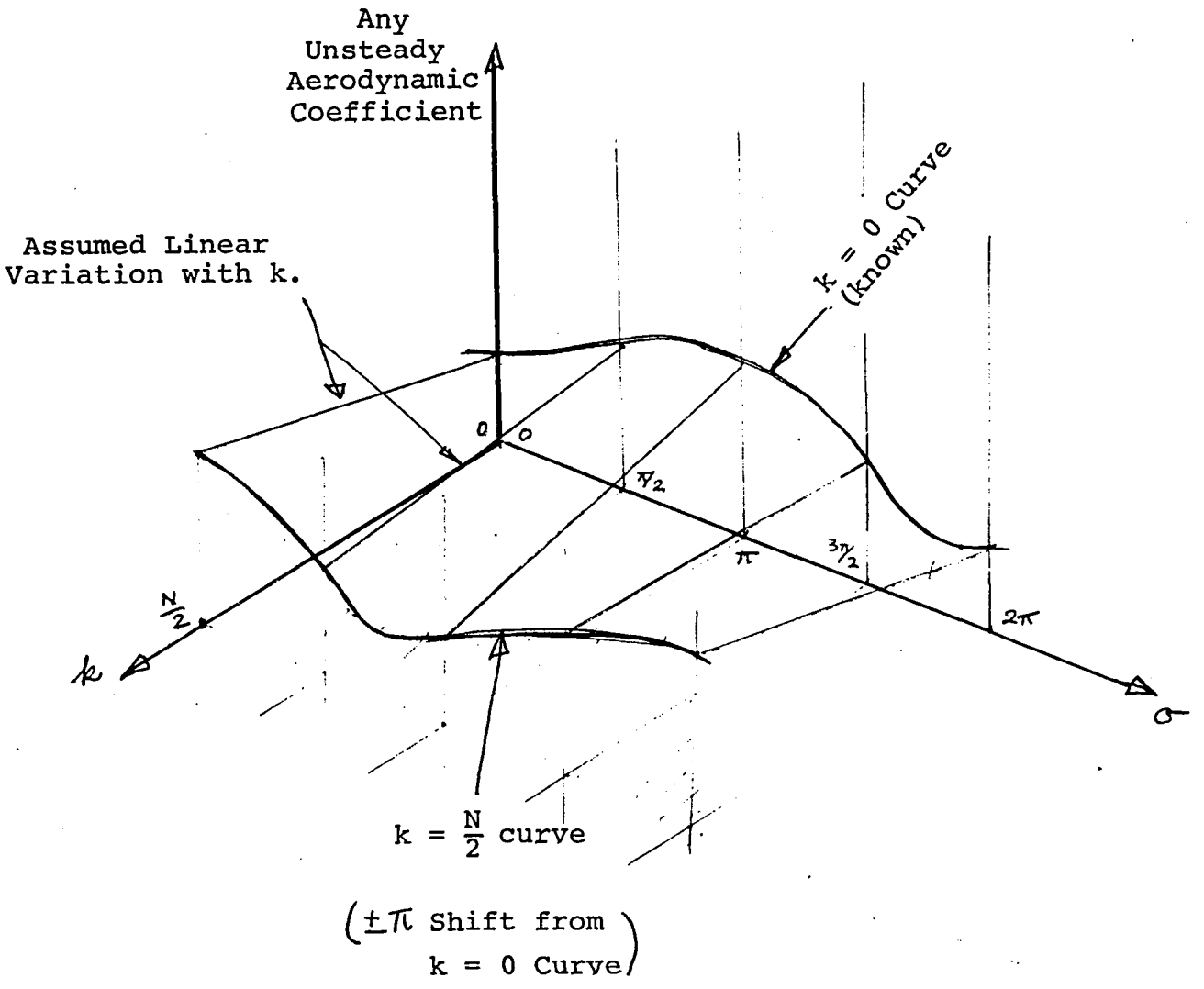

SKETCH OF PLAUSIBLE VARIATION OF UNSTEADY AERODYNAMIC COEFFICIENT WITH k and σ

FIGURE E1

APPENDIX F

EIGENVALUE PROBLEM OF CYCLIC STRUCTURES WITH PRESCRIBED MISTUNING

Structures exhibiting geometric cyclicity with rotational symmetry are considered. Each cyclic segment is permitted a prescribed mistuning in its mass and stiffness properties. The resulting equations of motion of the mistuned structure are expressed in terms of a set of "symmetric components". For a modal formulation, the symmetric components are expanded as a linear combination of the normal modes of the tuned structure for a set of harmonic numbers. The transformed motion equations yield a reduced eigenvalue problem, the degree of reduction being dependent upon the number of tuned normal modes and the harmonic numbers selected. Linearized perturbation theory can be used at this stage to express the eigenvalues of the mistuned structure as a function of those of the tuned structure with small perturbations. If this step is followed, the reduced eigenvalue problem evolves into a set of linear, algebraic equations in the unknown perturbations implying great savings in computational efforts.

F.1 Notation

N — No. of segments $(n = 1, 2, \cdots, N)$

k — Harmonic number $(k = 0, 1, 2, \cdots, k_L$, and N/2 for N even)

k_L = (N-2)/2 for N even; = (N-1)/2 for N odd.

$[M]$ = $[M_{aa}]$, mass matrix for the tuned cyclic segment

$[\Delta M]^n$ — Perturbation mass matrix for segment n, size axa

$[K]$ = $[K_{aa}]$, stiffness matrix for the tuned cyclic segment

$[\Delta K]^n$ — Perturbation stiffness matrix for segment n, size axa

$\{u\}^n = \{u_a\}^n$, displacement d.o.f. in the nth. segment, size axl

$\{\bar{u}\}^x$ — Symmetric components; $x = 0, (1c, 1s), \cdots, (k_L c, k_L s), N/2$ size axl

$\{\bar{u}\}^{K,k}$ — Independent symmetric components for harmonic k, i.e., symmetric components after the intersegment compatibility constraints are applied. Size (internal d.o.f. + side 1 d.o.f.) x 1 = K x 1

F.2 Eigenvalue Formulation

Equations of motion for the mistuned nth. segment are

$$[M + \Delta M^n]\{\ddot{u}\}^n + [K + \Delta K^n]\{u\}^n = \{0\} \quad . \qquad F(1)$$

In order to introduce the symmetric components, consider the sum over the segments,

$$\sum_{n=1}^{N} \left\{ [M + \Delta M^n]\{\ddot{u}\}^n + [K + \Delta K^n]\{u\}^n \right\} = \{0\}$$

Rearranging,

$$[M]\sum_n \{\ddot{u}\}^n + \sum_n [\Delta M]^n \{\ddot{u}\}^n + [K]\sum_n \{u\}^n + \sum_n [\Delta K]^n \{u\}^n = \{0\} \quad . \qquad F(2)$$

By the definition of the symmetric components in terms of $\{u\}^n$, (see NASTRAN THEORY, 4.5-2 Eqn. (2)), Equations F(2) become

$$[N[M] + [\Delta\bar{M}]^{0,oc}]\{\ddot{u}\}^0 + \sum_{k=1}^{k_L} \left([\Delta\bar{M}]^{kc,oc} \{\ddot{u}\}^{kc} + [\Delta\bar{M}]^{ks,oc} \{\ddot{u}\}^{ks} \right)$$

$$+ [\Delta\bar{M}]^{\frac{N}{2},oc} \{\ddot{u}\}^{\frac{N}{2}} + \text{"K-terms"} = \{0\} \quad , \qquad F(3)$$

where

$$[\Delta\bar{M}]^{0,oc} = \sum_{n=1}^{N} [\Delta M]^n$$

$$[\Delta\bar{M}]^{kc,oc} = \sum_n \left(\cos[(n-1)ka] [\Delta M]^n \cos[(n-1).0.a] \right) \quad , \quad a = \frac{2\pi}{N}$$

and $$[\Delta\bar{M}]^{\frac{N}{2},oc} = \sum_n (-1)^{n-1} [\Delta M]^n \quad .$$

Similarly, for a given Harmonic No. H ($=1,2,..,k_L$) form the sum

$$\sum_{n=1}^{N}\left(\cos[(n-1)Ha]\left[[M+\Delta M^n]\{\ddot{u}\}^n+[K+\Delta K^n]\{u\}^n\right]\right) = \{0\}\ .$$

Rearrangement and introduction of the symmetric components and $\{u\}^n$ definitions result in

$$[\Delta\bar{M}]^{0,Hc}\{\ddot{u}\}^0+\sum_{k=1}^{k_L}[\Delta\bar{M}]^{kc,Hc}\{\ddot{u}\}^{kc}+\sum_{k=1}^{k_L}[\Delta\bar{M}]^{ks,Hc}\{\ddot{u}\}^{ks}$$

$$+\left[\tfrac{N}{2}[M]+[\Delta\bar{M}]^{(k=H)c,Hc}_{(-H)}\right]\{\ddot{u}\}^{Hc}$$

$$+[\Delta\bar{M}]^{\frac{N}{2},Hc}\{\ddot{u}\}^{\frac{N}{2}}+\text{"K-terms"}=\{0\}\ , \qquad (4)$$

where

$$[\Delta\bar{M}]^{0,Hc}=\sum_{n=1}^{N}[\Delta M]^n\cos[(n-1)Ha]\ ,$$

$$[\Delta\bar{M}]^{kc,Hc}=\sum_{n}\left[\cos[(n-1)ka][\Delta M]^n\cos[(n-1)Ha]\right]\ ,$$

$$[\Delta\bar{M}]^{ks,Hc}=\sum_{n}\left[\sin[(n-1)ka][\Delta M]^n\cos[(n-1)Ha]\right]\ ,$$

and

$$[\Delta\bar{M}]^{\frac{N}{2},Hc}=\sum_{n}\left[(-1)^{n-1}[\Delta M]^n\cos[(n-1)Ha]\right]\ .$$

A set of equations similar to F(4) is obtained when $H = N/2$ for even N, and we have

$$[\Delta\bar{M}]^{0,\frac{N}{2}c}\{\ddot{u}\}^0+\sum_{k=1}^{k_L}\left([\Delta\bar{M}]^{kc,\frac{N}{2}c}\{\ddot{u}\}^{kc}+[\Delta\bar{M}]^{ks,\frac{N}{2}c}\{\ddot{u}\}^{ks}\right)$$

$$+\left[N[M]+[\Delta\bar{M}]^{\frac{N}{2},\frac{N}{2}c}\right]\{\ddot{u}\}^{\frac{N}{2}}+\text{"K-terms"}=\{0\}\ , \qquad (5)$$

with

$$[\Delta\bar{M}]^{0,\frac{N}{2}c} = \sum_{n=1}^{N} [\Delta M]^n \cos\left[(n-1)\tfrac{N}{2}a\right]$$

$$= \sum_n (-1)^{n-1} [\Delta M]^n \quad ,$$

$$[\Delta\bar{M}]^{kc,\frac{N}{2}c} = \sum_n \left[\cos[(n-1)ka][\Delta M]^n (-1)^{n-1}\right] ,$$

$$[\Delta\bar{M}]^{ks,\frac{N}{2}c} = \sum_n \left[\sin[(n-1)ka][\Delta M]^n (-1)^{n-1}\right] ,$$

and

$$[\Delta\bar{M}]^{\frac{N}{2},\frac{N}{2}c} = \sum_{n=1}^{N} \left[(-1)^{n-1}[\Delta M]^n (-1)^{n-1}\right]$$

$$= \sum_n [\Delta M]^n \quad .$$

The intersegment compatibility constraints are unchanged from NASTRAN THEORY 4.5-6 Eqn. (15), and are

$$\{\bar{u}\}^0 = [G_{ck}(0)]\{\bar{u}\}^{K,0} ,$$

$$\{\bar{u}\}^{kc} = [G_{ck}(k)]\{\bar{u}\}^{K,k} ,$$

$$\{\bar{u}\}^{ks} = [G_{sk}(k)]\{\bar{u}\}^{K,k} ,$$

F(6)

and

$$\{\bar{u}\}^{N/2} = [G_{ck}(\tfrac{N}{2})]\{\bar{u}\}^{K,\frac{N}{2}} .$$

Introducing the constraint Equations F(6) into Equations F(3), F(4) and F(5) yields, respectively,

$$[N[M] + [\Delta\bar{M}]^{0,oc}][G_{ck}(0)]\{\ddot{\bar{u}}\}^{K,0} + \sum_{k=1}^{k_L}\left([\Delta\bar{M}]^{kc,oc}[G_{ck}(k)] + [\Delta\bar{M}]^{ks,oc}[G_{sk}(k)]\right)\{\ddot{\bar{u}}\}^{K,k} + [\Delta\bar{M}]^{\frac{N}{2},oc}[G_{ck}(\tfrac{N}{2})]\{\ddot{\bar{u}}\}^{K,\frac{N}{2}} + \text{"K-terms"} = \{0\}, \quad (H=0), \qquad F(7)$$

$$[\Delta\bar{M}]^{0,Hc}[G_{ck}(0)]\{\ddot{\bar{u}}\}^{K,0} + \sum_{\substack{k=1\\(-H)}}^{k_L}[\Delta\bar{M}]^{kc,Hc}[G_{ck}(k)]\{\ddot{\bar{u}}\}^{K,k} + \sum_{k=1}^{k_L}[\Delta\bar{M}]^{ks,Hc}[G_{sk}(k)]\{\ddot{\bar{u}}\}^{K,k} + \left[\tfrac{N}{2}[M][G_{ck}(H)] + [\Delta\bar{M}]^{(k=H)c,Hc}[G_{ck}(H)]\right]\{\ddot{\bar{u}}\}^{K,H} + [\Delta\bar{M}]^{\frac{N}{2},Hc}[G_{ck}(\tfrac{N}{2})]\{\ddot{\bar{u}}\}^{K,\frac{N}{2}} + \text{"K-terms"} = \{0\}, \quad (H=1,2,\cdots,k_L), \qquad F(8)$$

and

$$[\Delta\bar{M}]^{0,\frac{N}{2}c}[G_{ck}(0)]\{\ddot{\bar{u}}\}^{K,0}$$

$$+\sum_{k=1}^{k_L}\left([\Delta\bar{M}]^{kc,\frac{N}{2}c}[G_{ck}(k)]+[\Delta\bar{M}]^{ks,\frac{N}{2}c}[G_{sk}(k)]\right)\{\ddot{\bar{u}}\}^{k,k}$$

$$+\left[N[M]+[\Delta\bar{M}]^{\frac{N}{2},\frac{N}{2}c}\right][G_{ck}(\tfrac{N}{2})]\{\ddot{\bar{u}}\}^{K,\frac{N}{2}}$$

$$+\text{"K-terms"}=\{0\}\ ,\ (H=\tfrac{N}{2})\ . \qquad F(9)$$

Now, the following steps complete the definition of the equations of motion for the mistuned cyclic structure in the symmetric components.

(1) Premultiply Equations F(7), F(8) and F(9) by $[G_{ck}(0)]^T$, $[G_{ck}(H)]^T$ and $[G_{ck}(\frac{N}{2})]^T$, respectively.

(2) With the use of terms like $\sin[(n-1)H\alpha]$ instead of $\cos[(n-1)H\alpha]$, obtain results similar to those of step (1) above.

(3) Note that $\sin[(n-1)H\alpha] \equiv 0$ for $H=0$ and $N/2$, N even.

Note also that $[G_{sk}(0)] \equiv 0 \equiv [G_{sk}(\frac{N}{2})]$.

(4) Add the corresponding results (same H) of steps (1) and (2) above.

(5) The result is the complete equations of motion for the mistuned cyclic structure in terms of the independent symmetric components, i.e.,

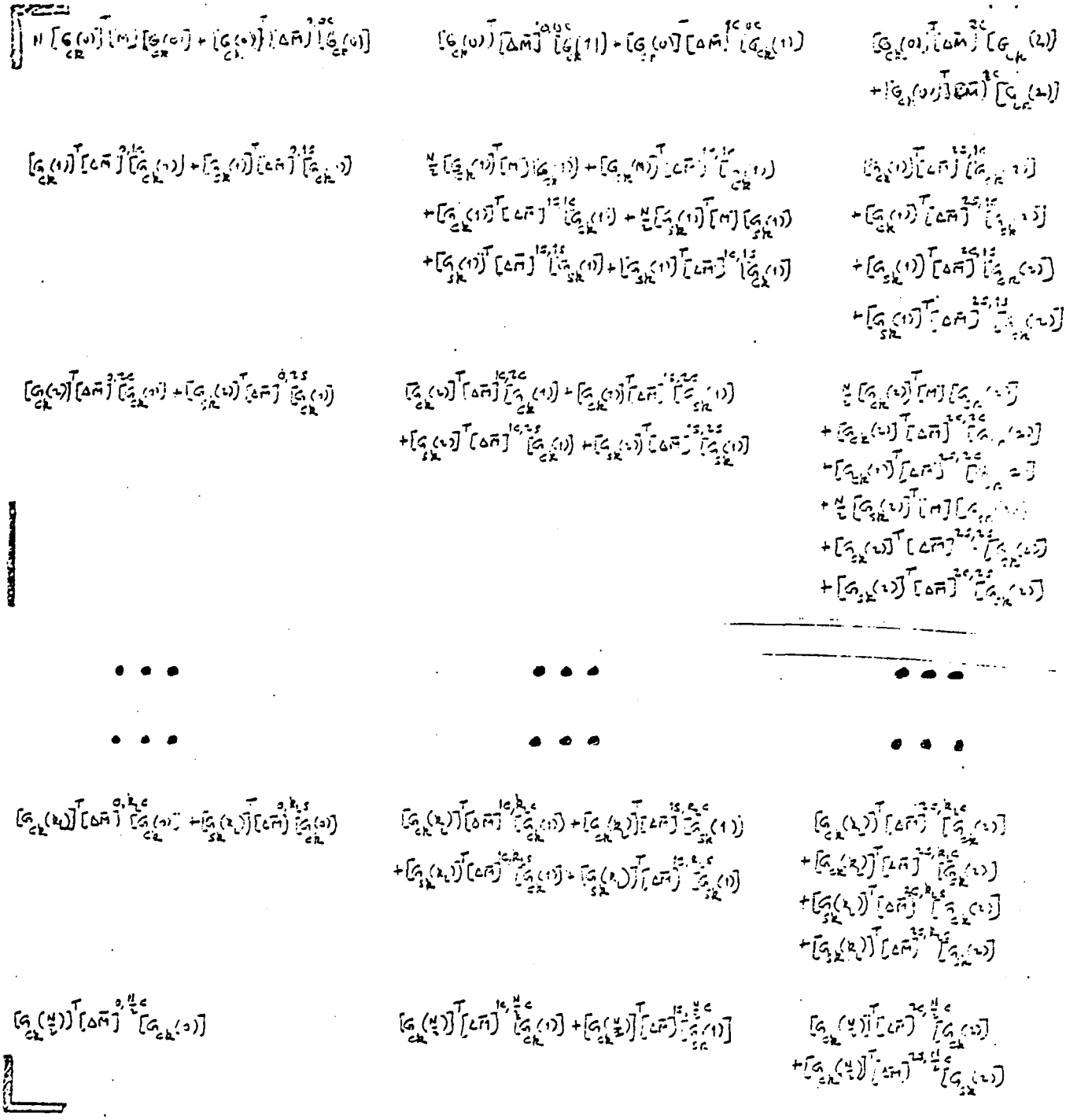

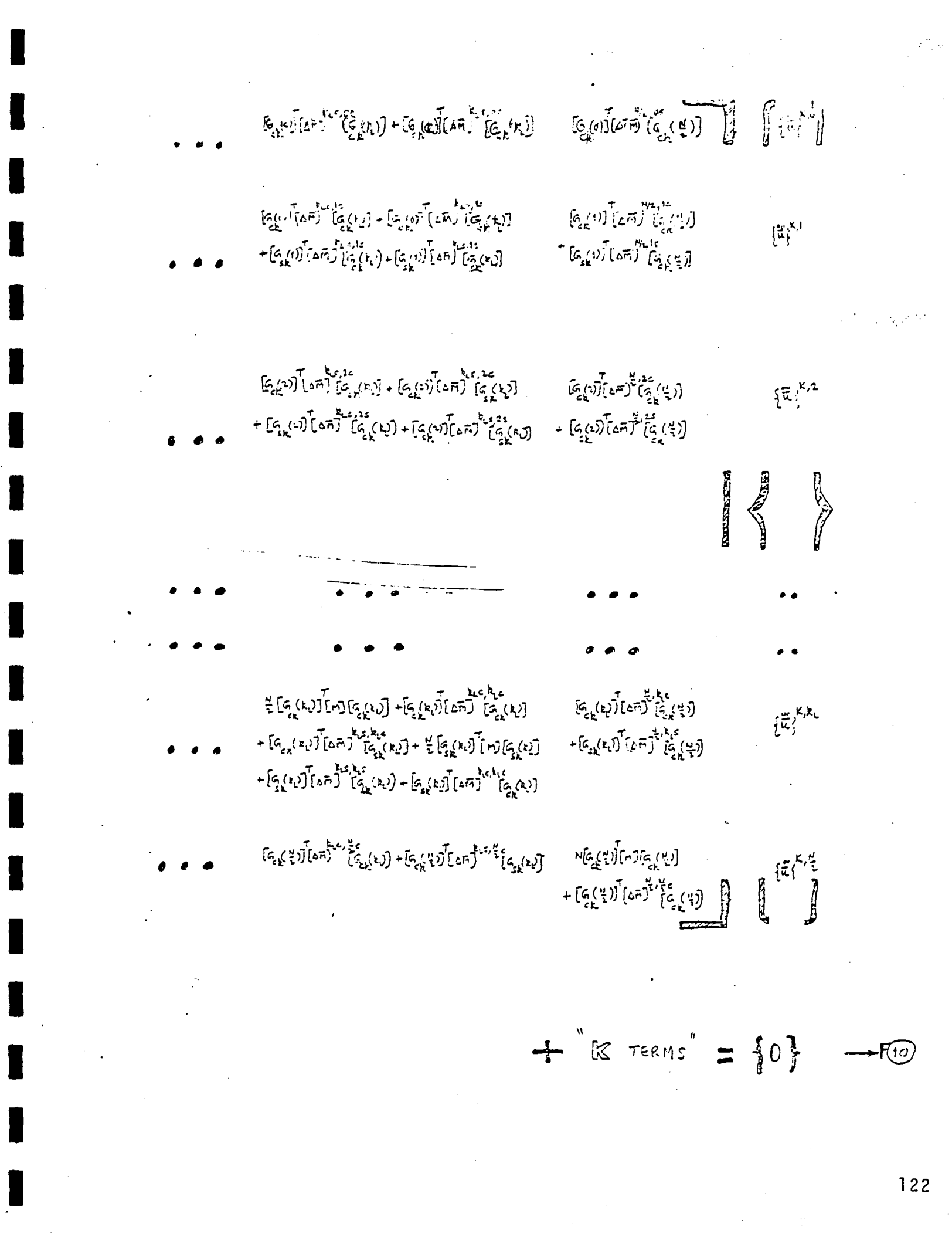

+ "K TERMS" = {0} → F(10)

Equations F(10) illustrate the coupling between the independent symmetric components of various harmonic numbers in a mistuned cyclic structure. The coupling may be seen to depend only on the mass and stiffness perturbations, and these equations degenerate into the sets of harmonically decoupled equations in the symmetric components for a tuned cyclic system.

.3 Mistuned Solution

In their present form, Equations F(10) imply a huge eigenvalue problem comparable in size to the one that would evolve if the entire mistuned structure was considered without regard to its geometric periodicity. However, expansion of the mistuned modes in terms of subsets of the tuned cyclic system harmonic families may be used to greatly reduce the size of the mistuned eigenvalue problem. Further, if small ΔM and ΔK perturbations are assumed, the eigenvalue problem can be reduced to a set of algebraic equations in the unknown eigenvalue perturbations.

As the first step towards the solution, Equations F(10) are written as

$$[\bar{\bar{M}}]^K \{\ddot{\bar{\bar{u}}}\}^K + [\bar{\bar{K}}]^K \{\bar{\bar{u}}\}^K = \{0\} \quad , \qquad F(11)$$

where

$$\{\bar{\bar{u}}\}^K = \begin{Bmatrix} \{\bar{u}\}^{K,0} \\ \{\bar{u}\}^{K,1} \\ \vdots \\ \{\bar{u}\}^{K,k_L} \\ \{\bar{u}\}^{K,\frac{N}{2}} \end{Bmatrix}$$

Introducing $\{\bar{u}\}^K = \{\bar{U}\}^K e^{i\omega t}$ into Equations F(11) results in

$$\left[-\omega^2 [\bar{\bar{M}}]^K + [\bar{\bar{K}}]^K\right] \{\bar{\bar{U}}\}^K = \{0\} \quad , \qquad F(12)$$

where ω^2 are the eigenvalues of the mistuned system and

$$\{\bar{\bar{U}}\}^{K.} = \begin{Bmatrix} \{\bar{U}\}^{K,0} \\ \{\bar{U}\}^{K,1} \\ \vdots \\ \{\bar{U}\}^{K,k_L} \\ \{\bar{U}\}^{K,\frac{N}{2}} \end{Bmatrix}$$

We now expand $\{\bar{U}\}^{K,k}$ as a linear combination of subsets of tuned normal modes of various harmonic numbers. That is,

$$\{\bar{U}\}^{K,k} = [\bar{\phi}]^{K,0}_{\text{Tuned}} \{\bar{\eta}\}^{K,0}_{k} + [\bar{\phi}_T]^{K,1} \{\bar{\eta}\}^{K,1}_{k} + \cdots + [\bar{\phi}_T]^{K,k_L} \{\bar{\eta}\}^{K,k_L}_{k} + [\bar{\phi}_T]^{K,\frac{N}{2}} \{\bar{\eta}\}^{K,\frac{N}{2}}_{k} .$$

Note here that each $\{\bar{\eta}\}^{K,k}_{k}$ may be of arbitrary order, generally <<a. Then,

$$\{\bar{\bar{U}}\}^{K} = [\bar{\bar{\Phi}}]^{K} \{\bar{\bar{\eta}}\}^{K} , \qquad F(13)$$

where

$$\{\bar{\bar{\eta}}\}^K = \begin{Bmatrix} \{\bar{\eta}\}_0^{K,0} \\ \{\bar{\eta}\}_0^{K,1} \\ \vdots \\ \{\bar{\eta}\}_0^{K,N/2} \\ \hline \{\bar{\eta}\}_1^{K,0} \\ \{\bar{\eta}\}_1^{K,1} \\ \vdots \\ \{\bar{\eta}\}_1^{K,\frac{N}{2}} \\ \hline \vdots \\ \hline \vdots \\ \hline \vdots \\ \hline \{\bar{\eta}\}_{N/2}^{K,0} \\ \{\bar{\eta}\}_{N/2}^{K,1} \\ \vdots \\ \{\bar{\eta}\}_{N/2}^{K,N/2} \end{Bmatrix}$$

Substituting Equations F(13) into Equations F(12), and premultiplying by $[\bar{\bar{\Phi}}^K]^T$, a reduced eigenvalue problem results,

$$\left[-\omega^2 [\bar{\bar{M}}]^K + [\bar{\bar{K}}]^K\right] \{\bar{\bar{\eta}}\}^K = \{0\} \quad , \qquad \text{F (14)}$$

where $[\bar{\bar{M}}]^K = [\bar{\bar{\Phi}}^K]^T [\bar{M}]^K [\bar{\bar{\Phi}}]^K$

and

$[\bar{\bar{K}}]^K = [\bar{\bar{\Phi}}^K]^T [\bar{K}]^K [\bar{\bar{\Phi}}]^K$

are the generalized mass and stiffness matrices. This may be solved by standard means.

Alternatively, perturbation techniques using the tuned system results can provide another approach to mistuned solutions.

If the Equations F(14) represent a pth. order system, the associated characteristic equation can be written as

$$b_p(\omega^2)^p + b_{p-1}(\omega^2)^{p-1} + \cdots + b_1(\omega^2) + b_0 = 0 \quad . \qquad F(15)$$

We now assume that an eigenvalue of the perturbed system is a small change from that of the unperturbed system, i.e.

$$\omega^2 = \omega_0^2 + \Delta(\omega_0^2) = \omega_0^2(1+\mu) \quad , \quad \mu \ll 1 \quad . \qquad F(16)$$

Equation F(16) is substituted into Equation F(15) and the first order terms are retained in the expansion of $(1+\mu)$ in integral powers of p. Collecting terms in μ, we obtain

$$\Delta(\omega_0^2) = \mu\omega_0^2 = -\omega_0^2 \left[\frac{b_0 + b_p(\omega_0^2)^p + b_{p-1}(\omega_0^2)^{p-1} + \cdots + b_1(\omega_0^2)}{p\,b_p(\omega_0^2)^p + (p-1)b_{p-1}(\omega_0^2)^{p-1} + \cdots + 1\cdot b_1(\omega_0^2)} \right] \quad . \qquad F(17)$$

Equations F(17), F(16) and F(14) yield the desired eigenvalues and the eigenvectors for the mistuned cyclic structure, and would be solved separately for each.

In summary, a method is developed and shown to systematically reduce the huge problem of determining the eigenvalues and eigenfunctions of a mistuned cyclic structure to a

substantially smaller, practical and computationally efficient set of algebraic equations. The accuracy of the method would largely be governed by

a) the experience of the user in the qualitative and the quantitative selection of the tuned normal modes of various harmonic numbers to represent the mistuned motion, and,

b) the degree of mass and stiffness mistuning in the light of the use of linearized perturbation theory.

Two guides to the selection of the $\overline{\eta}$'s to be retained in Equations F(13) are

(1) the bandwidth over which mistuned system eigenvalues are required,

(2) the spectrum of the particular distribution of ΔM and ΔK considered in the perturbation.

F.4 The Use of Measured Modes

Section 14 of the NASTRAN Theoretical Manual describes methods whereby representation of part of a structure by its orthogonal vibration modes is permitted in analyzing the modes of the whole structure. This feature can be effectively used for the analysis of mistuned cyclic structures such as bladed discs.

Laboratory measurements of individual blade natural frequencies and mode shapes, (and perhaps those of the disc) are used to define the generalized mass and stiffness matrices associated with the normal modal coordinates. Multipoint constraints between the degrees of freedom at the blade-disc attachment then complete the definition of the mistuned bladed disc assembly.

In NASTRAN, the generalized modal properties of the "substructure" are assigned to "scalar elements" connected appropriately to represent that portion of the structure. In a similarly modelled bladed disc, the mass and stiffness matrices of the total structure are used to derive the $[\Delta M]^{\sim}$ and $[\Delta K]^{\sim}$ perturbations in each segment. This forms the input to the analysis presented in the previous section wherein such mistuning is prescribed.

Thus, the use of the measured modes (blade modes and disc finite element model, or, both blade and disc modes) can be made compatible with the method developed for prescribed mistuning in bladed discs with rotational cyclic symmetry.

F.5 Closure

In practice the differences in the two approaches may be summarized as:

1. Prescribed Mistuning

   Relatively many degrees of freedom in the blades, but controllable mistuning spectrum.

2. Measured Modes

   Relatively few degrees of freedom in the problem but in general, the mistuning spectrum will be "broadband random".

SYMBOLS

a	Fourier coefficients
A	Generalized airforce matrix for aerodynamic modes
C	Matrix of modal pressure coefficients
D	Assumed structural damping
f	Blade geometry revision factors in static analysis
F	Generalized forcing function
G	Transformation matrix, grid points/streamline
G_{ck}, G_{sk}	Transformation matrices (Eq. B5)
I	Number of structural modes, chordwise weighting matrix
k	Reduced frequency, harmonic number
K	Stiffness matrix, Number of "independent symmetric components
L	Blade semichord
M	Mass matrix
n	Cyclic segment number
N	Cyclic segments/bladed disc
p	Differential pressure
P	Load vector, cascade theory pressure points/ streamline
q	Generalized coordinates
Q	Generalized aerodynamic force matrix
Q'	$= Q/(1/2\ \rho V^2)_{ref.}$
R	Streamline mean radius
S	Streamlines/blade
t	time
T	Coordinate transformation matrix, kinetic energy
u	Physical degrees of freedom
$\overline{u}$	"Symmetric components" in cyclic analysis

U	Strain energy
V	Free stream velocity
W	Virtual work, spanwise integration vector
x,y,z	Streamline rectangular coordinates
X,Y,Z	Basic rectangular coordinates
β	Blade angle
ε	Convergence parameter
η	Aerodynamic modal coordinates
θ	Rotational degrees of freedom
λ	Real eigenvalues
ν	Streamline angle
ξ	Structural modal coordinates
ρ	Fluid density
σ	Interblade phase angle
$\emptyset$	Structural mode shapes
Φ	Aerodynamic mode shapes
Ψ	Differential pressure distribution in aerodynamic modes
ω	Circular frequency

Subscripts

b	Blade
c	Disc
g	Grid point on streamline, chordwise aerodynamic mode on each streamline
i	Chordwise structural mode on streamline

n	Normal to local blade chord
p	Cascade theory pressure point on streamline
r	Blade root
s	Streamline
t	Blade tip

Superscripts

a	Analysis set
A	Aerodynamic
b	Basic coordinate system
d	Differential
e	Elastic
g	Global coordinate system
K	Independent solution set in "symmetric components"
l	Local (streamline) coordinate system
n	Cyclic segment n
NA	Nonaerodynamic
0,kc, ks,N/2	Fourier components (Equation B2)

REFERENCES

1. Fleeter, S. (Ed.), "Aeroelasticity in Turbomachines", Proceedings of Workshop held at Detroit Diesel Allison, Junel-2, 1972.

2. Platzer, M. F., "Transonic Blade Flutter - A Survey," Shock and Vibration Digest, July 1975.

3. Mikolajczak, A. A., "Technology Status for Blade Flutter in Axial Turbomachinery," Journal of Fluids Engineering, Trans. ASME, September 1976.

4. Platzer, M. F., "Unsteady Flows in Turbomachines: A Review of Current Developments," Shock and Vibration Digest, December 1978.

5. Sisto, F., "Review - A Review of the Fluid Mechanics of Aeroelasticity in Turbomachines," Journal of Fluids Engineering, Trans. ASME, March 1977.

6. Fleeter, S., "Aeroelasticity Research for Turbomachine Applications," Journal of Aircraft, Vol. 16, No. 5, May 1979.

7. The NASTRAN Manuals, NASA SP-221-224(05), December 1978.

8. Srinivasan, A. V., Lionberger, S. R., and Brown, K. W., "Dynamic Analysis of an Assembly of Shrouded Blades Using Component Modes," Journal of Mechanical Design, Trans. ASME, July 1978.

9. Thomas, D. L., "Dynamics of Rotationally Periodic Structures," Intl. Journal for Numerical Methods in Engg., Vol. 14, 1979.

10. Ehrich, F. F., "A Matrix Solution for the Vibration Modes of Nonuniform Disks," Journal of Applied Mechanics, March 1956.

11. Tobias, S. A., and Arnold, R. N., "The Influence of Dynamical Imperfection on the Vibration of Rotating Disks," Proc. Inst. of Mech. Engrs., Vol. 171, 1957.

12. Whitehead, D. S., "Effect of Mistuning on the Vibration of Turbomachine Blades Induced by Wakes, "Journal of Mech. Engg. Sci., Vol. 8, No. 1, 1966.

13. Ewins, D. J., "The Effects of Detuning Upon the Forced Vibrations of Bladed Disks," Journal of Sound and Vibration, Vol. 9, No. 1, 1969.

14. Ewins, D. J., "Vibration Characteristics of Bladed Disc Assemblies," Journal of Mech. Engg. Sci., Vol. 15, No. 3, 1973.

15. El-Bayoumy, L. E., and Srinivasan, A. V., "Influence of Mistuning on Rotor Blade Vibrations," AIAA Journal. Vol. 13, No. 4, April 1975.

16. Srinivasan, A. V., and Frye, H. M., "Effects of Mistuning on Resonant Stresses of Turbine Blades, " Winter Annual Meeting ASME, New York, December 1976.

17. Ewins, D. J., and Sadasiva Rao, Y. V. K., "A Theoretical Study of the Damped Forced Vibration Response of Bladed Discs," Winter Annual Meeting ASME, New York, December 1976.

18. Ewins, D. J., "Vibration Modes of Mistuned Bladed Disks," Journal of Engg. for Power, Trans. ASME, July 1976.

19. Hearsey, R. M., "A Revised Computer Program for Axial Compressor Design," ARL-75-0001, Vol. I and II, Wright-Patterson AFB, January 1975.

20. Katsanis, T., and McNally, W. D., "FORTRAN Program for Calculating Velocities and Streamlines on the Hub-Shroud Mid-Channel Flow Surface of an Axial - or Mixed-Flow Turbomachine," Vol. I, User's Manual, NASA TN-D7343, July 1973.

21. Kurzrock, J. W. and Novick, A. S., "Transonic Flow around Compressor Rotor Blade Elements", U.S.A.F. - A.P.L. T.R.-73-69, Vols. I & II. (G.M. Corporation, DDAD-EDR-7892 Vols. I & II).

22. Rao, B. M., and Jones, W. P., "Unsteady Airloads for a Cascade of Staggered Blades in Subsonic Flow," 46th Propulsion Energetics Review Meeting, Monterey, CA., September 1975.

23. Goldstein, M. E., Braun, W., and Adamczyk, J. J., "Unsteady Flow in a Supersonic Cascade with Strong In-Passage Shocks", Journal of Fluid Mechanics, Vol. 83, Part 3, December 1977.

24. Delaney, R. A., and Kavanogh, P.,"Transonic Flow Analysis in Axial-Flow Turbomachinery Cascades by a Time - Dependent Method of Characteristics," Trans. A.S.M.E., Vol. 98, 1976 Series A.

25. Verdon, J. M., and McCune, J. E., "Unsteady Supersonic Cascade in Subsonic Axial Flow," AIAA Journal, Vol. 13, No. 2, February 1975.

26. Elchuri, V., and Smith, G. C. C.,"NASTRAN Level 16 Theoretical Manual Updates for Aeroelastic Analysis of Bladed Discs", NASA CR 159823 BAT Report No. D2536-941002.

27. Elchuri, V., and Gallo, A. M., "NASTRAN Level 16 User's Manual Updates for Aeroelastic Analysis of Bladed Discs", NASA CR 159824, BAT Report No. D2536-941003.

28. Gallo, A. M., and Dale, B., "NASTRAN Level 16 Programmer's Manual Updates for Aeroelastic Analysis of Bladed Discs", NASA CR 159825, BAT Report No. D2536-941004.

29. Elchuri, V.,and Gallo, A. M., "NASTRAN Level 16 Demonstration Manual Updates for Aeroelastic Analysis of Bladed Discs", NASA CR 159826, BAT Report No. D2536-941005

30. Bisplinghoff, R. L., Ashley, H., Halfman, R. L., Aeroelasticity, Addison-Wesley Publ. Co., Inc., 1955.

31. Gradshteyn, I. S., and Ryzhik, I. M., Tables of Integrals, Series and Products, Academic Press, 1965.

1. INTERBLADE PHASE ANGLE (σ) AND HARMONIC NUMBER (k) IN TUNED BLADED DISK DYNAMICS

This addendum discusses the discrete values of interblade phase angle that should be considered in conducting flutter analyses of tuned bladed disks.

Consider a disk with N blades exhibiting a harmonic travelling wave motion in which there are "k" waves round the disk. Let the oscillatory frequency at any point on the disk be ω. A reference blade, say number one, then performs oscillations with respect to some suitably chosen time reference,

$$u_1 = U e^{i\omega t}$$

Blade two performs similar oscillations shifted by a phase lag $\pm \sigma$,

$$u_2 = U e^{i(\omega t \pm (2-1)\sigma)}$$

in which +, - denote waves travelling with or against the blade numbering sense.

Similarly

$$u_n = U e^{i(\omega t \pm (n-1)\sigma)}$$

Since the total phase shift around the disk is $\pm 2\pi k = N\sigma$

we must have $\sigma = \pm \frac{2\pi k}{N}$.

If waves of equal amplitude occur in both directions,

then
$$u_n = U e^{i\omega t}\left(e^{i(n-1)\sigma} + e^{-i(n-1)\sigma}\right)$$

$$= 2U e^{i\omega t} \cos (n-1)\sigma$$

$$= 2U e^{i\omega t} \cos\left[(n-1), \frac{2\pi k}{N}\right]$$

This is a standing wave of harmonic order 'k'.

Two features distinguish standing waves from travelling waves:

1. No interblade phase angle occurs on standing waves, but does on travelling waves.
2. Maximum blade amplitude varies from blade to blade on standing waves but does not on travelling waves.

On a flexible N-bladed disk, eigenvalues occur as follows:

N even	$k = 0, \frac{N}{2}$	- simple eigenvalues
	$k = 1, 2..\frac{N-2}{2}$	- double eigenvalues
N odd	$k = 0$	- simple eigenvalues
	$k = 1, 2... \frac{N-1}{2}$	- double eigenvalues

Travelling wave pairs are associated with double eigenvalues. For a travelling wave, the local oscillation period is $\frac{2\pi}{\omega}$, in which time the wave travels an angle $\pm \frac{2\pi}{k}$. Thus the angular wave speed is $\pm \frac{\omega}{k}$ rads./second.

Thus, in a flexible bladed disk, the interblade phase angle is <u>constrained</u> to discrete values $\sigma = \pm \frac{2\pi k}{N}$

$$\text{where } k = 0, 1 \ldots . \frac{N}{2} \quad , \quad N \text{ even} .$$

$$= 0, 1 \ldots . \frac{N-1}{2} \quad , \quad N \text{ odd.}$$

For a "rigid" disk, (which strictly never exists), the blades are ideally <u>INDEPENDENT</u>, and interblade phase angles could be arbitrary, subject only to the condition

$$\sum_{n=1}^{N} \sigma_{n+1,n} = 2\pi p , \qquad p = 0, \pm 1 \ldots$$

It is assumed that this does not occur in practice. An arbitrary distribution could however, be expanded as a finite Fourier series and treated appropriately in terms of "pseudo-harmonic numbers."

2. SPURIOUS MODES IN NASTRAN CYCLIC SYMMETRY ANALYSIS OF AXISYMMETRIC STRUCTURES

In conducting cyclic modal analysis of an axisymmetric structure using the NASTRAN cyclic symmetry capability, modes of other (higher) harmonic numbers than those of the selected harmonic number are sometimes obtained. This note discusses a probable cause of these spurious modes and possible remedies.

With reference to section 4.5 of the NASTRAN Theoretical Manual, the 'analysis' set ('a' set) physical degrees of freedom (dof's) in any section n for a given harmonic number "k" are given by

$$\{u\}^{n,k} = \{\bar{u}\}^{kc} \cos\left(2\pi k\frac{(n-1)}{N}\right) + \{\bar{u}\}^{ks} \sin\left(2\pi k\frac{(n-1)}{N}\right)$$

The $u^{n,k}$ include the dof's on the interior and the two boundaries of the sector.

The corresponding eigenvalue problem for modal analysis is posed in (an independent) K set dof's consisting of both $\bar{u}^{kc}$ and $\bar{u}^{ks}$ for all the interior and one of the two boundaries,

$$\left[\bar{K}^{k} - \omega^2 \bar{M}^{k}\right]\{\bar{u}\}^{k} = \{0\}$$

where

$$\bar{K}^{k} = G_{ck}^{T} K G_{ck} + G_{sk}^{T} K G_{sk}$$

$$\bar{M}^{k} = G_{ck}^{T} M G_{ck} + G_{sk}^{T} M G_{sk}.$$

The transformation matrices G_{ck} and G_{sk} define the intersegment compatibility conditions for a given harmonic number k. However, it is observed that both G_{ck} and G_{sk} are actually functions of (k/N) instead of k alone, suggesting similar G matrices for a given k/N ratio.

In axisymmetric structures, where the choice of the smallest representative sector is arbitrary (and hence the choice of the total number of sectors N) it is, therefore, possible for a series of (k,N) pairs to satisfy the same intersegment compatibility condition. Thus, given enough internal dof's to define mode shapes, modes of harmonic numbers other than the selected harmonic k can manifest themselves.

One possible remedy is to define a representative sector with only boundary dof's i.e., small enough to eliminate all interior dof's as suggested in the NASTRAN Theoretical Manual, section 4.5. An alternative development for cyclic modal analysis is also discussed briefly in BAT's original Technical Proposal to NASA LERC, Report no. D2528-953001, Volume I, June 1976, on Finite Element Modal Analysis of a Bladed Shrouded Disk.

In cyclic structures as distinct from axisymmetric structures, this problem should not arise.

3. ON THE DEFINITION OF BLADE AND FLOW ANGLES

In order to facilitate independent steady state and flutter analysis of a bladed-shrouded disc, the pertinent definitions have been grouped as those for

(a) static aerothermoelastic design/analysis (RF 16, DISP Approach)

(b) modal flutter and subcritical roots analyses (RF 9, AERO Approach)

It is noted that if data (STREAML1 and STREAML2 bulk data cards) for (b) type analyses for a compressor stage are obtained as partial output of (a) type analysis, the variables are automatically redefined, if required, to be consistent with (b) type analyses.

(a.) Static Aerothermoelastic design/analysis

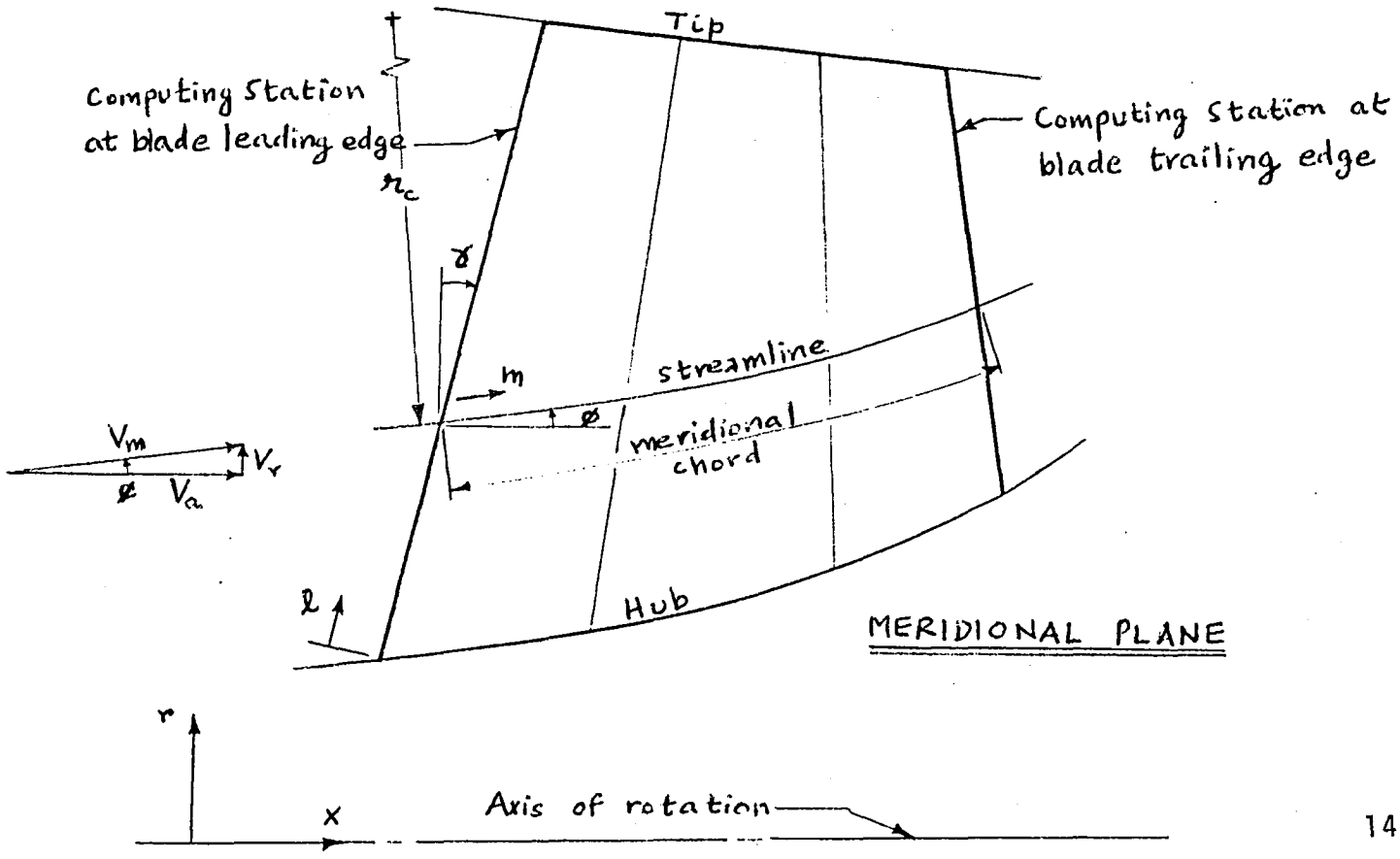

r	radial coordinate	
x	axial coordinate	
ℓ	computing station coordinate (zero at bub)	
m	meridional direction	
r_c	radius of curvature of streamline	shown positive
γ	station lean angle	
ϕ	streamline slope angle	
V_r	radial velocity	
V_a	axial velocity	
V_m	meridional velocity	

Typical Rotor Section on Streamline
(cannot be drawn in 2-d)

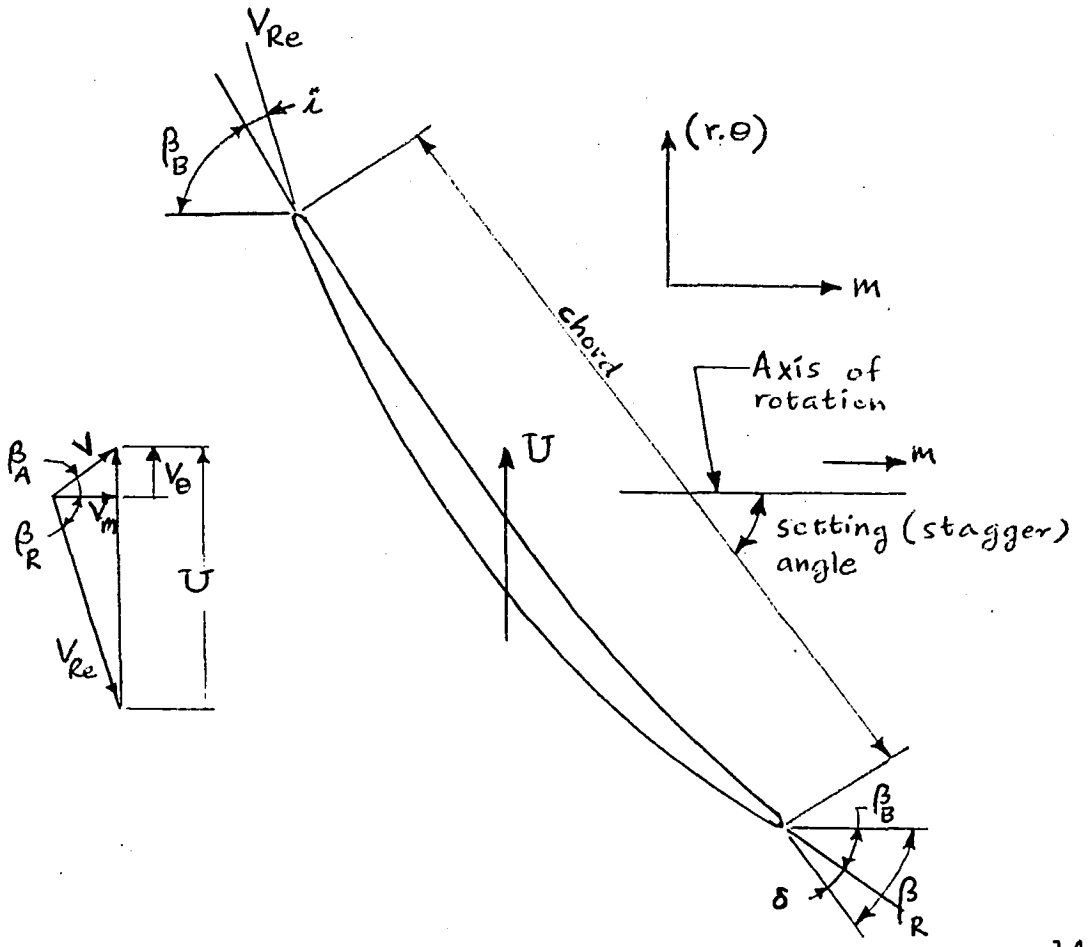

V	absolute (total) velocity
V_θ	tangential velocity
V_{Re}	relative velocity
β_A	absolute flow angle
U	blade speed
$\beta_R = \beta_B + \delta$	at blade trailing edge
$\beta_R = \beta_B + i$	at blade leading edge
β_R	relative flow angle
β_B	blade angle
δ	deviation angle
i	incidence angle

shown negative (typical rotor)

Note:

If the blade section drawing below is made in the (r.θ-x) plane, instead of (r.θ-m) plane, we get "cylindrical plane" angles.

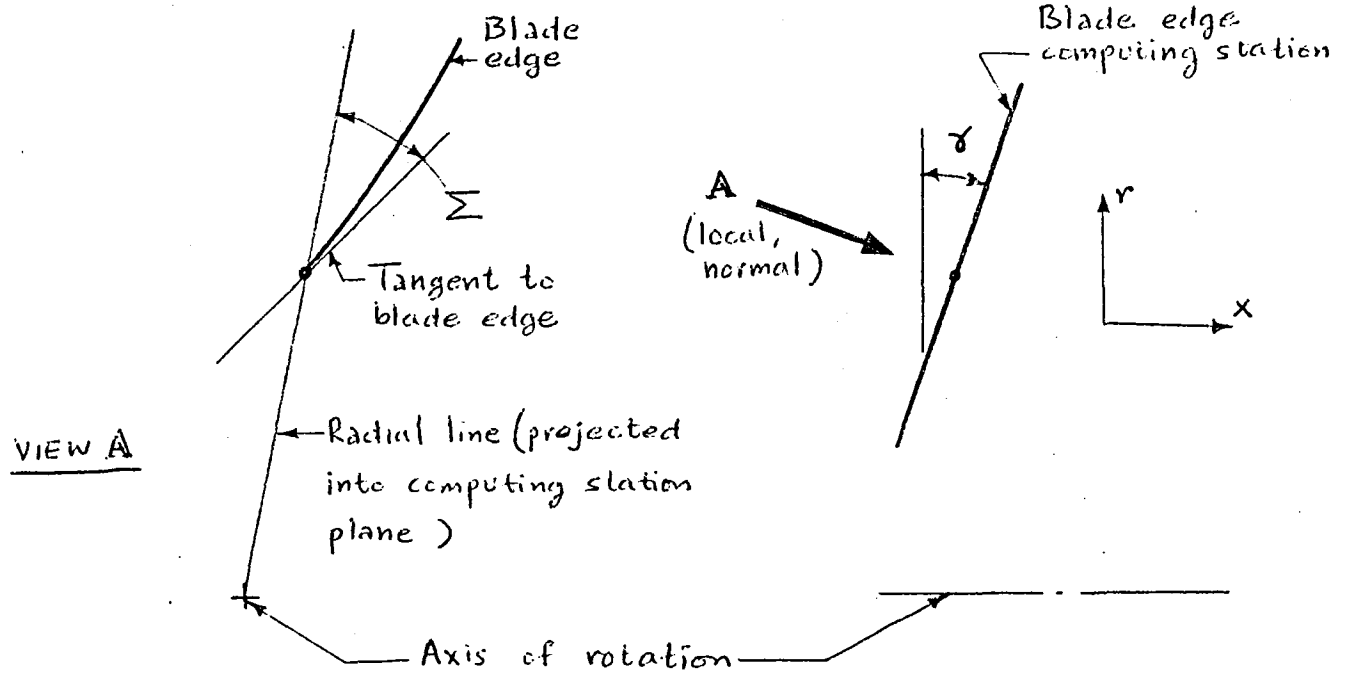

Σ	Blade lean angle	shown positive
γ	station lean angle	shown positive

(b.) Modal Flutter and Subcritical roots analyses

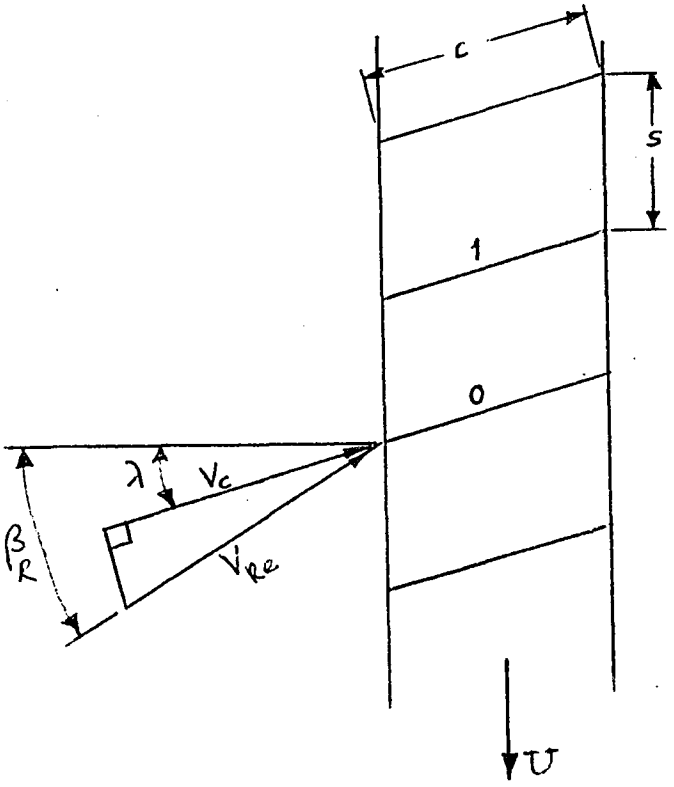

c	blade chord
s	blade spacing
U	blade speed
λ	stagger angle
β_R	relative flow angle
V_c	cascade inflow relative velocity
V_{Re}	relative flow velocity
0	reference blade
1	first blade

All angles are shown positive. A positive interblade phase angle σ implies the first blade leads the reference blade by σ .